

Copyright
by
John Alexander McMillan
2016

**The Thesis Committee for John Alexander McMillan
Certifies that this is the approved version of the following thesis:**

Physical Modeling of the Pile over Pile Condition

**APPROVED BY
SUPERVISING COMMITTEE:**

Supervisor:

Robert B. Gilbert

Kenneth H. Stokoe

Physical Modeling of the Pile over Pile Condition

BY

John Alexander McMillan, B.S. in Civil Engr.

Thesis

Presented to the Faculty of the Graduate School of

The University of Texas at Austin

in Partial Fulfillment

of the Requirements

for the Degree of

Master of Science in Engineering

The University of Texas at Austin

August 2016

DEDICATION

This one goes out to the lovely Mary Crawford James.

ACKNOWLEDGEMENTS

I would like to first thank my advisor, Dr. Robert Gilbert, for his advice and guidance during my time at UT. I had a few hiccups along the way, jumping from one topic to another in my last semester at the University, but he always managed to find me work when I needed it. His classes were pretty good, too, I suppose. I would also like to thank my second reader, Dr. Kenneth Stokoe, for his input on this project. Our meetings were always something I could look forward to, as he could always temper the technical talk with his wealth of anecdotes, which sometimes tied in to the topic at hand, but more frequently didn't. I would also like to thank my academic mentor at The Citadel, Professor Kaitlin Marley, for first getting me interested in the field of geotechnical engineering and graduate study.

I would like to thank my dear friend William Livingston. From already being one of my closest friends and confidantes from my time at The Citadel, Will Livingston moved to Texas for work around the same time that I moved for school. Being stuck in the objectively miserable town of Bay City with his job, he made it his mission to come visit in Austin as frequently as possible. I could always expect to have long conversations on the most serious aspects of life whenever this occurred, usually while sitting in my driveway and splitting a case of Lonestars.

I would like to thank Sorin Secara, for helping me get through grad school by suffering right alongside me. I met Sorin on my first day of orientation for the geotech department, and we became best of friends almost immediately. After a first year filled

with adventures and late nights of struggling to finish assignments on time, we decided that we had to be roommates, and so our adventures continued. I'll always remember some of our most difficult times in grad school as some of my favorite, as they brought out the dark humor in both of us that kept us plowing ahead without spiraling into depression.

I'd like to thank Mary Crawford James, for motivating me to finish strong in every way possible. I probably wrote half of this thesis as a result of her keeping me on track when my mind wandered to other things, such as catching Pokémon, the possibility of intelligent life in the universe, memes, how much I don't like sand, or CiCi's Pizza. Plus, she's really cute.

Finally, I'd like to thank my parents, for encouraging me to pursue an education, and starting me off early with Texas on my mind.

ABSTRACT

Physical Modeling of the Pile over Pile Condition

John Alexander McMillan, M.S.E.

The University of Texas at Austin, 2016

Supervisor: Robert B. Gilbert

In certain conditions, the need may exist for installing an open ended pile over an already placed pile as a means of remediation or increasing the capacity of the existing foundation. The objectives of this program of testing were to investigate the presence of an existing pile's effect on the drivability of an outer pile, and on the pull-out resistance of an outer pile.

Laboratory testing was conducted using normally consolidated test beds to model offshore conditions that would be reflective of the typical scenario in which such a method would be implemented. First, a series of tests were conducted with single piles to determine the set-up time for the inner pile. This set-up time was then used in the pile-over-pile tests to model a fully set-up condition for the existing pile. Three series of pile over pile tests were conducted, modeling various diameter ratios between the two piles.

For each test series, three pile over pile tests were conducted in the same test bed, with a free field control test with a pile of the same diameter as the outer pile used as a comparison. A separate test bed was used to run seismic testing, with a geophone sensor array, to better understand how the properties of the test bed changed with time around the pile.

The major conclusion was that there is no discernible increase in push-in resistance due to an inner pile, provided the piles do not come into contact. The pull-out capacity is similarly unaffected and is consistent with the prediction based on the API design method. If piles come into contact, the push in resistance increased. Spacers placed at the top of the inner pile were shown to mitigate the problem of pile to pile contact.

TABLE OF CONTENTS

TABLE OF CONTENTS	IX
LIST OF TABLES	XIII
LIST OF TABLES	XIII
LIST OF FIGURES	XIV
Chapter 1 Introduction.....	1
1.1 Background on Pile over Pile Testing	1
1.2 Objectives of Thesis.....	1
1.3 Organization of Thesis	2
Chapter 2 Literature Review.....	4
2.1 Introduction.....	4
2.2 Pile Set-Up	4
2.3 Pile Pull-Out Capacity	6
2.4 Undrained shear strength determination	7
2.5 Use of Shear Wave Velocity Measurements	9
2.6 Conclusion	15

Chapter 3	Experimental Equipment and Facility	16
3.1	Introduction.....	16
3.2	Test beds	16
3.3	Test Piles.....	19
3.4	Loading Apparatus.....	21
3.4.1	Load Frame	21
3.4.2	Pulley System and Loading Cables.....	23
3.4.3	Motor.....	25
3.4.4	Load Cell.....	26
3.5	Seismic Testing Equipment	27
3.6	Data Acquisition and Control Systems	28
3.6.1	Pile Testing	29
3.6.2	Seismic Testing.....	32
3.7	Conclusion	33
Chapter 4	Methodology	34
4.1	Introduction.....	34
4.2	T-bar Testing.....	34
4.3	Normally consolidated test bed construction	36

4.4	Seismic Test Bed Construction.....	41
4.5	Pile Installation	45
4.6	Pile Pull-Out.....	52
4.7	Seismic Readings.....	52
4.8	Conclusion	54
Chapter 5	Results.....	55
5.1	Introduction.....	55
5.2	Single pile setup tests.....	55
5.3	Pile over pile tests	62
5.3.1	Test Series 1: 2-inch over 1.5-inch	63
5.3.2	Test Series 1 Retest: 2-inch over 1.5-inch	68
5.3.3	Test Series 2: 3-inch over 2-inch	73
5.3.4	Test Series 3: 4-inch over 3-inch	77
5.4	Conclusion	81
Chapter 6	Analysis of Results from Pile over Pile Testing	82
6.1	Correcting Measured Load for Buoyancy.....	82
6.2	Push-in Resistance	83
6.2.1	Push-In Resistance in Free-Field Soil.....	83

6.2.2 Push-In Resistance Outer Pile.....	85
6.3 Pull-out capacity	92
6.3.1 Pull-Out Capacity during Set-Up.....	92
6.3.2 Pull-Out Capacity after Set-Up.....	93
6.4 Conclusion	104
Chapter 7 Seismic Testing of Monopile.....	106
7.1 Introduction.....	106
7.2 Results.....	106
7.3 Conclusion	110
Chapter 8 Conclusion and Recommendations.....	112
8.1 Conclusions.....	112
8.2 Recommendations.....	113
REFERENCES	115
VITA	118

LIST OF TABLES

Table 1	Summary of the primary consolidation in UT test beds (Lee 2008).	17
Table 2	Pile model dimensions	20
Table 3	Configuration of Test Series 1: 2 inch over 1.5 inch diameter piles.	48
Table 4	Configuration of Test Series 2: 3 inch over 2 inch diameter piles....	49
Table 5	Configuration of Test Series 3: 4 inch over 3 inch diameter piles....	50
Table 6	Measurements from Test Series 1	66
Table 7	Measurements from Test Series 1 retest	71
Table 8	Measurements from Test Series 2.....	75
Table 9	Measurements from Test Series 3.....	79
Table 10	Predicted pullout force based on T-bar tests run prior to pile installation and T-bar tests run after final pile removal.....	96
Table 11	Composite weights of outlier pile systems exhibiting gapping behavior	102

LIST OF FIGURES

Figure 1	Example of setup time prediction (Bogard and Matlock 1990).....	5
Figure 2	Penetrometer test results in normally consolidated kaolinite	8
Figure 3	Generalized Crosshole arrangement for shear wave measurement in small kaolinite test bed (Jung 2005)	10
Figure 4	Typical shear wave signal monitored in the small kaolinite test bed	11
Figure 5	Undrained shear strength vs. depth determined by penetration tests in Test Bed 3 (from Vanka, 2004)	13
Figure 6	Shear wave velocity versus depth determined by penetrating type bender element tests (Jung 2005).....	14
Figure 7	Relationship between undrained shear strength and shear wave velocity in the kaolinite slurry in Test Bed 3	15
Figure 8	55 gallon plastic barrel used for test bed construction.....	19
Figure 9	General design of model piles.....	20
Figure 10	Aluminum loading frame (Coffman 2003)	22
Figure 11	Cantilevered wooden arm used for testing next to tank (McCarthy 2011)	23
Figure 12	Pulley system mounted to load frame (McCarthy 2011)	24
Figure 13	Motor mounted to load frame (El-Sherbiny 2005)	25
Figure 14	Lebow Load cell	26
Figure 15	28 Hz model GS-14 geophone soldered to shielded twisted pair cable	27
Figure 16	Water proofed geophone sensor sealed with epoxy in plastic canister	28

Figure 17	Flow chart of the DAQ and control system used for the loading apparatus (Huang 2015).....	29
Figure 18	User interface developed for data acquisition (Huang 2015)	30
Figure 19	National Instruments data acquisition box.....	31
Figure 20	User interface for motion control system (Huang 2015)	32
Figure 21	Data acquisition system used for the geophones	33
Figure 22	T-bar at initial penetration of soil surface.....	35
Figure 23	Relationships developed between water content and undrained shear strength for normally consolidated kaolinite (Lee 2008).....	37
Figure 24	Typical layering process of normally consolidated test beds	38
Figure 25	Test Bed 3, Test Series 1 actual water contents at time of construction	39
Figure 26	Test Bed 4, Test Series 2 water contents at time of construction	40
Figure 27	Geophone layout at 23" embedment.....	41
Figure 28	Geophone arrangement at 15 inch embedment.....	42
Figure 29	Geophone arrangement at 7 inch embedment.....	42
Figure 30	Geophone arrangement in the seismic test bed.....	43
Figure 31	Spiral arrangement of geophones in the test bed	44
Figure 32	Installation of a 1.5 inch diameter pile.....	46
Figure 33	Configuration of Test Series 1: 2 inch over 1.5 inch diameter piles.....	48
Figure 34	Configuration of Test Series 2: 3 inch over 2 inch diameter piles.....	49
Figure 35	Configuration of Test Series 3: 4 inch over 3 inch diameter piles.....	50
Figure 36	Measurements taken after pile Installation	51

Figure 37	Calibration of the geophone with the pile as source configuration ..53
Figure 38	T-bar Results for Test Bed 1 before pile installation.....56
Figure 39	Results from Setup Tests of 1.5-inch piles57
Figure 40	Pull-out load/ Push-in capacity versus pull-out Displacement58
Figure 41	Pullout capacity/push-in capacity versus Time for 1.5-inch diameter piles.....59
Figure 42	T-bar Results for setup tests of 3-inch diameter piles, Test Bed 5 ...60
Figure 43	Results from setup tests of 3-inch Piles62
Figure 44	Pullout capacity/push-in capacity vs. time for 3-inch diameter piles62
Figure 45	Typical Pile configuration used for PoP and setup testing63
Figure 46	Example of inner pile making contact with outer pile visible from the surface.....64
Figure 47	T-bar test results for Test Series 1, Test Bed 3 before PoP tests were run65
Figure 48	Push in capacities of 2-inch piles over 1.5-inch piles.....66
Figure 49	Push in vs. Pullout results from Test Series 167
Figure 50	T-bar test results for Test Series 1, Test Bed 3 after PoP tests were run68
Figure 51	Spacers used on 1.5-inch piles for retest of Test Series 2.....69
Figure 52	T-bar test results for Test Series 1 retest, Test Bed 8 before PoP tests were run70
Figure 53	Push in capacities of 2-inch piles over 1.5-inch piles with spacers..71
Figure 54	Push in vs. Pullout results from retest of Test Series 1 with spacers72

Figure 55	T-bar test results for retest of Test Series 1, Test Bed 8 after PoP tests were run	73
Figure 56	T-bar test results for Test Series 2, Test Bed 4 before PoP tests were run	74
Figure 57	Push in capacities of 3-inch piles.....	75
Figure 58	Push in vs. Pullout results from Test Series 2.....	76
Figure 59	T-bar test results for Test Series 2, Test Bed 4 after PoP tests were run	77
Figure 60	T-bar test results for Test Series 3, Test Bed 6 before PoP tests were run	78
Figure 61	Push in capacities of 4-inch piles.....	79
Figure 62	Push in vs. Pullout results from Test Series 3.....	80
Figure 63	Predicted Push in Resistance vs. Measured Push in Resistance for 1.5-inch Piles.....	84
Figure 64	Predicted Push in Resistance vs. Measured Push in Resistance for 3-inch Pile Tests.....	85
Figure 65	Predicted push in capacity vs. measured push in capacities for 2-inch piles pushed over 1.5-inch piles.....	86
Figure 66	Percentage 2-inch PoP capacity higher than free field 2-inch capacity	87
Figure 67	Predicted push in capacity vs. measured push in capacities for 3-inch piles pushed over 2-inch piles.....	87
Figure 68	Percentage 3-inch PoP capacity higher than free field 3-inch capacity	88

Figure 69	Predicted push in capacity vs. actual push in capacity for 4-inch piles pushed over 3-inch piles	88
Figure 70	Percentage 4-inch PoP capacity higher than free field 4-inch capacity	89
Figure 71	Predicted push in capacity vs. actual push in capacity of 2-inch piles pushed over 1.5-inch piles with spacers	90
Figure 72	Percentage 2-inch PoP capacity higher than free field 2-inch capacity for test with spacers	90
Figure 73	Free-body Diagram of Lateral Contact Force and Soil Resistance on Outer Pile	91
Figure 74	Predicted and actual percent setup for 1.5-inch and 3-inch diameter piles	92
Figure 75	Free body diagram for pile pull-out with end bearing	93
Figure 76	Free body diagram for "gapping" behavior at base of pile with no end bearing.....	94
Figure 77	Ratio of predicted pull out resistance to measured pull out resistance for 1.5-inch Piles.....	97
Figure 78	Ratio of predicted pull out resistance to measured pull out resistance for 3-inch Pile Tests.....	98
Figure 79	Ratio of predicted pull out resistance to measured pull out resistance of 2-inch piles over 1.5-inch piles.....	98
Figure 80	Ratio of predicted pull out resistance to measured pull out resistance of 2-inch piles over 1.5-inch piles – Retest with spacers	99

Figure 81	Ratio of predicted pull out resistance to measured pull out resistance of 3-inch piles over 2-inch piles.....	99
Figure 82	Ratio of predicted pull out resistance to measured pull out resistance of 4-inch piles over 3-inch piles.....	100
Figure 83	Soil retained on 2 inch pile after pull-out	101
Figure 84	Normalized pull out force in tests that displayed possible gapping behavior.....	102
Figure 85	Comparison of predicted resistance based on fully plugged behavior to measured resistance in piles that displayed possible gapping behavior	103
Figure 86	Comparison of predicted resistance based on fully plugged behavior with gapping at base of pile to measured resistance in piles that displayed possible gapping behavior	104
Figure 87	Average shear wave velocities vs. time from seismic test bed	107
Figure 88	Change in Vs with time in the small kaolinite test bed (Jung 2005).....	107
Figure 89	T-bar results for seismic test bed, Test Bed 7	108
Figure 90	Undrained shear strength versus shear wave velocity	109
Figure 91	Undrained shear strength versus shear wave velocity in a kaolinite slurry (Jung, 2005) compared to results from seismic test bed	109

Chapter 1 INTRODUCTION

1.1 BACKGROUND ON PILE OVER PILE TESTING

In certain situations, existing deep foundations may require remediation, or the capacity to be increased. A pile may be damaged in a number of ways, and removal of the pile could prove to be prohibitively impractical or expensive. A pile may also be determined to have an inadequate capacity after installation, which needs to be increased. In both of these scenarios, removing the pile entirely could prove to be an impracticality, therefore, a different approach would need to be considered. One way to remediate both situations, would be to install a larger pile over the already existing pile. A plan to ensure that these aspects are adequately accounted for in pile design includes a program of physical modeling to be conducted at The University of Texas at Austin (UT).

1.2 OBJECTIVES OF THESIS

The overall objective of the physical modeling is to examine the possibility of using a pile installed over an already existing pile by providing data to assist in developing appropriately conservative pile driving resistance prediction aspects unique to the Pile-over-Pile (PoP) concept. Specific objectives are to quantify the effects of the following:

1. Shear strength changes in the test beds used for driven piles:

Evaluate shear strength changes in the soil surrounding the existing pile before installation and after installation through use of several methods, destructive and non-destructive.

2. Push-in resistance as a result of inner pile presence:

Evaluate the contribution to soil resistance to driving of the outer pile from the presence of the inner pile.

3. Pull-out resistance as a result of inner pile presences:

Evaluate the contribution to soil resistance to pull out of the outer pile from the presence of the inner pile.

In order to fulfill these objectives, small scale models were constructed to properly model the pile over pile condition. Inner piles were installed in normally consolidated test beds with a designed continuously increasing undrained shear strength profile, and were allowed a proper amount of time to setup. After the predetermined setup period, outer piles were installed over the inner piles. These outer piles were then removed at varying time intervals. Additionally, the increase in the undrained shear strength was measured using T-bar tests, as well as seismic crosshole style test in a specially constructed test bed.

1.3 ORGANIZATION OF THESIS

This thesis is organized with a literature review presented first. Next, the experimental facilities and equipment used for testing are detailed. Next, the methodologies for testing and test bed construction are described. After that, the actual results from the testing are presented for all pile tests. The next section presents an analysis of the results from all model pile testing. Following this, a section on the seismic

testing, summarizing both its results and analysis is presented. Finally, the conclusions and recommendations are presented in the final section of the thesis.

Chapter 2 LITERATURE REVIEW

2.1 INTRODUCTION

The objective of this section is to review the prior research on pile set up and capacity. These are all issues that are important to consider in the installation of a pile over another pile. Additionally, the use of seismic testing in undrained shear strength characterization is another important aspect of this program of research and its history is examined.

2.2 PILE SET-UP

After installation, a pile's capacity is usually not at its peak value. Observations of numerous pile tests have shown that over time, the capacity of a pile increases. This is known as the set-up effect. Model tests conducted by Olson on suction caissons in normally consolidated test beds demonstrated a marked increase in pull-out resistance over time (Olson 2003). He specifically details the change in side resistance with time, and looked at the dissipation of excess pore pressures. Matlock and Bogard also examined this in a series of full scale tests (Bogard and Matlock 1990), both their own, and real pile load test data that they collected from other data sets. All of their information came from tests using open ended driven piles. They attempted to find correlations between time after pile installation, and the capacity of the pile. Using data from various tests, they first determined an empirical method to determine the degree of axial capacity realized using consolidation theory, and related to the diameter of the pile and its wall thickness. They then applied this to create a prediction model for setup with time (Figure 1).

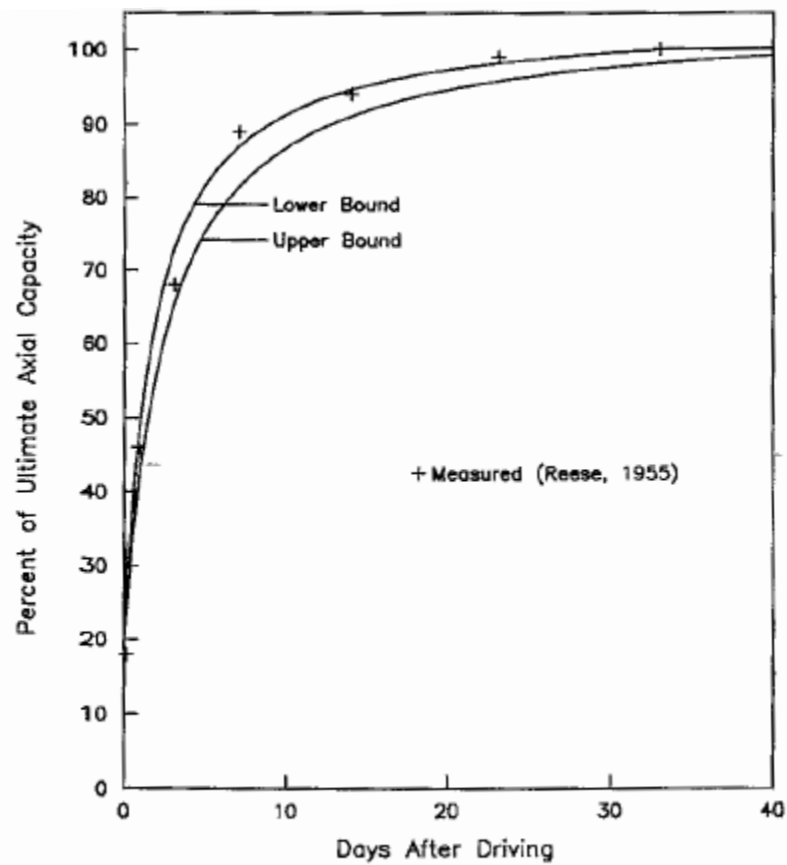


Fig 5. Load Tests in San Francisco Bay

Figure 1 Example of setup time prediction (Bogard and Matlock 1990)

For the case of pile over pile testing, the setup time was an important consideration, as the inner pile would likely be fully setup in the real world scenarios discussed. Any model testing would need to allow the inner pile to fully setup so its full capacity could be realized prior to installing an outer pile.

2.3 PILE PULL-OUT CAPACITY

Many methods have been used to predict the capacity of a pile in compression and extension. In clay, several methods include the lambda method, which limits shaft friction with increasing pile length (Vijayvergiya and Focht 1972). Another take on the lambda method was developed to take into account the ratio of the length of the pile to its diameter (Kolk and van der Velde 1996). Finally, a model was created to take into account cavity expansion with time after a pile is installed (Randolph 2003).

The API method is one of the most commonly employed, particularly in the field of offshore structures, and breaks the capacity of the pile down in to two components: the side shear, and the end bearing (API 2011). In the case of axial pullout, API specifies that "The pile capacity in tension, Q_t , is less than or equal to, but shall not exceed $Q_{f,c}$, the total shaft friction capacity in compression." (API 2011) The following equation is specified by API to in

$$Q = Q_{f,c} + Q_p$$

where

$$Q_{f,c} = \sum_{\text{Pile Length}} \alpha S_u C_{side} dL$$

S_u = Undrained shear strength

α = Empirical skin friction factor

C_{side} = Outside circumference of pile

dL = Interval of length along pile

and where

$$Q_{p,net} = 9S_u A_{tip}$$

S_u = Undisturbed undrained shear strength

A_{tip} = Area of pile tip (fully enclosed area for fully plugged and 0
for unplugged)

Based on the criteria established for axial capacity of a pile in extension, this same formula can be used to predict the axial capacity of a pile being pulled-out.

For the pile over pile testing being considered, due to certain testing constraints, the most practical way to test the capacity of any given pile after setup is through extension rather than compression. The API method for predicting the axial capacity provides a good starting point check and prediction for the capacity of the piles being tested, due to its relative simplicity, and precedent of use in offshore deep foundation design.

2.4 UNDRAINED SHEAR STRENGTH DETERMINATION

In order to understand the results from testing, it was also necessary to be able test the kaolinite. Due to its softness, undisturbed samples were not possible to obtain, limiting testing to in-situ methods. Vane shear, cone penetration test (CPT), T-bar, and T-ball are four typical options for in-situ measurements

Vane shear testing has been used extensively in shear strength characterization (Fugelsang and Steensen-Bach 1991, El-Gharbawy and Olson 1999). However, for the scale of testing, it was an impractical method for several reasons. Measurements can only be taken at intervals, giving a non-continuous soil profile, and making the test relatively slow. Vane shear tests were also shown by Vanka (2004) to provide a lower estimate of undrained shear strength than the CPT, T-bar, or T-ball tests (Figure 2).

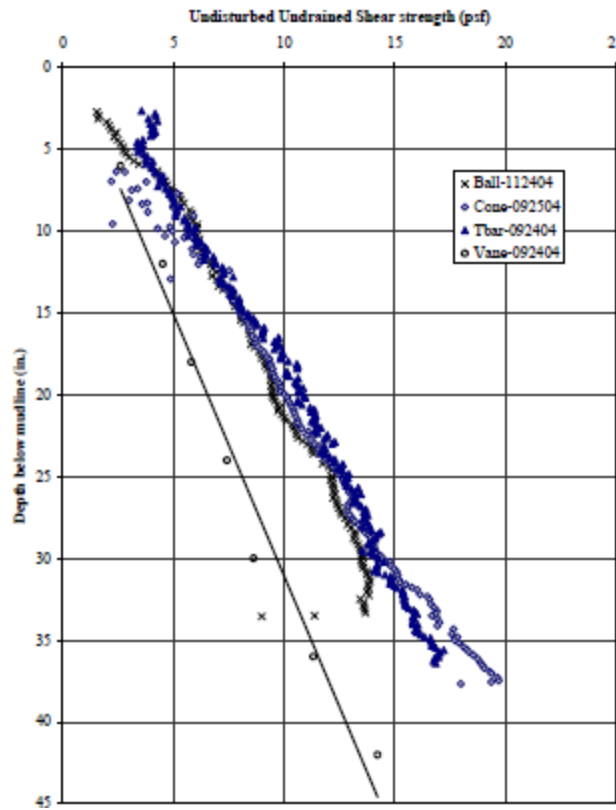


Figure 2 Penetrometer test results in normally consolidated kaolinite

The CPT also has problems for lab use in kaolinite. While it does provide a continuous profile of undrained shear, the reliability of this data is low in clay as soft as the kaolinite being used in the pile over pile lab testing. For the PoP tests, a profile with an increase in undrained shear strength of 6psf/ft was desired, with the strength being 0 psf at the soil surface and increasing from there. The CPT has demonstrated difficulty in registering such low resistance on its load cell (Boylan and Long 2007). This, coupled with the need for corrections due to overburden and pore pressure, made the CPT a less desirable option for in-situ testing.

The T-bar and T-ball tests were initially proposed in response to the problems with the vane-shear and CPT tests by Stewart and Randolph (1991). They have since become popular for in-situ lab testing (Horse and Randolph 2001, El-khatib et. al. 2002, Lee 2008). These tests are also able to create a continuous profile of undrained shear strength, and have been used extensively in the facilities that were used for the pile over pile testing (Coffman, Jung, Lee, El-Sherbiny, Vanka, Huang etc.) Based on the ease of testing, reliability of results, and precedent set in the lab facilities, the T-bar test was selected for determining the undrained shear strength of the kaolinite as needed.

2.5 USE OF SHEAR WAVE VELOCITY MEASUREMENTS

The final objective of this project, was to observe the changes in undrained shear strength in the test beds using non-destructive means. While tests such as the T-bar and CPT can give an accurate measure of shear strength, they are destructive, causing disturbance in the soil, and substantially limiting the number of times they can be run. This was of particular concern given the relatively small confines of the normally consolidated test beds being used for model testing (55 gallon barrels). The goal of seismic testing was to obtain as many readings as needed without causing any disturbance in the soil test beds. While much work has been done to determine a relationship between shear wave velocity, shear modulus, effective stress, and void ratio (Hardin and Drnevich 1972), the relationship between shear wave velocity and undrained shear strength is questionable and not as well studied.

Small scale lab testing of kaolinite using shear waves was performed at University of Texas by Men Jae Jung in 2005. Using bender elements, he set out to perform small

scale crosshole tests in kaolinite slurry in an effort to observe the shear stiffness of the soil, and then correlate it to geotechnical parameters. The preliminary system that he created to measure shear waves is shown in Figure 2.3.

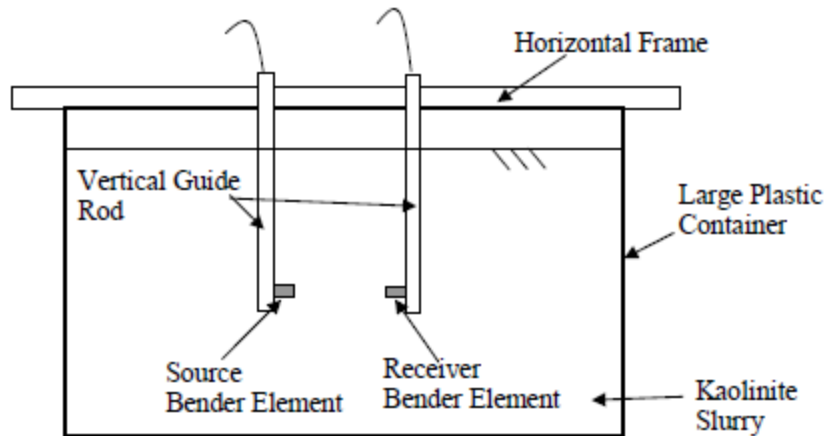


Figure 3 Generalized Crosshole arrangement for shear wave measurement in small kaolinite test bed (Jung 2005)

Using one bender element as a source, and the second element as a receiver, he could generate a shear wave, receive it with the second element, and use the time difference and known distance to compute the shear wave velocity of the kaolinite (Figure 4).

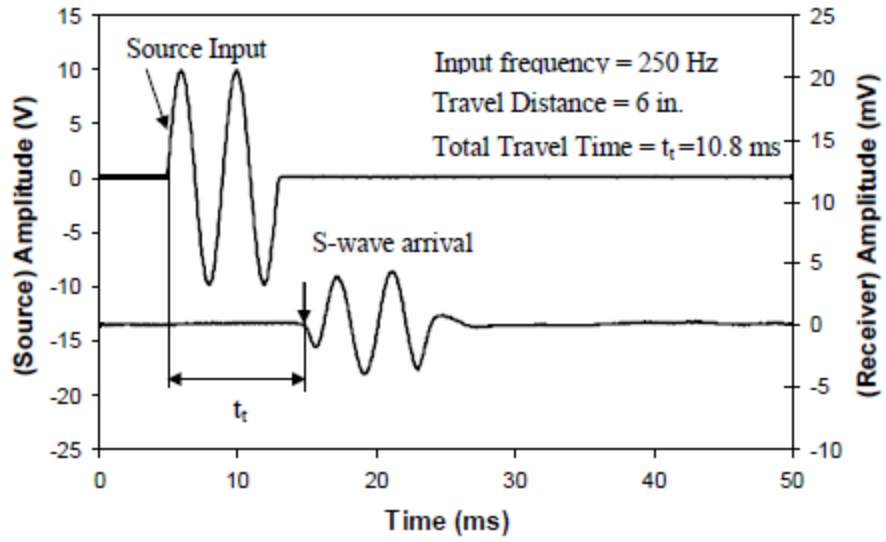


Figure 4 Typical shear wave signal monitored in the small kaolinite test bed

This output could be used to determine the travel time, and shear wave velocity, as shown in the following equation.

$$V_s = L/t_s$$

Where:

$$t_s = t_t - t_{cal}$$

L is the tip to tip distance between elements

t_t is the total travel time of the shear wave through the system

t_{cal} is the delay time in the system from the wave traveling through the elements, coating, cables, and hardware

These preliminary tests were purely to observe the change in shear wave velocity with time in a kaolinite slurry, and to establish an approach for much larger scale testing in a test bed with suction caissons installed. One of Jung's kaolinite test beds would be 6

feet deep, and 4 feet by 8 feet in plan, and constructed with a kaolinite slurry that was allowed to consolidate under its own weight over the course of a year. The other test bed was of the same dimensions but constructed earlier in the same manner and allowed to similarly consolidate (Vanka 2004). He then implemented a similar crosshole type setup of seismic instrumentation with the same intention of measuring shear wave velocities. The full details of his test bed setup and instrumentation can be found in chapters 3 and 4 of his thesis.

Of particular interest to this was, was Jung's attempt to correlate shear wave velocity to undrained shear strength, using the data collected previously on the undrained shear strength of Test Bed 3 by Vanka. Using the best fit line equation for the increase in strength with depth in Test Bed 3 and the equation for the best fit line of the increase in shear wave velocity with depth, a simple solution for the relationship between shear wave velocity and undrained shear strength was created for the normally consolidated kaolinite.

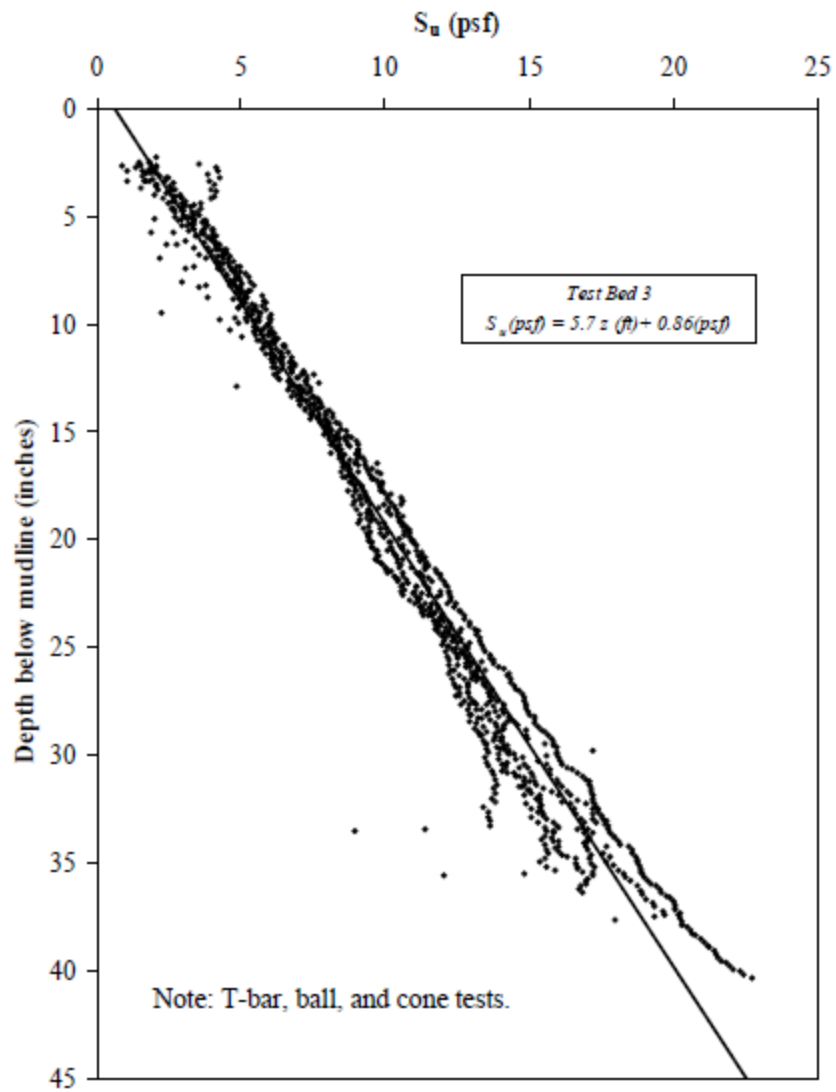


Figure 5 Undrained shear strength vs. depth determined by penetration tests in Test Bed 3 (from Vanka, 2004)

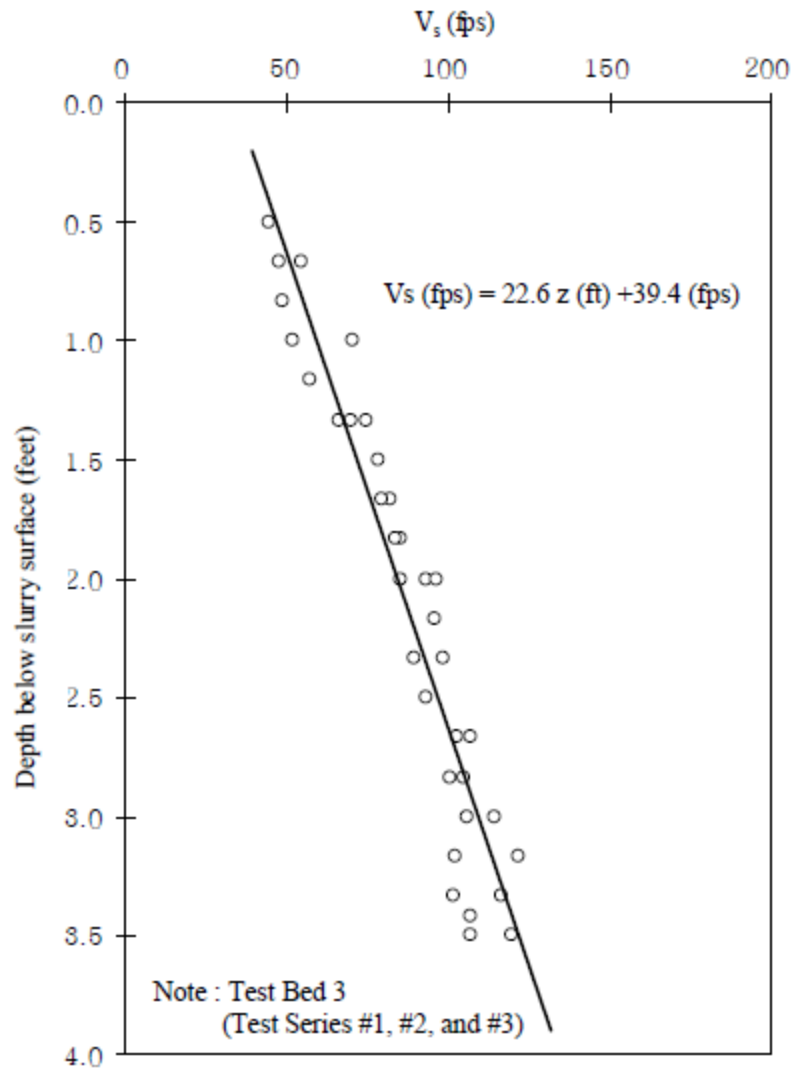


Figure 6 Shear wave velocity versus depth determined by penetrating type bender element tests (Jung 2005)

Using the data from Figures 5 and 6, Jung developed the linear relationship between undrained shear strength and shear wave velocity shown in Figure 7.

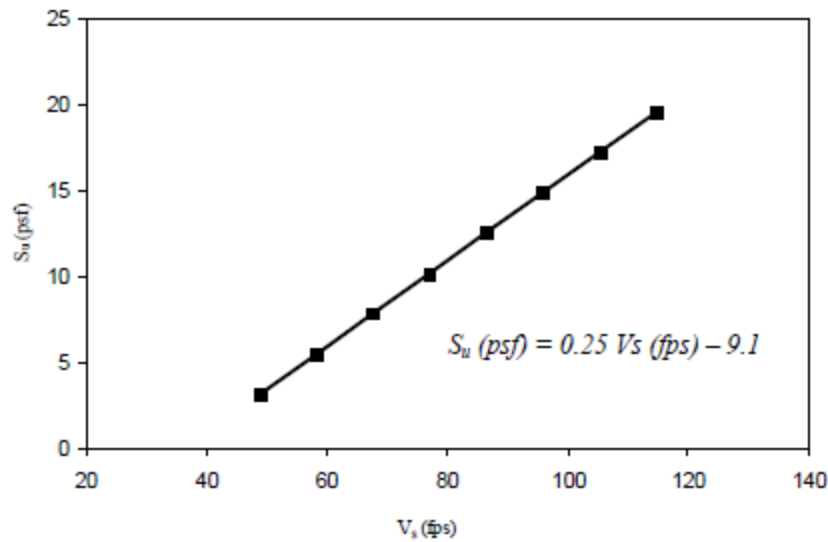


Figure 7 Relationship between undrained shear strength and shear wave velocity in the kaolinite slurry in Test Bed 3

Ideally, using this correlation, measurements of shear wave velocity could be used to determine the undrained shear strength of the soil in the pile over pile testing. Setting up an array of geophone sensors, and using a similar crosshole method could allow for a constant means of observing the increase in shear strength in the test bed before and after a pile was installed.

2.6 CONCLUSION

Many tests have been performed on single piles to establish models to predict their capacity, and their resistance to pull-out. In order to properly model the pile over pile condition as it would occur in the field, an examination of setup time was necessary. A setup time initially needed to be determined appropriately for the inner pile, as shown by Matlock and Bogard. Determination of the undrained shear strength of the test beds would also be conducted using T-bar testing and seismic testing.

Chapter 3 EXPERIMENTAL EQUIPMENT AND FACILITY

3.1 INTRODUCTION

All tests were conducted at the J.J. Pickle Research Campus of The University of Texas at Austin, in Building 120. This building contained all of the equipment and systems needed for the project.

3.2 TEST BEDS

In order to test the piles, it was necessary to create soil test beds modeling the offshore condition. In order to realistically model the offshore conditions that the pile over pile testing was modeling, it was necessary to use a normally consolidated soil profile, with linearly increasing strength.

Kaolinite has a long history of usage for model testing of various types of foundations. Examples of this include axial testing of suction caissons (El-Gharbawy and Olson 1999, Coffman 2003). In general, kaolinite is an easy to work with medium for model testing, and there was an established precedent in the lab facilities used for this testing which further made it a practical choice for the model pile over pile testing (Luke 2002, Coffman 2004, Vanka 2004, El-Sherbiny 2005, Jung 2005, Morvant 2008, and Lee 2008).

The kaolinite that was used for the pile over pile modeling had been used many times before in the lab facilities. According to the manufacturer, Kaolin Company, it has a mean particle size of $0.7\mu\text{m}$ with a specific gravity ranging from 2.58 to 2.61 (El-Sherbiny 2005). It has a liquid limit ranging from 54% and 61% and a plasticity index ranging between 20% and 27% (Chen and Randolph 2004, El-Sherbiny 2005). Finally, it

has a Unified Soil Classification System (USCS) classification of Low Plasticity Clay (CL), according to the Modified Plasticity Chart (ASTM D2488).

In the past, the process of creating a normally consolidated clay profile was extremely time consuming, as the consolidation times required were very long for beds of only a few feet of depth. The initial method of construction of these test beds in the UT lab facility was to create a slurry of the clay at a very high water content (around 150%), pour it into the test beds, and then allow it to consolidate. Lee details the methodology and properties of five of these test beds that were created for model suction caisson research and torpedo pile research (Luke 2002, Coffman 2004, Vanka 2004, El-Sherbiny 2005, and Morvant 2008) in his thesis. For each of these test beds, water contents were taken throughout the duration of their consolidation, along with settlement measurements (Table 1).

Test Bed	Date of consolidation start	Final measurement date	Average water content at placement	Average water content after consolidation	Initial thickness	Final thickness	Total settlement	Total consolidation period		t_{60} days	Approximate c_v ft ² /days
			%	%	(in)	(in)	(in)	(days)	(months)		
1	6/19/2001	2/19/2002	158	117	57	42	15	246	8	27	0.16
2	6/19/2001	1/19/2002	158	109	60	42.5	16.5	214	7	34	0.14
3	3/20/2003	5/24/2004	155	108	66.6	50.8	15.8	431	14	18	0.34
4	3/17/2004	6/19/2005	142	114	61.3	47.8	13.5	461	15	50	0.10
5	11/28/2006	5/6/2007	139	109	60	49	11	159	5	18	0.27

Table 1 Summary of the primary consolidation in UT test beds (Lee 2008)

Further details on the determination of c_v can be found in Section 3 of Lee's thesis. Using the data from the construction of the five test beds and their subsequent consolidation, Lee developed a series of target water contents with depth that would create a normally consolidated soil profile in a kaolinite test bed. By mixing layers of kaolinite with the varying water contents, and then pouring them into a barrel in layers, a

normally consolidated soil profile could be created for testing that was ready to use in 2 weeks as opposed to 2 years. From this information, Lee created a general method of normally consolidated test bed construction detailed in his conclusions. Lee's thesis was used as a guide for test bed construction, but several changes to his approach were made, as detailed in the methodology of this report.

An embedment depth of approximately 24 inches was desired for the piles, therefore, the test beds needed to typically be 2 inches deeper than this. 55 gallon barrels were ultimately decided on as the best vessel to place the test beds in. Since each test bed could only run one test series at any given time, and each test series required almost two weeks from soil layering to final pile removal, multiple test beds were needed in order to allow tests to be run concurrently. one steel barrel, and three plastic barrels were used for test bed construction (Figure 8).



Figure 8 55 gallon plastic barrel used for test bed construction

All barrels were 23 inches in diameter, and 36 inches in height. The barrels were placed on four wheel dollies so that they could be moved from underneath the loading frame for testing, and then moved to the side for other barrels as needed.

3.3 TEST PILES

In order to model the pile over pile condition, a series of pile models were created from aluminum. Three specific pile over pile configurations were desired (Table 2).

Length (in)	D _{outer} (in)	t _o (in)	D _o /t	D _{inner} (in)	t _i (in)	D _i /t
24	2	0.049	40.8	1.5	0.049	30.6
24	3	0.065	46.2	2	0.049	40.8
24	4	0.125	32	3	0.065	46.2

Table 2 Pile model dimensions

These three different pile sizes were cut from aluminum pipe to lengths varying between 30 and 42 inches, depending on the needs of the specific test configuration. After cutting, holes were drilled to allow a transverse threaded rod to be installed. This was supported with washers, with the purpose of holding weight plates on either side, which were used to install the piles. While different configurations and embedment depths existed depending on the test series, all of the inner and outer pile configurations more or less followed the scale and design shown in Figure 9.

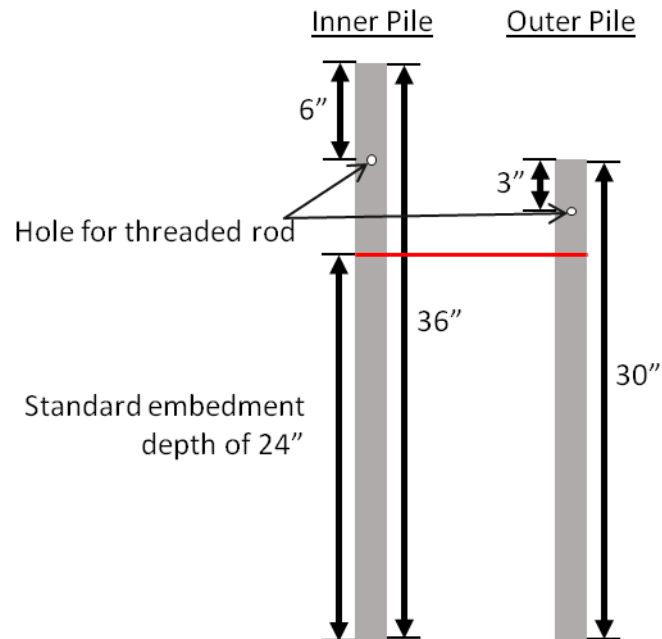


Figure 9 General design of model piles

3.4 LOADING APPARATUS

In order to install and remove the model piles, as well as perform T-bar tests, a loading apparatus was needed.

3.4.1 Load Frame

The load frame was movable, and was 5 feet wide and 4.7 feet tall. It was constructed from 4 inch wide C channel aluminum. This frame was mounted over the tank to 3x3x3/8 inch aluminum angle measuring 40 inches in length on either side. The angle mount allowed the frame to be moved along the long dimension of the steel tank. The dimensions of the frame can be seen in Figure 10.

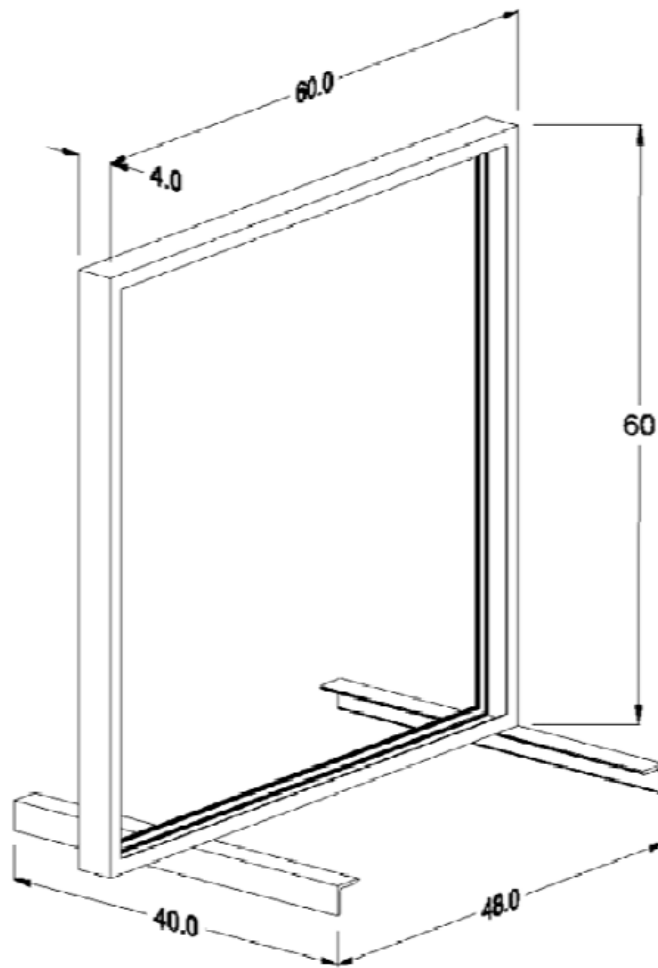


Figure 10 Aluminum loading frame (Coffman 2003)

The load frame consisted of an aluminum rectangular frame mounted on top of a large steel tank that was 4 feet by 8 feet in plan, and 6 feet in height. The frame also had a large aluminum angle mounted to the bottom angle used to straddle the tank. The motor used for loading was mounted to this plate so that it could move with the load frame.

In order to be able to use the load frame for tests being performed next to the steel tank it was mounted on, a 2x6 8 foot long wooden arm had been mounted to the top of

the load frame so that it cantilevered 5 feet out from the end of the load frame itself (Figure 11). The arm was configured with a pulley system detailed in the following section.



Figure 11 Cantilevered wooden arm used for testing next to tank (McCarthy 2011)

3.4.2 Pulley System and Loading Cables

The pulley system mounted to the load frame was made up of six 6 inch diameter fiberglass pulleys. One of these pulleys was a driving pulley, while the other five were directional, as shown in Figure 12.

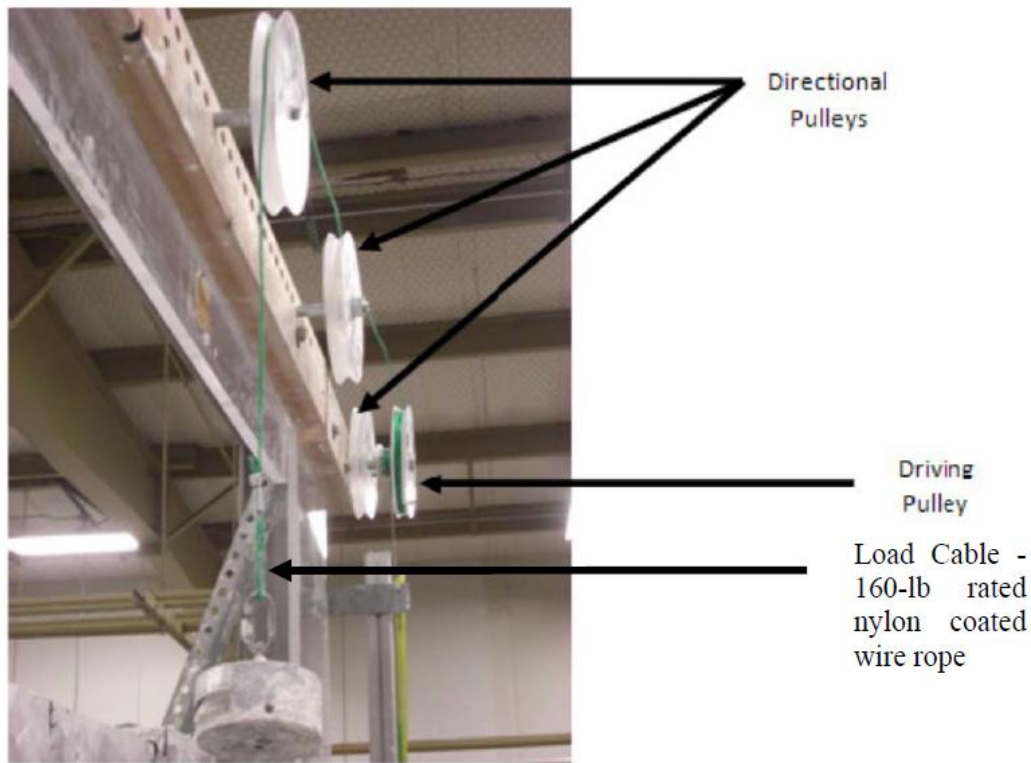


Figure 12 Pulley system mounted to load frame (McCarthy 2011)

The driving pulley was two connected 6 inch diameter pulleys mounted about a 1.8 inch diameter metal pulley. The motor was connected to this driving system by a cable connected to the smaller metal pulley between the two. The small pulley is used to give a higher range of displacements than the motor stroke alone would allow, by giving a pulley ratio of 1:3.25. Any displacement of the motor would give 3.25 times the motor displacement on the cable connected to the pulley system.

This pulley system was spooled with a McMaster Carr, 160-lb rated nylon coated wire, as seen in Figure 13. This cable was used for both the connection of the motor to the driving pulley, and the driving pulley to the directional pulleys and load cell.

3.4.3 Motor

The motor used for displacements had previously been used with the load frame for a large number of tests, such as those conducted by El-Gharbawy (1998), El-Sherbiny (2005), Coffman (2003), Lee (2008), and McCarthy (2011). The motor was a Superior Electric SLO-SYN MH112-ff-206 stepper motor with both a horizontal and vertical actuator (Figure 14). The motor itself had 12.5 inches of stroke, which when paired with the pulley system, allowed for 40.625 inches of displacement in the actual testing cable. This was only used with the vertical actuator for the testing conducted for the project.

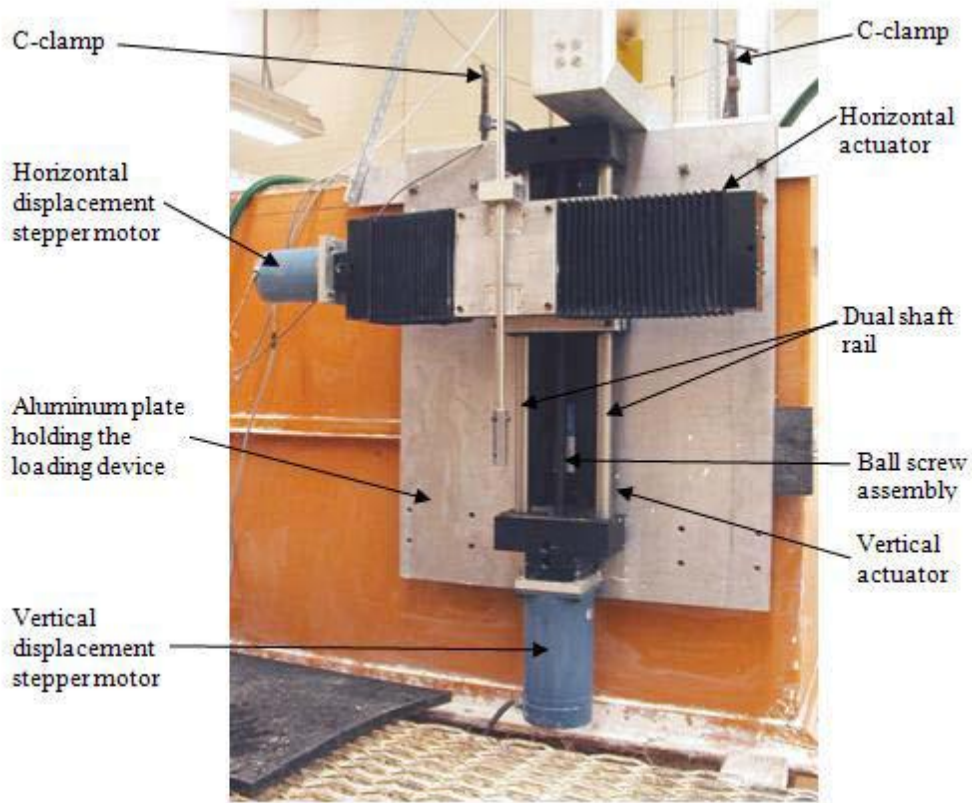


Figure 13 Motor mounted to load frame (El-Sherbiny 2005)

The motor was mounted to the load frame as shown, with the drive cable connected to the vertical actuator.

3.4.4 Load Cell

A load cell was attached to the end of the load cable off of the cantilevered end for testing being conducted on the floor next to the load frame. A 100 pound rated Lebow model load cell was used (Figure 14). This load cell measured the weight of the pile that was attached to it, and the change due to soil resistance during installation. When removing a pile, the load cell measured both the weight of the pile, and the total resistance caused by the soil.



Figure 14 Lebow Load cell

3.5 SEISMIC TESTING EQUIPMENT

The seismic instrumentation decided on for the test beds required 20 individual geophones. 28 Hz Model GS-14 geophones manufactured by Geospace. This model has a weight of 0.67 oz. (0.042 lb), a diameter of 0.66 inches, and a height of 0.68 inches (Geospace). The geophones were then each individually connected at the positive and negative terminals to 20 foot lengths of shielded twisted pair cable, which was stripped of its casing just enough to allow the connection at the end. The connections were soldered in place to each geophone (Figure 15). Additionally, each geophone was labeled with a unique number to keep track of with during data acquisition.



Figure 15 28 Hz model GS-14 geophone soldered to shielded twisted pair cable

Because the geophone sensors were going to be embedded in fully saturated kaolinite, it was also necessary to water proof them, along with their connection to the cable. This waterproofing was accomplished using 1 inch diameter, 1.375 inch height plastic canisters. Each geophone sensor was placed inside one of these containers with the soldered end sticking out the top, and then the canister was filled with epoxy until the

exposed portion of the cable was completely submerged. After ensuring that the sensor was level inside the canister, the epoxy was allowed to dry for 24 hours. The resulting waterproofed geophone sensor could then be connected to the data acquisition system as needed (Figure 16)



Figure 16 Water proofed geophone sensor sealed with epoxy in plastic canister

3.6 DATA ACQUISITION AND CONTROL SYSTEMS

Two data acquisition and control systems were used during testing. The pile installation and removal was controlled and recorded by one DAQ, while the seismic testing was controlled and recorded by a separate one.

3.6.1 Pile Testing

The data acquisition and motion control system for the load frame setup is the same that were used by Huang (2015). The data acquisition program was written in LabVIEW, and records measurements from the load cell and the LMT and outputs the data as a text file. The system designed to both control the motion of the motors, and the output of the sensors is shown in Figure 17.

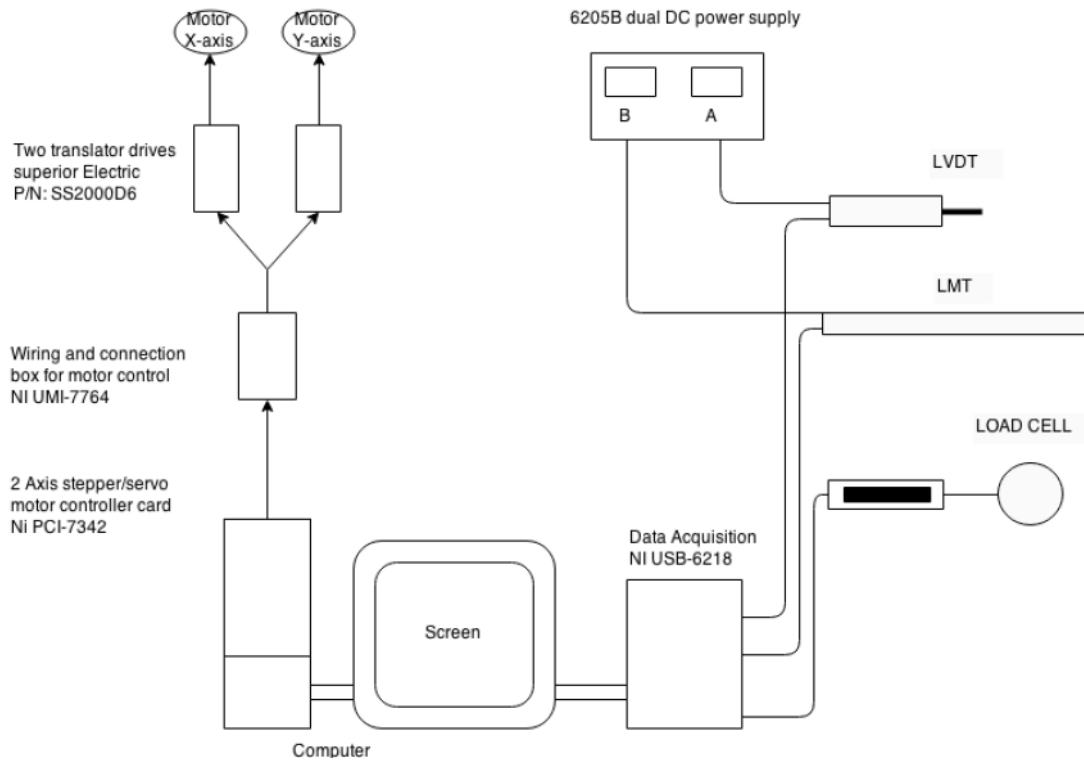


Figure 17 Flow chart of the DAQ and control system used for the loading apparatus (Huang 2015)

The full LabVIEW program written can also be found in Appendix II of Huang's thesis (Huang 2015). The LabVIEW program provides a convenient user interface that shows the outputs from the connected sensors as shown in Figure 18.

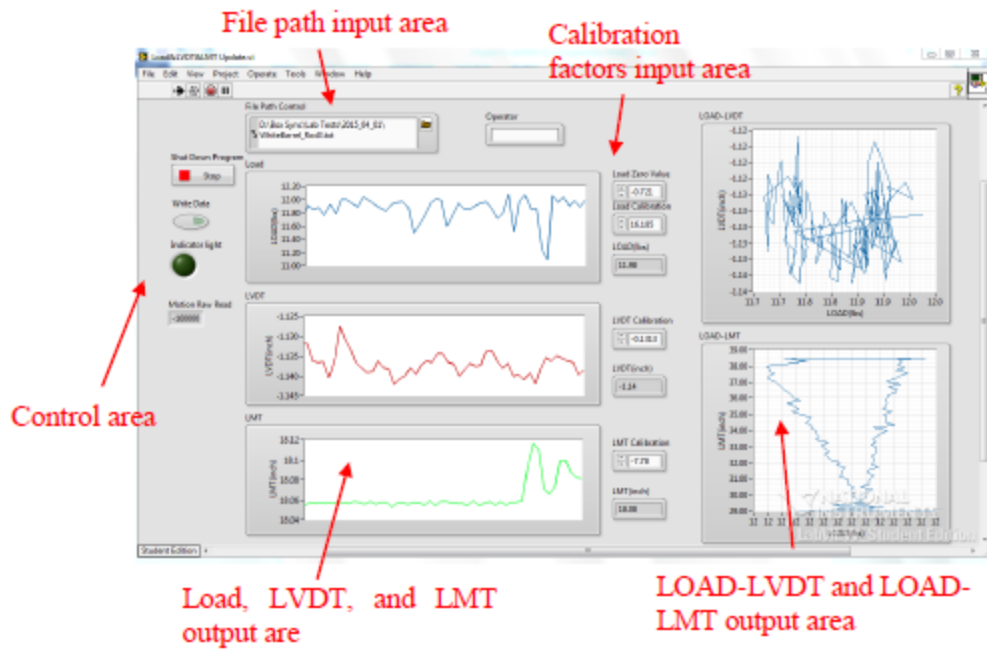


Figure 18 User interface developed for data acquisition (Huang 2015)

The actual hardware used to sample the data was a DAQ box and motor control card produced by National Instruments (Figure 19).

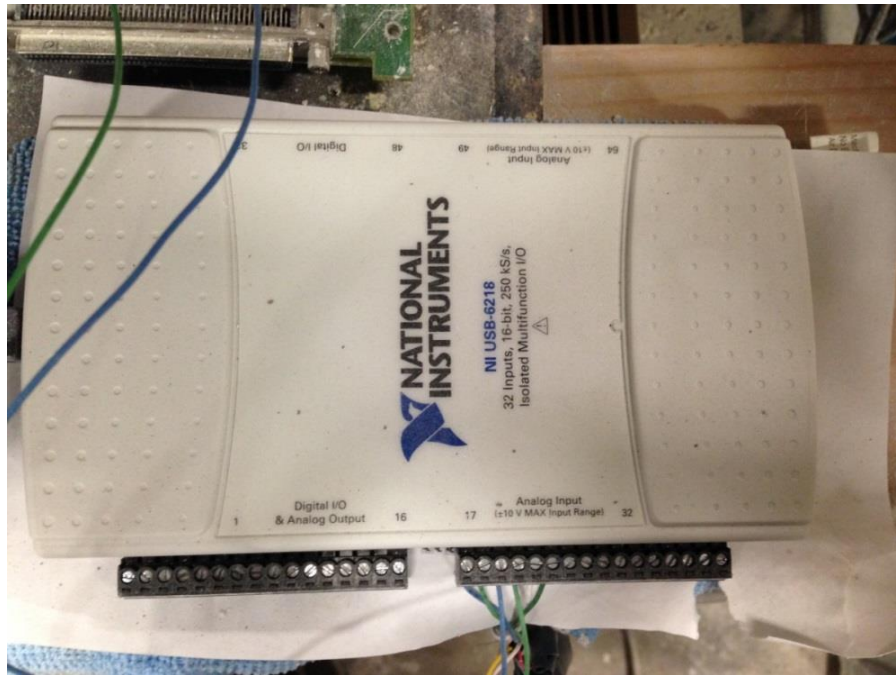


Figure 19 National Instruments data acquisition box

Using this interface, the data from pile installation could be observed in real time as it was also collected and written to the desired file path. In the pile over pile testing, only the load cell reading and LMT reading were necessary, so the LVDT portion was irrelevant.

The motion control program for the motor was also written by Huang in LabVIEW. His program has inputs for several variables: "(1)Target Position: the position the electric motor goes to;(2)Velocity: the speed of the electric motor during moving; (4)Deceleration: the rate of the change of Velocity when stop[ped]; (5) Jerk: the rate of the change of Acceleration and Deceleration" (Huang 2015). This can be seen in Figure 20.

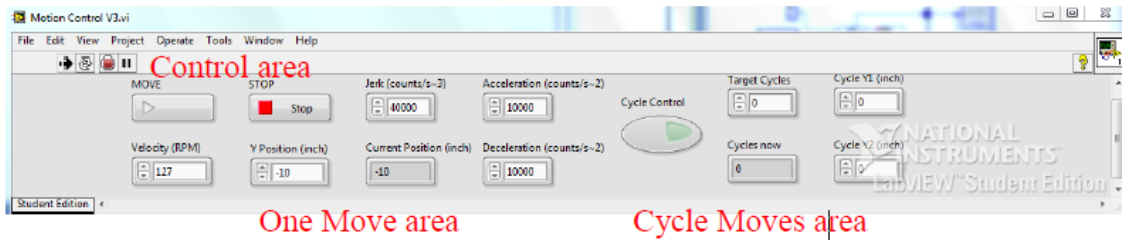


Figure 20 User interface for motion control system (Huang 2015)

After the desired inputs are entered into the input boxes, the motor can be moved with the "MOVE" command button. By integrating the motion control system with the data acquisition system, both the testing and data collection could all be controlled from the computer monitor, as shown in Figure 17.

3.6.2 Seismic Testing

For seismic testing, the geophone sensors were all connected to a DAQ manufactured by ABACUS. All the shielded cables connected to individual geophones were run to the DAQ setup, as shown in Figure 21.



Figure 21 Data acquisition system used for the geophones

The software program used to analyze the data was written in ABACUS, and the output of the tests was viewable as wave forms plotted with time. Using these wave forms, the shear wave arrival time could be picked off and used as needed.

3.7 CONCLUSION

For the program of testing, existing facilities and equipment were in place to complete most of the required work. The main addition to these facilities were the pile models and test beds needed to conduct the pile installation.

Chapter 4 METHODOLOGY

4.1 INTRODUCTION

This chapter contains the methodology for all the tests performed, as well as the details on the construction of the test beds used for testing.

4.2 T-BAR TESTING

T-bar tests were used to measure the undrained shear strength of the test beds in-situ. The T-bar is a 4 inch acrylic rod with a 1 inch diameter. The acrylic rod was attached in its center to the a steel rod 3/8 inches in diameter. This rod was then loaded with weights totaling 15 pounds, and attached to the load frame described in section 3.3. It was then allowed to push into the soil at a controlled rate of 0.8 in/sec. The load cell and LMT setup created a continuous profile of force in the rod and displacement of the rod. The undrained shear strength was then determined using the following equation (El-Sherbiny 2005):

$$S_u = \frac{(F_{total} - F_{rod})}{N_c \times A}$$

Where:

F_{total} =Total measured resistance from the load cell

F_{rod} =Measured resistance from standalone rod test

N_c =Bearing capacity factor (10.5)

A =Area of the T-bar (4 inch²)

N_c is the bearing capacity factor. From Randolph and Houlsby (1984), a plasticity solution was developed for limiting pressure on a T-bar moving perpendicular to its axis in a purely cohesive soil. This gave a range of N_c values of 9 to 12 for a fully smooth and fully rough bar, respectively. For the sake of this testing, an average value of 10.5 was used, based on precedent set in normal practice (Stewart and Randolph, 1994).



Figure 22 T-bar at initial penetration of soil surface

For each series of T-bar tests, one test was run in an undisturbed area, followed by two more in the same spot for remolded strength. Then, a final test with just the rod was run to obtain values for F_{rod} . After each penetration, the T-bar and rod were cleaned. In

order to minimize disturbance, T-bar tests were performed at the end of test bed consolidation prior to pile installation, a process typically taking six days from time of construction. They were also performed at the end of testing for a profile of undrained shear strength for the test bed. In the case of the standard pile over pile tests, the initial T-bar tests were performed in the center, with the final T-bar test series run between two of the pile locations about the same distance out from the center.

4.3 NORMALLY CONSOLIDATED TEST BED CONSTRUCTION

Test beds were constructed in 55 gallon drums to a depth of at least 24 inches to allow embedment of the test piles. The methodology used generally follows the procedure described by Lee in his construction of normally consolidated test beds, although several changes were made.

Using the kaolinite soil from the large tanks previously discussed, individual layers of soil were created in 5 gallon buckets typically filled to around the 4 gallon mark to allow the addition of water. A linearly increasing, 6 psf/ft, shear strength profile was desired. For the calculations for the desired water contents at different depths, $c/p=0.19$, $\gamma_{\text{water}}=62.4$ pcf, $G_s=2.58$ for the kaolinite, and $S=100\%$, based on the properties of the kaolinite. Lee established a relationship between the undrained shear strength profiles he measured in these test beds and the measured water contents (Figure 23).

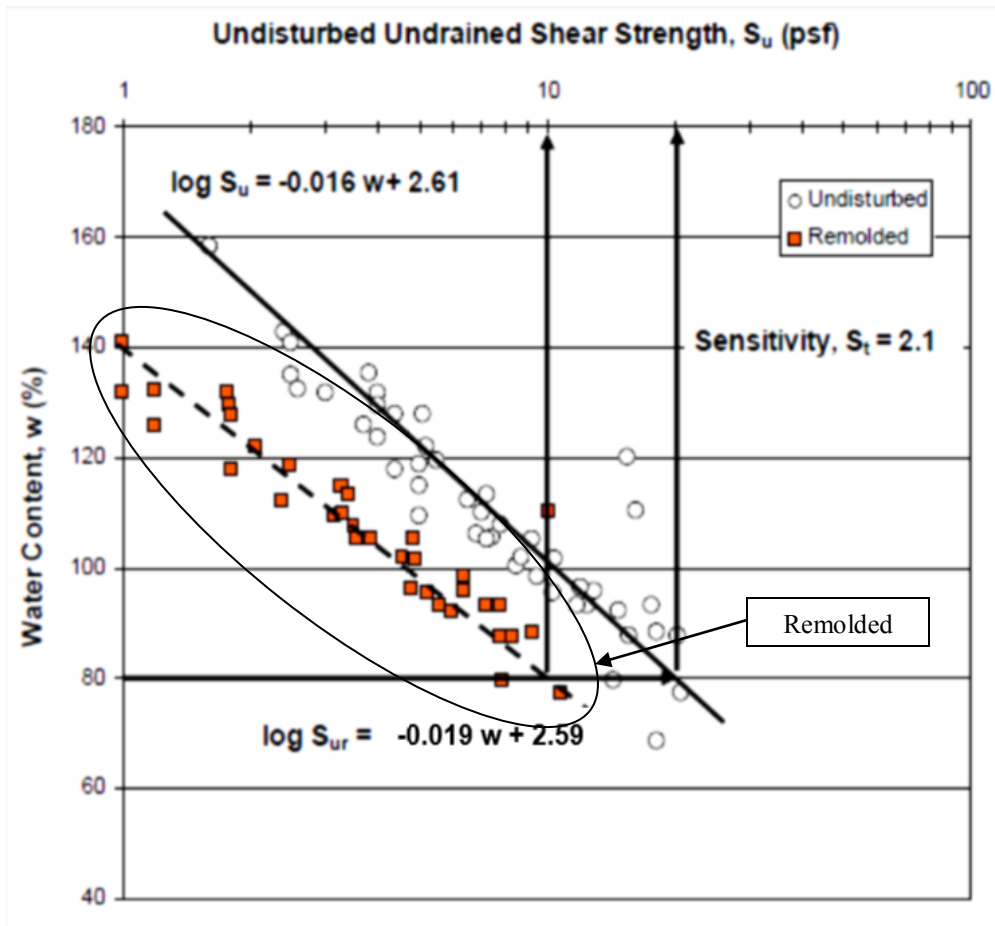


Figure 23 Relationships developed between water content and undrained shear strength for normally consolidated kaolinite (Lee 2008)

Using this data from Lee, the target water content for the desired NC soil profile at a given depth can be determined based on the equation of the trend developed for the remolded undrained shear strength of the kaolinite clay.

$$\log S_u = -0.019w + 2.59 \rightarrow w_{target} = \frac{(2.59 - \log S_u)}{0.019}$$

Where:

S_u =Undrained shear strength

w_{target} = Target water content

Using the 6 psf/ft desired strength, the water contents needed at different depths were determined for the test beds (Figure 25, 26). By mixing the soil in layers, a soil profile with increasing strength with depth could be created. These individual layers were then added to the 55 gallon barrel test bed to ensure that the layers remained separate. A typical test barrel was created from 10 separate buckets of soil, and each barrel was added starting with the highest undrained shear strength layer at the bottom, to the lowest undrained shear strength layer at the top (Figure 24). The actual water contents initially present in Test beds 3 and 4 were recorded as well (Figure 25 and 26).

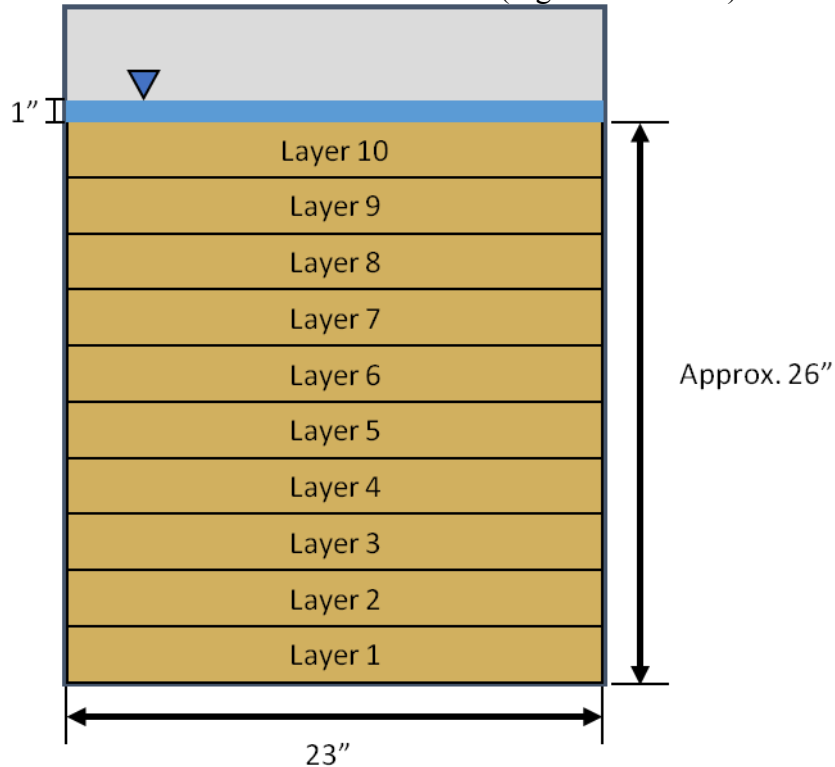


Figure 24 Typical layering process of normally consolidated test beds

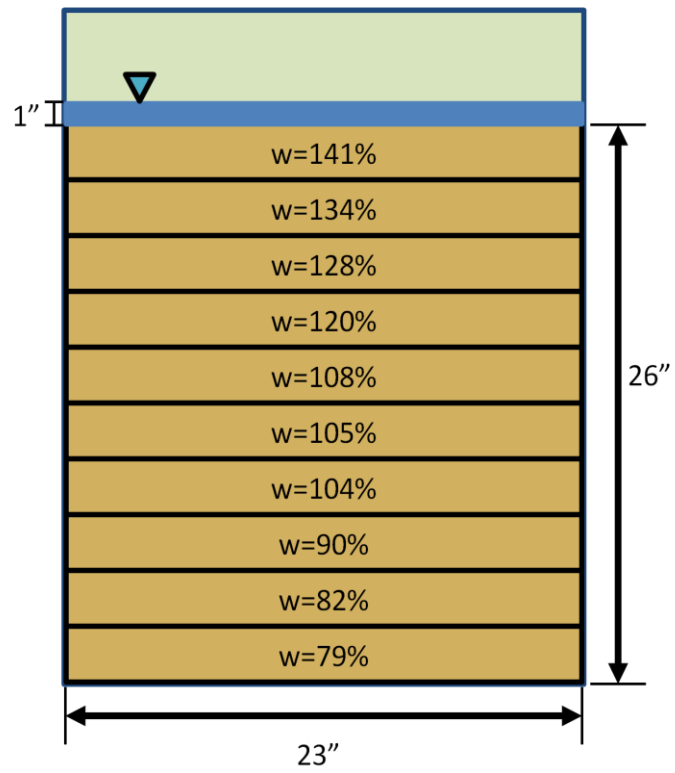


Figure 25 Test Bed 3, Test Series 1 actual water contents at time of construction

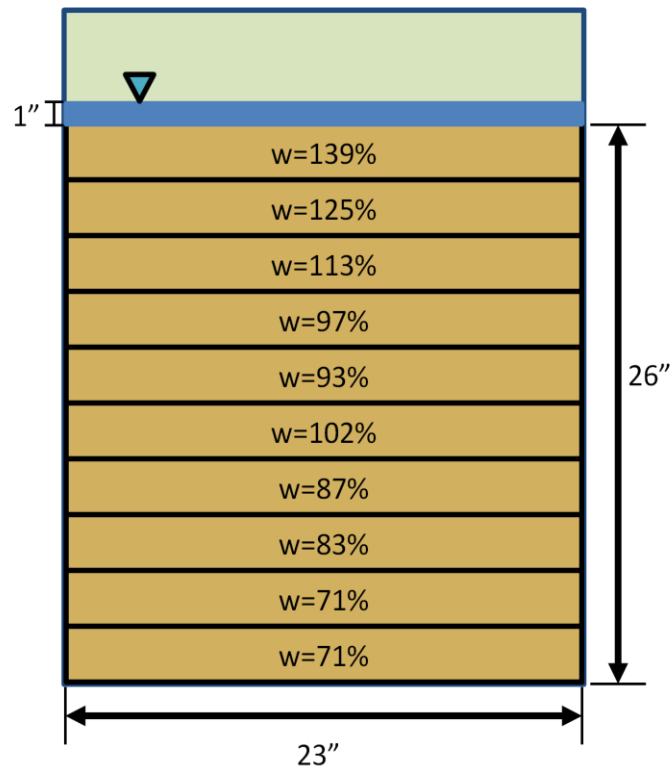


Figure 26 Test Bed 4, Test Series 2 water contents at time of construction

The layer heights were approximate, as variations in water content and fill level in the individual mixing buckets made the individual layer thickness difficult to precisely predict. However, this method of mixing in buckets and then layering provided a satisfactory profile. After the layering of the soil, about an inch of water was added to the top to prevent desiccation of the upper soil layers. The entire test bed was then allowed to consolidate for 6 days, and at this point, a T-bar test was run. If the profile provided by the T-bar test closely matched the 6psf/ft undrained shear strength profile, then the test bed was ready for pile installation.

4.4 SEISMIC TEST BED CONSTRUCTION

The seismic measurements required the least amount of disturbance possible, therefore, they were run in a special test bed constructed to contain a single 4 inch diameter pile with a wall thickness of 0.065 inches. The sensor configuration that was settled on would maximize the available space in the test bed while allowing readings to be made at a variety of spacings (Figures 27, 28, 29 and 30).

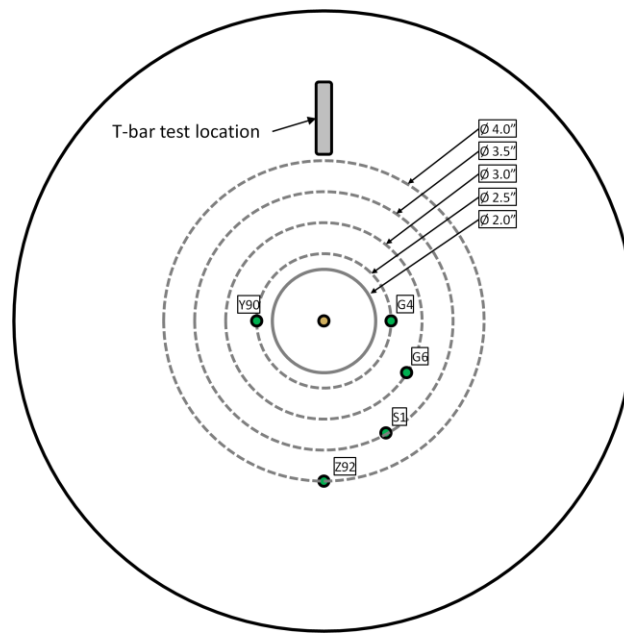


Figure 27 Geophone layout at 23" embedment

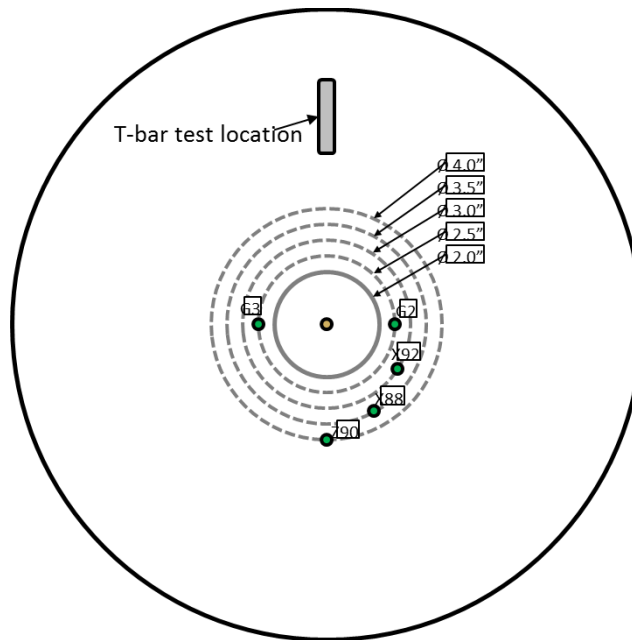


Figure 28 Geophone arrangement at 15 inch embedment

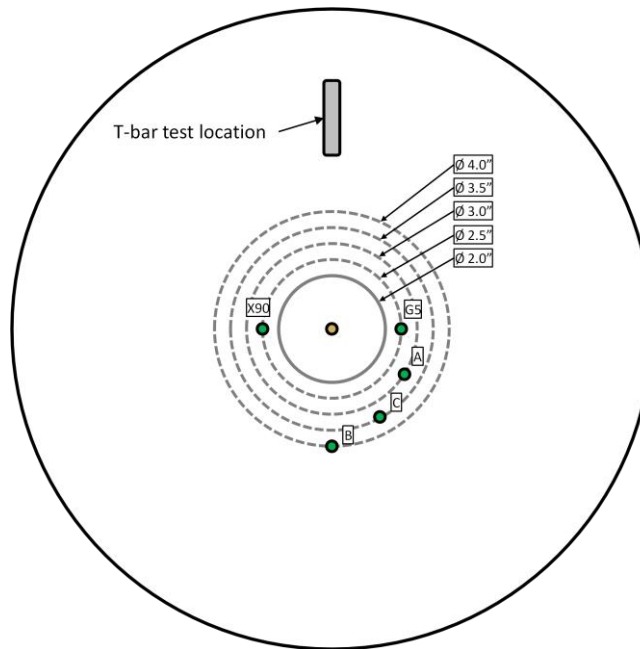


Figure 29 Geophone arrangement at 7 inch embedment

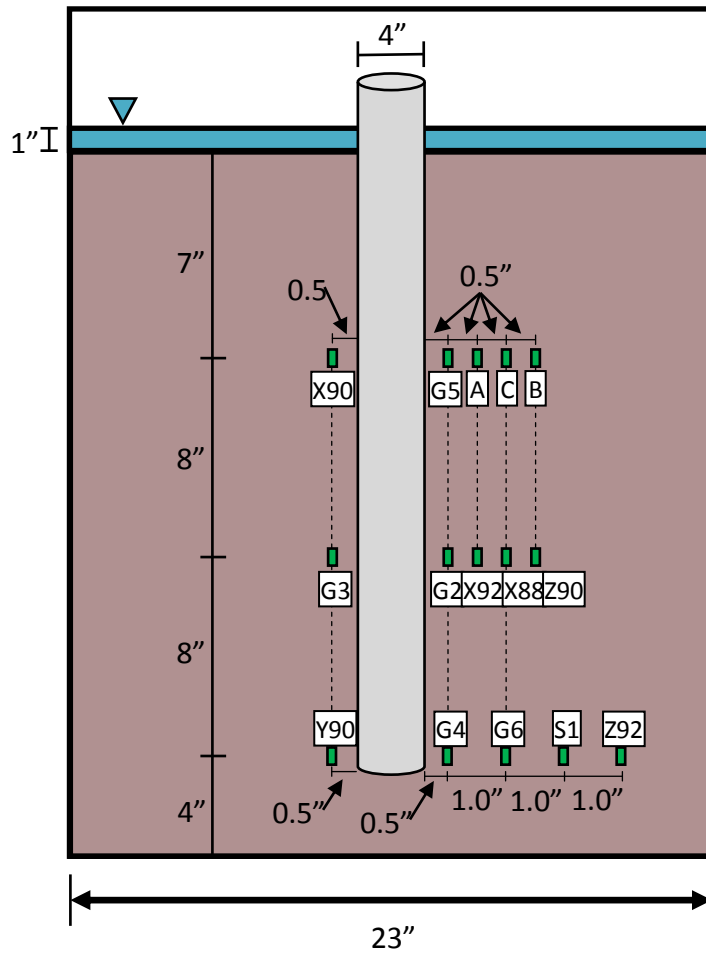


Figure 30 Geophone arrangement in the seismic test bed

The sensors were very tightly spaced, with those nearest to the pile designed to only be within 0.25 inches of its outer wall. Each sensor was unique and registered in the data acquisition system for testing.

The construction of the test bed followed the same process described in Section 4.2, with some slight variations. After the desired soil profile was mixed in separate buckets, the soil was layered, with a wooden rod secured to the bottom of the barrel with the depth of the soil marked on it, with 0 being the base of the barrel. Once the layers

reached the depths that were selected for sensor placement (4 inches, 12 inches, and 20 inches), the sensors were placed directly into the soil at the exact intervals shown in Figure 29. The cables connected to the sensors were run directly to one side of the barrel, taped to its wall, and then run up the side and out of the barrel, to connect to the DAQ (Figure 31).



Figure 31 Spiral arrangement of geophones in the test bed

After each set of sensors was installed, the layering process continued in the same manner, with extra care being taken not to disturb the newly placed sensor array. The final layer ended at a height of 27 inches from the bottom of the barrel. Water was once again added to the surface.

4.5 PILE INSTALLATION

For this project, two types of pile installations were run: monopile installation, and pile over pile installation. These two procedures are detailed below.

For monopile tests, each pile was installed using the load frame and motor apparatus. The single pile was loaded with 10 or 15 lbs evenly distributed on a transverse threaded rod and secured with washers (Figure 32)

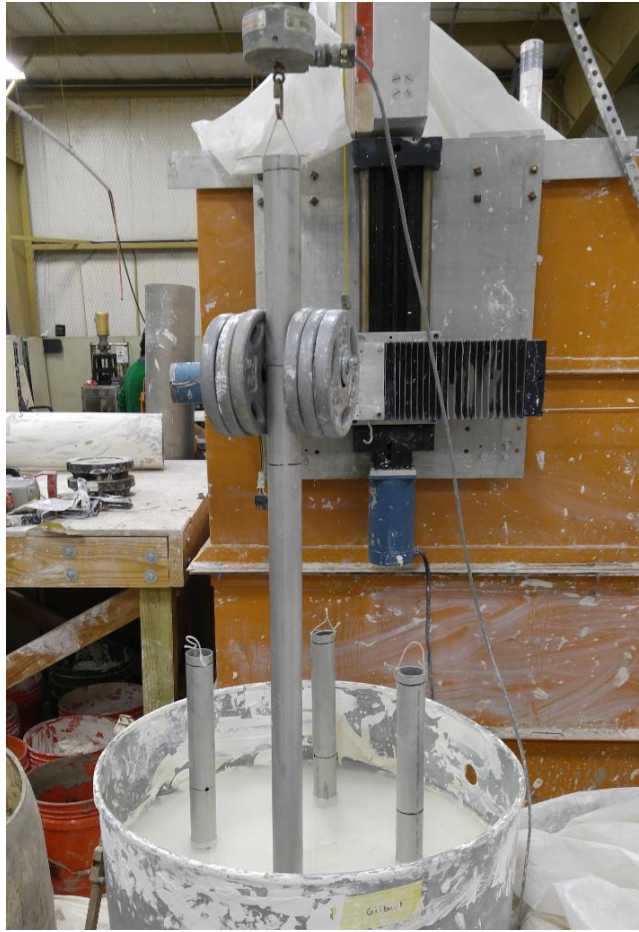


Figure 32 Installation of a 1.5 inch diameter pile

The rod was then secured to the load cell on the motorized frame apparatus. A level was used to check for plumbness, which could be adjusted by minor adjustments to the weights and the load cell attachment. The pile was then installed by lowering it with the motor at a constant rate of displacement of 0.8 in/sec (to match the installation rate of the T-bar), while recording continuous readings from the load cell and the LMT in the load frame apparatus. The piles were typically installed to a penetration of 24 inches into the test bed, which was monitored by a marking on the pile at that height of the pile

rather than the displacement readings given by the DAQ system, due to the elasticity of the cable system giving higher displacements than those actually occurring. While 24 inches was the standard, this was not always possible, due to variations in the test bed height, which ranged from 24 inches to 27 inches in depth, or limitations in motor stroke.

Once the pile reached the desired embedment, the motor was stopped, along with the load cell and LMT readings. The weights were then removed from the pile, and then the pile was disconnected from the load cell.

For pile over pile testing, the method described for the single piles was followed for the inner pile. The second outer pile was also installed using the load frame and threaded rod to place the weights in the mostly same manner as well. The only difference in the procedure was that the outer pile had to be centered over the inner pile prior to testing. This was achieved by moving the test bed barrel into position such that the inner pile was centered underneath the outer pile that was to be installed. The outer pile was then lowered with the motor at a much slower rate than the 0.8 in/sec rate used for actual installation over the "stick-up" portion of the inner pile. This "docking maneuver" was performed to prevent the outer pile from swinging prior to reaching the mudline.

The slow docking method was used to lower the outer pile to the mudline, at which point, the installation method described earlier was used to install the pile to full embedment, and then disconnect from the load frame.

Three test series were performed with varying configurations.

Test Series 1					
Test Bed Depth (in):	26	24 hour	48 hour	96 hour	Control
Embedment Depth	Inner Pile	24	24	24	22.5
	Outer Pile	23.5	23.8	24	-

Table 3 Configuration of Test Series 1: 2 inch over 1.5 inch diameter piles

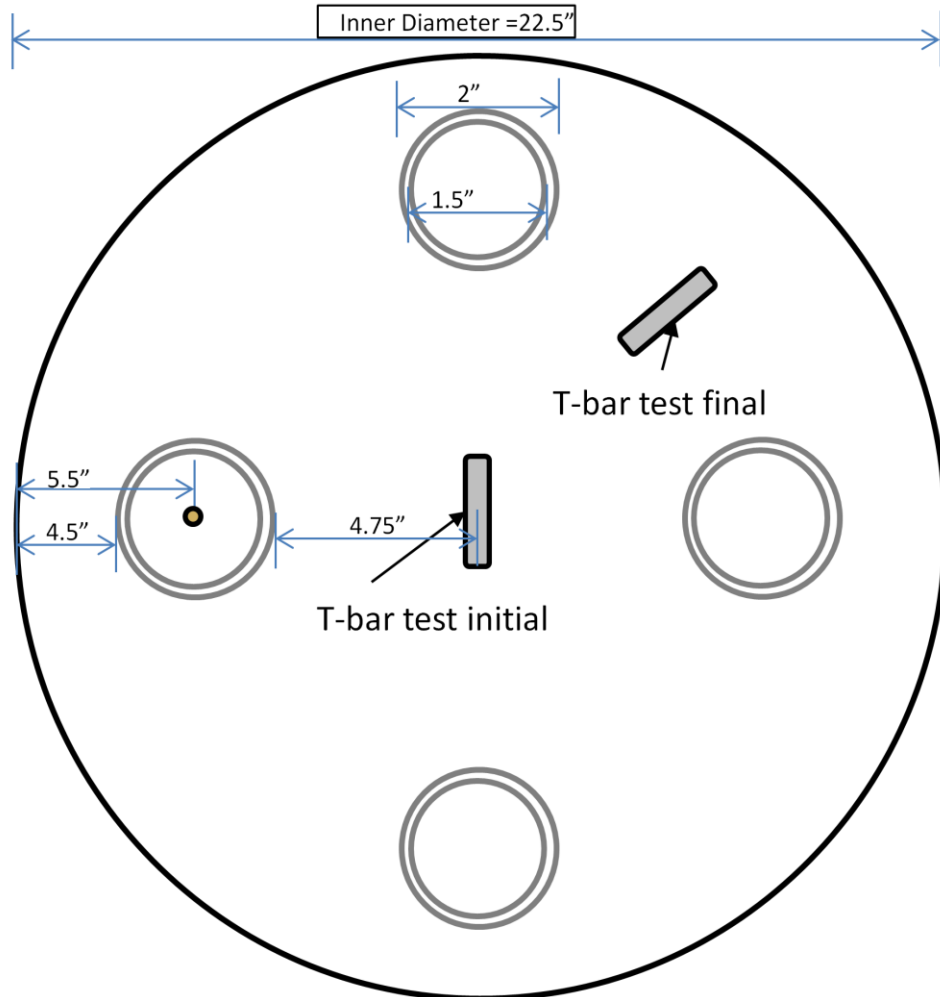


Figure 33 Configuration of Test Series 1: 2 inch over 1.5 inch diameter piles

Test Series 2					
Test Bed Depth (in):	26	24 hour	48 hour	96 hour	Control
Embedment Depth	Inner Pile	24.2	24	23.8	24
	Outer Pile	24	23	23	-

Table 4 Configuration of Test Series 2: 3 inch over 2 inch diameter piles

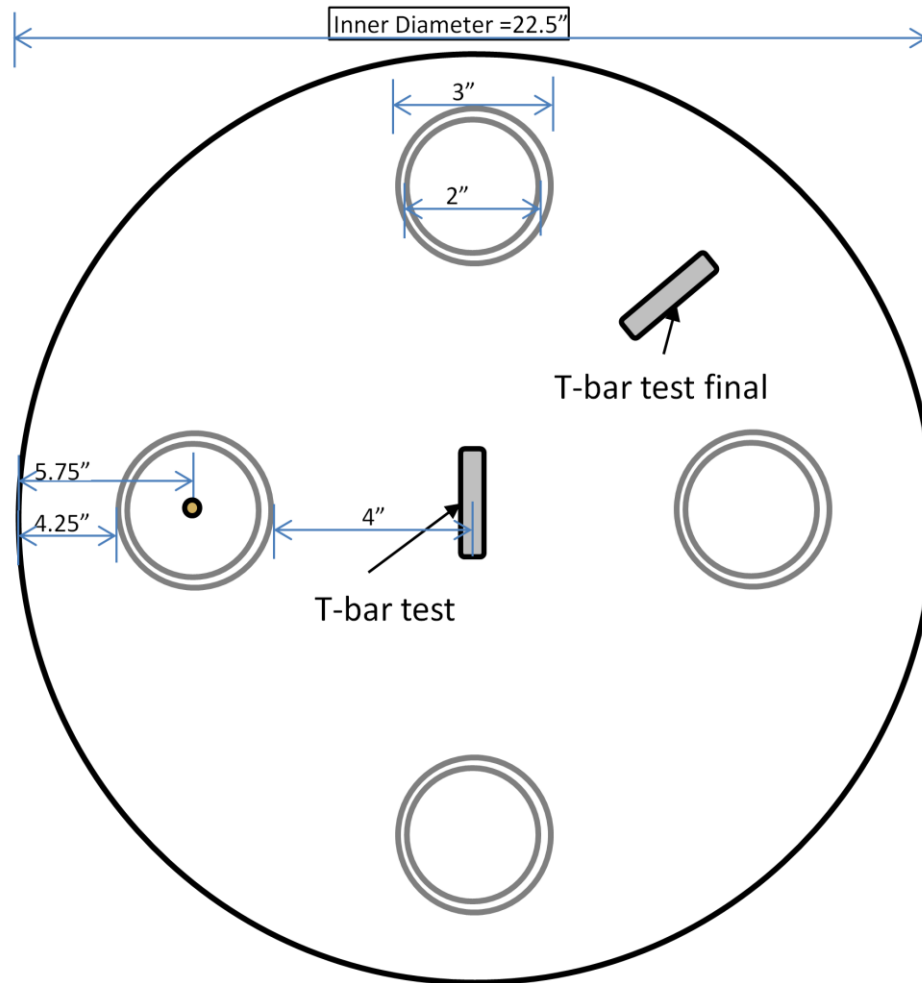


Figure 34 Configuration of Test Series 2: 3 inch over 2 inch diameter piles

Test Series 2					
Test Bed Depth (in):	26	24 hour	48 hour	96 hour	Control
Embedment Depth	Inner Pile	24	24	24	22.5
	Outer Pile	22	22	22.5	-

Table 5 Configuration of Test Series 3: 4 inch over 3 inch diameter piles

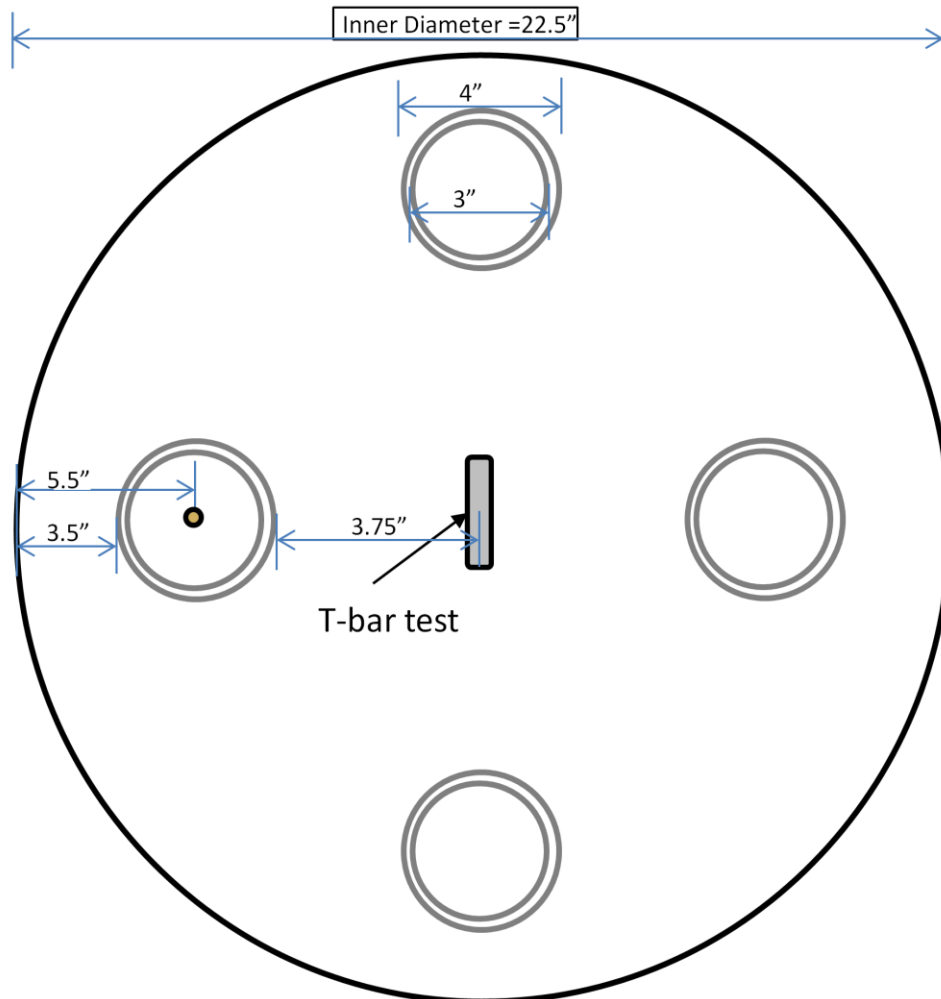


Figure 35 Configuration of Test Series 3: 4 inch over 3 inch diameter piles

After each installation, several physical measurements were taken. The plug height, which was the distance from the mudline of the test bed to the soil plug inside the inner pile or monopile, and the annulus height, which was the distance from the mudline of the test bed to the soil plug within the annulus between the two piles (Figure 36).

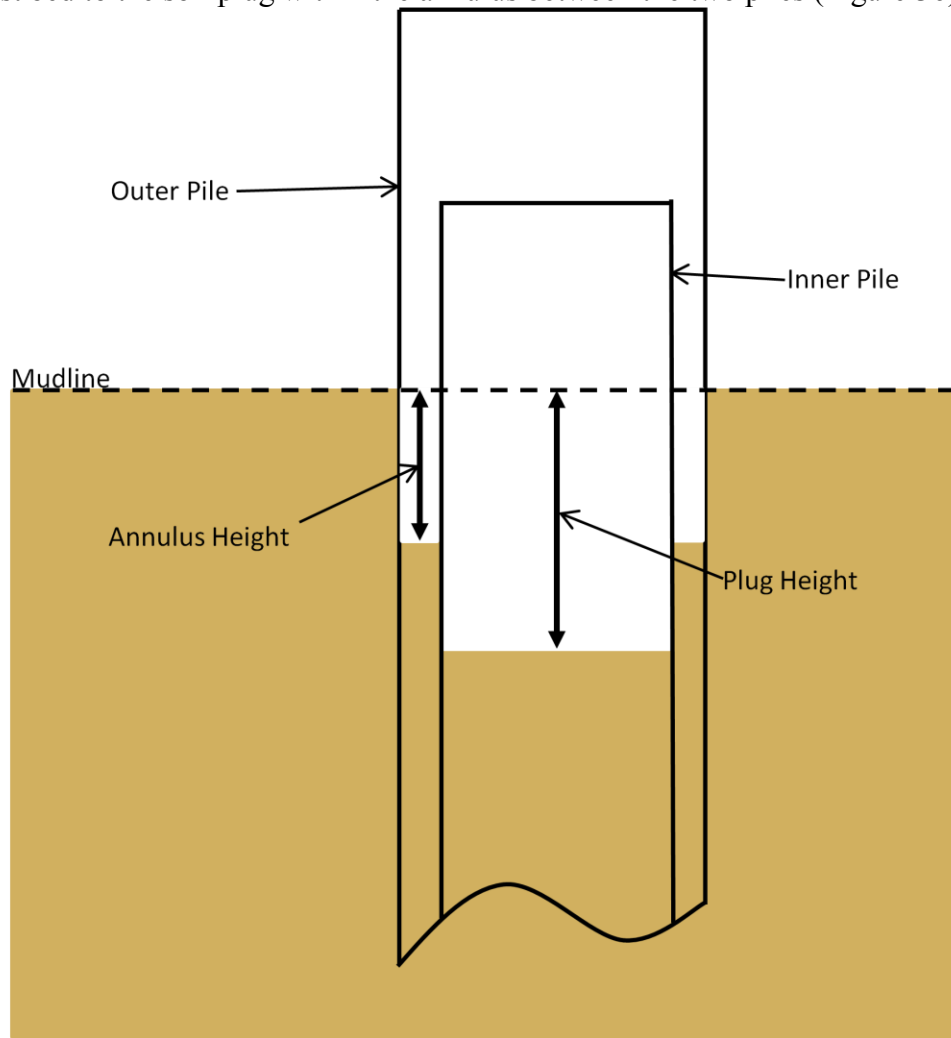


Figure 36 Measurements taken after pile Installation

4.6 PILE PULL-OUT

Piles were removed in the same manner for both single pile and pile over pile testing. The motor was lowered so that the load cell could be connected to the pile installed in the test bed. Once connected, the pile was pulled out of the test bed using a constant rate of displacement of 0.8 in/sec (to match the rate used for the T-bar), and continuous readings were taken from the load cell and the LMT. The motor and readings were stopped once the pile was fully pulled out from the test bed.

This procedure was followed for both monopile and pile over pile removal, but for the PoP test series, was only performed on the outer pile.

4.7 SEISMIC READINGS

Seismic readings were conducted using two separate methods, the pile as a source, and the sensor as the source.

To use the geophone as a source required an input voltage to displace, or ping, so to speak, the outer geophones in the array. The outer geophones were used as a source for the inner spiraled array of geophones at each sensor layer (Figure 4.29). The resulting wave arrival times that were registered on the other side of the array could be used with the known spacing of the geophones to determine the shear wave velocities in the kaolinite. This method of crosshole testing was used every day in the six days following the test bed creation and prior to the 4 inch pile installation.

To use the pile as the source, an instrumented hammer connected to the data acquisition system was tapped on the pile's tip that stuck up. The subsequent wave traveled down the pile and outward to all of the sensors. Once again, using the known

spacing of the sensors and the pile along with the shear wave arrival times at each sensor, the shear wave velocity could be determined. The pile was only used as a source after the 4 inch pile was installed in the seismic test bed.

Prior to any testing in the actual test bed, the travel time through the actual system (cables, geophones, DAQ, pile, electronic devices) had to be accounted for. For the pile as a source, this was accomplished by securing one of the geophone sensors to the 4 inch pile at each depth location the pile was going to be tested at. A test was then run using the instrumented hammer as the source at the top of the pile. The time difference between the hammer strike and the first shear wave arrival was then used as the calibration time for each depth.



Figure 37 Calibration of the geophone with the pile as source configuration

For the calibration time for the tests using a geophone as the source, two geophones were connected directly to each other. The source geophone was then "pinged." The time difference between the source ping and the first shear wave arrival time was used as the calibration time for all geophone source tests (Figure 37).

All seismic tests were performed as described, and subsequently corrected for the calibration times determined before testing.

4.8 CONCLUSION

All testing pile testing followed the same steps. First, a normally consolidated test bed was constructed, and allowed to consolidate, with a T-bar test being run the day of the first pile installations. Next, the inner piles were installed and allowed to set up. After set up, if conducting pile over pile testing, the outer piles were installed. These piles were then removed over a certain period of time, and a final T-bar test was conducted in most cases.

For the seismic testing, a normally consolidated test bed was constructed, this time, with geophone sensors being carefully placed at set intervals and spacings. A single T-bar test was run after construction, and geophone readings were taken daily throughout the consolidation period. After the consolidation period, a second T-bar test was conducted, and single pile was installed in the center of the test bed. Geophone readings were again taken daily following pile installation.

Chapter 5 RESULTS

5.1 INTRODUCTION

Before testing, a series of single pile setup tests were conducted to determine the setup time required for the inner piles prior to installation of the outer piles. This was conducted with a set of five 1.5 inch diameter piles in one test bed, and three 3 inch diameter piles in a second test bed.

After determination of the pile setup time, three pile over pile test series were conducted for the three pile diameter configurations specified: (1) 2 inch over 1.5 inch, (2) 3 inch over 2 inch, (3) 4 inch over 3 inch. Additionally, based on the results from the first pile over pile test series, a retest of test series 1 was conducted with spacers around the top of the inner 1.5 inch diameter piles.

5.2 SINGLE PILE SETUP TESTS

Before the first pile over pile tests were conducted, an initial test bed, Test Bed 1, was constructed as described for the purpose of running setup tests on the 1.5-inch diameter piles. The T-bar results, measured just prior to the pile installation, showed a normally consolidated profile (Figure 38). After the 1.5-inch piles were installed, the piles were pulled out from the test bed at intervals of 2 hours, 12 hours, 24 hours, 48 hours, and 96 hours (Figure 39 and Figure 40). The push-in resistance provides a local measurement of the undrained shear strength at the exact location of each pile; therefore, the ratio of the peak pull-out resistance to the peak push-in resistance provides a useful metric to isolate the effect of set-up time from other sources of variability (Figure 41).

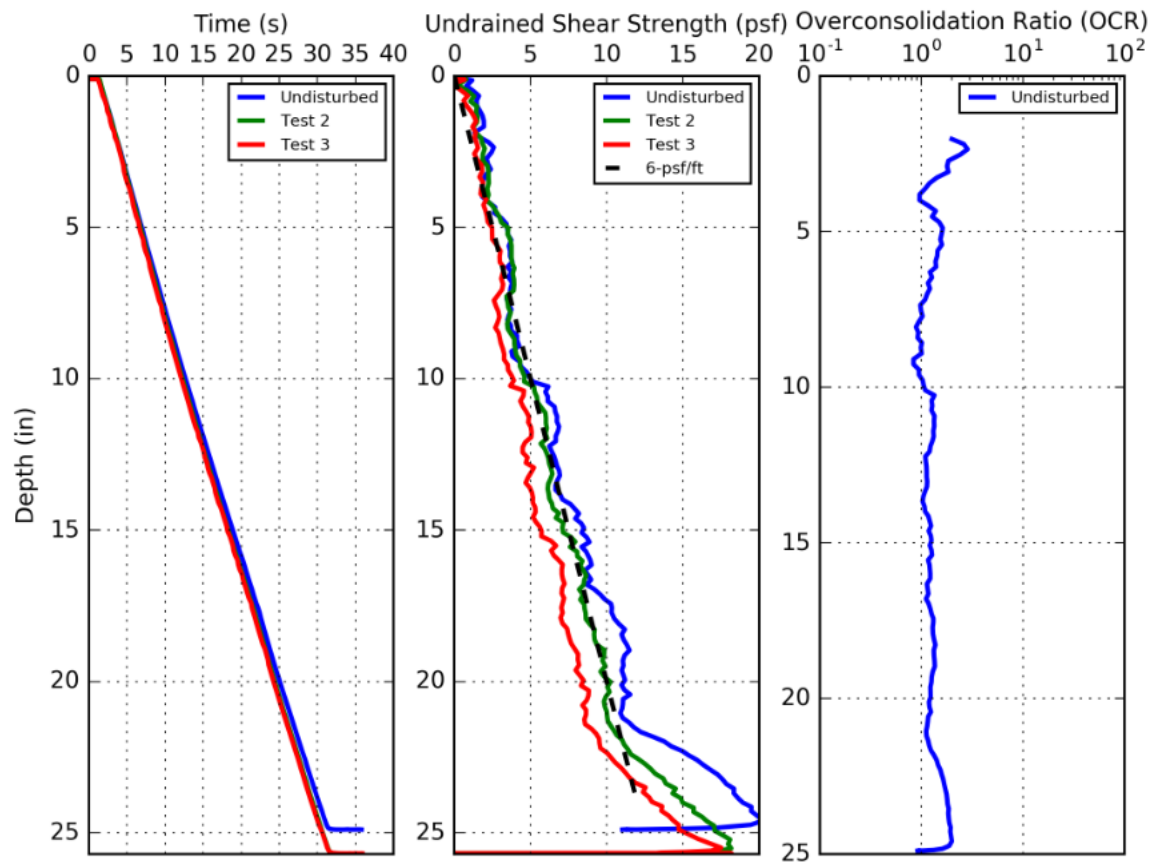


Figure 38 T-bar Results for Test Bed 1 before pile installation

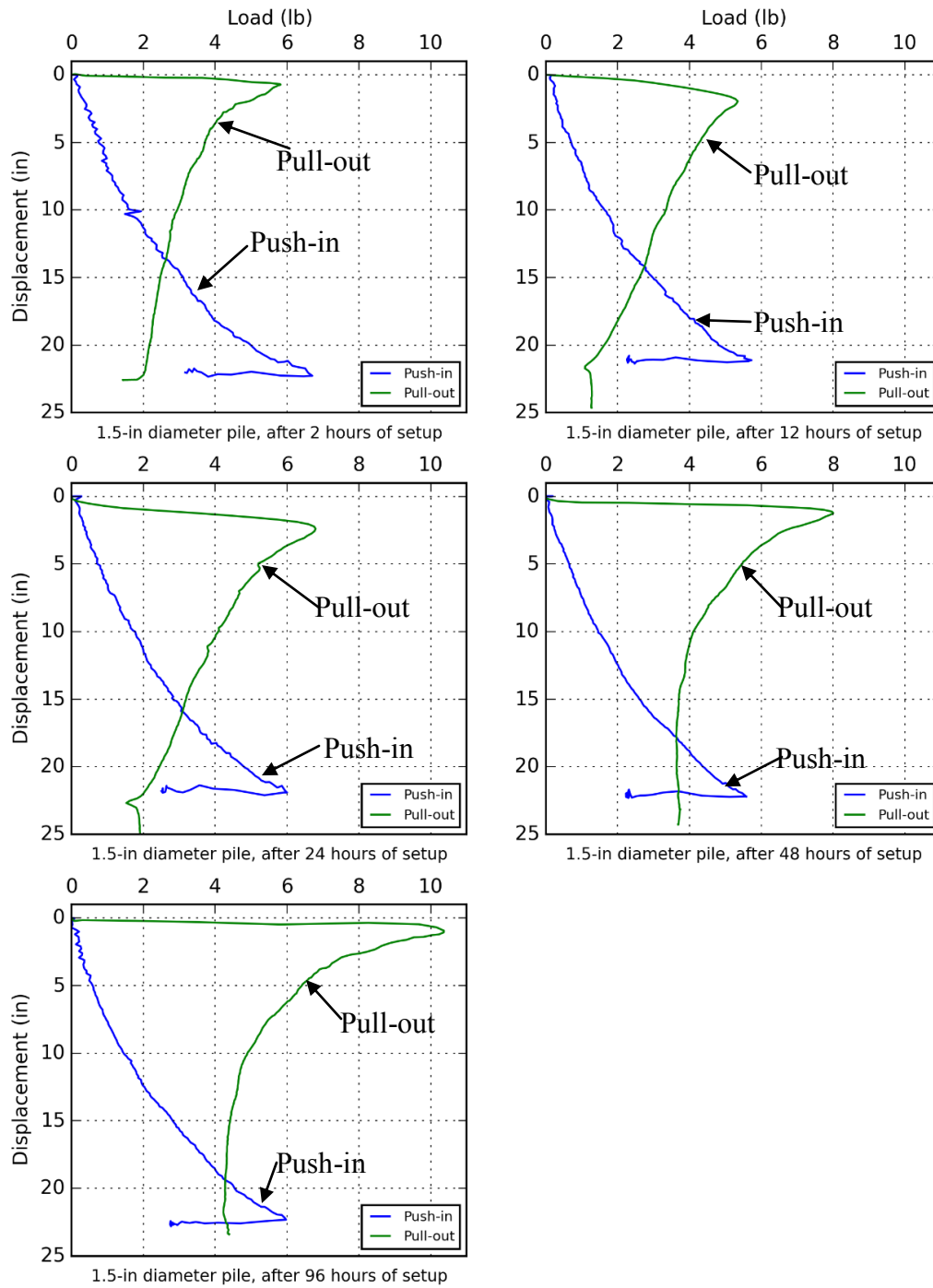


Figure 39 Results from Setup Tests of 1.5-inch piles

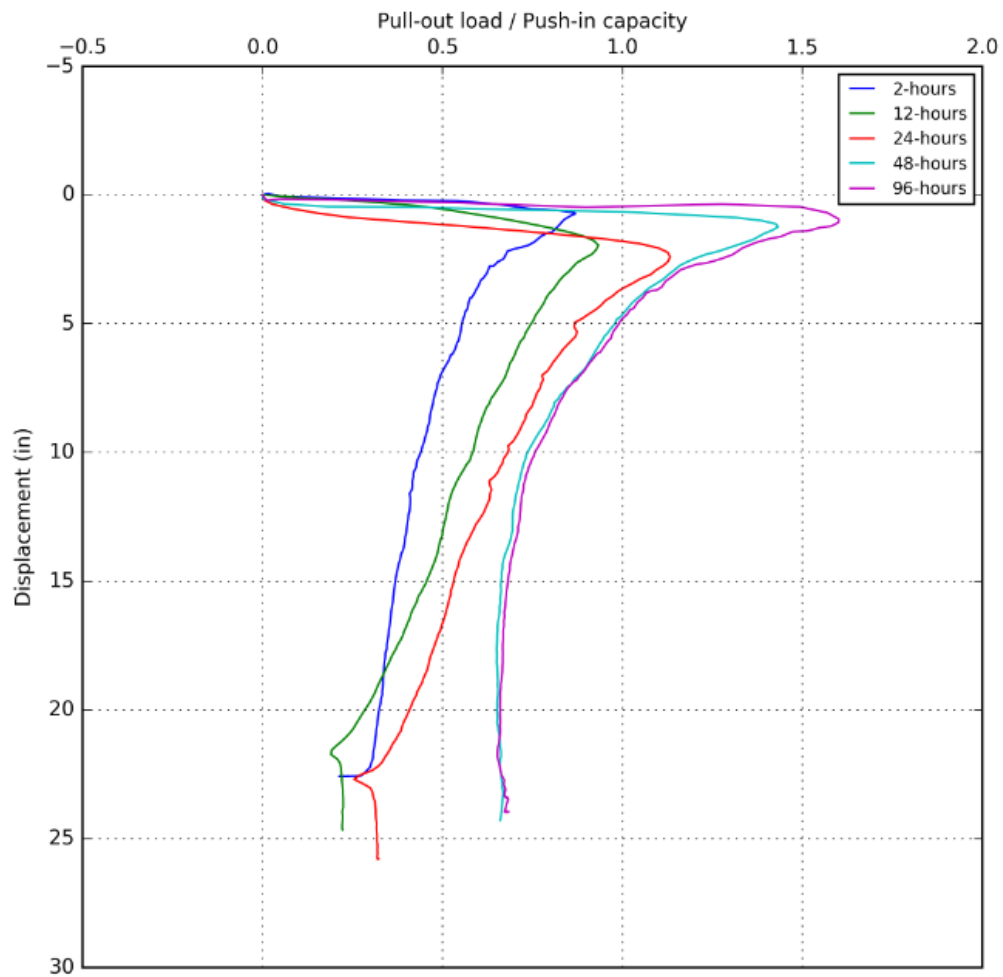


Figure 40 Pull-out load/ Push-in capacity versus pull-out Displacement

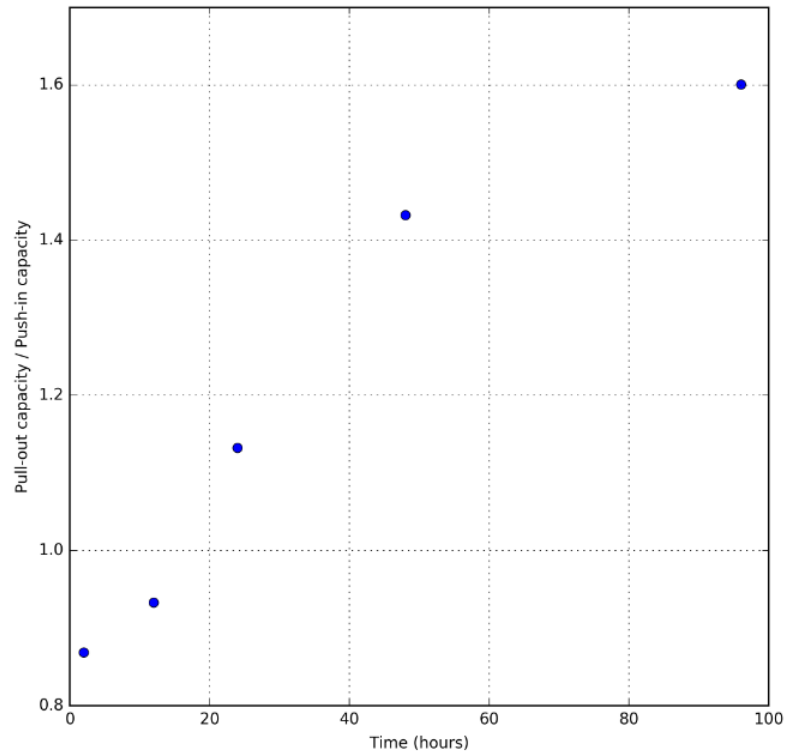


Figure 41 Pullout capacity/push-in capacity versus Time for 1.5-inch diameter piles

A similar series of tests was run on the 3-inch diameter piles in a separate normally consolidated kaolinite test bed (Figure 42). For this series, three tests were run with a pile being pulled out at the 24, 48, and 96 hour intervals. The push in and pullout results are shown in Figure 43 and the ratio of the peak pull-out resistance to the peak push-in resistance is shown in Figure 44.

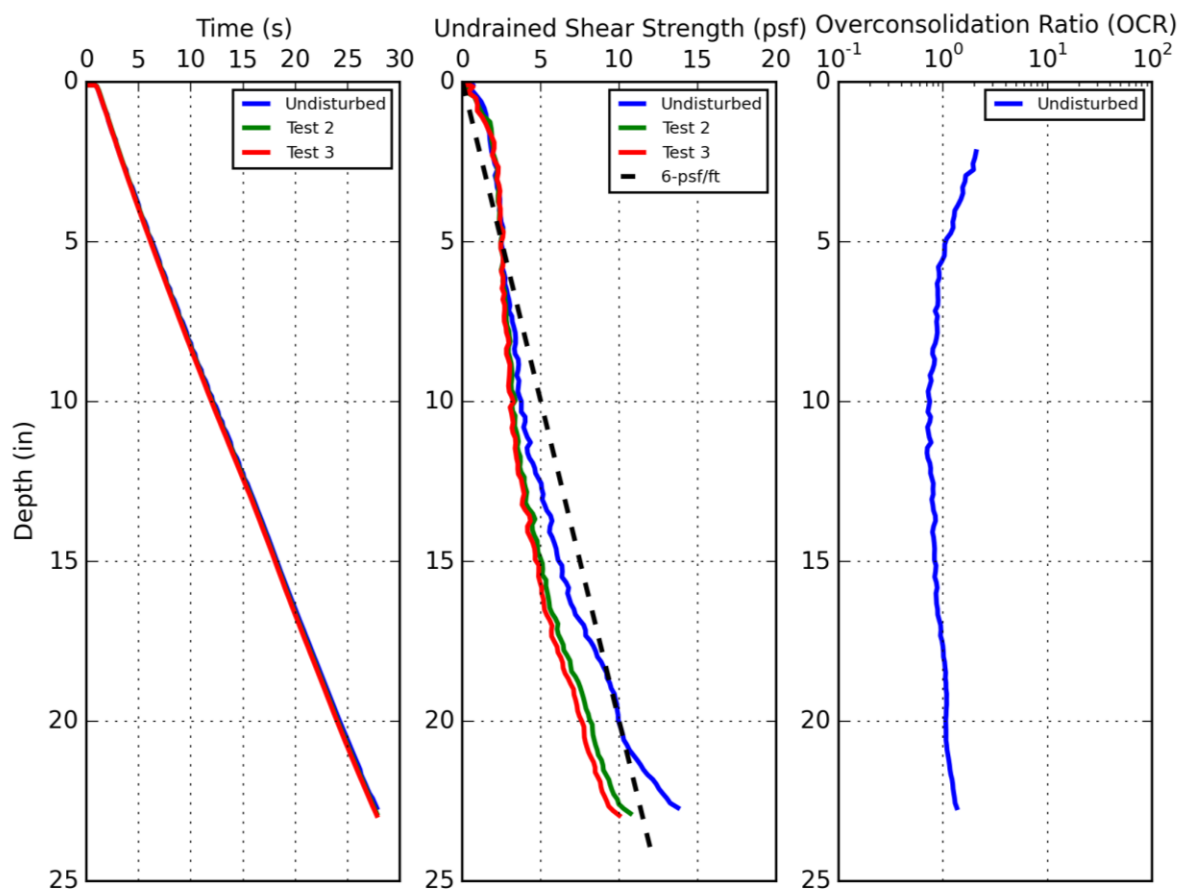


Figure 42 T-bar Results for setup tests of 3-inch diameter piles, Test Bed 5

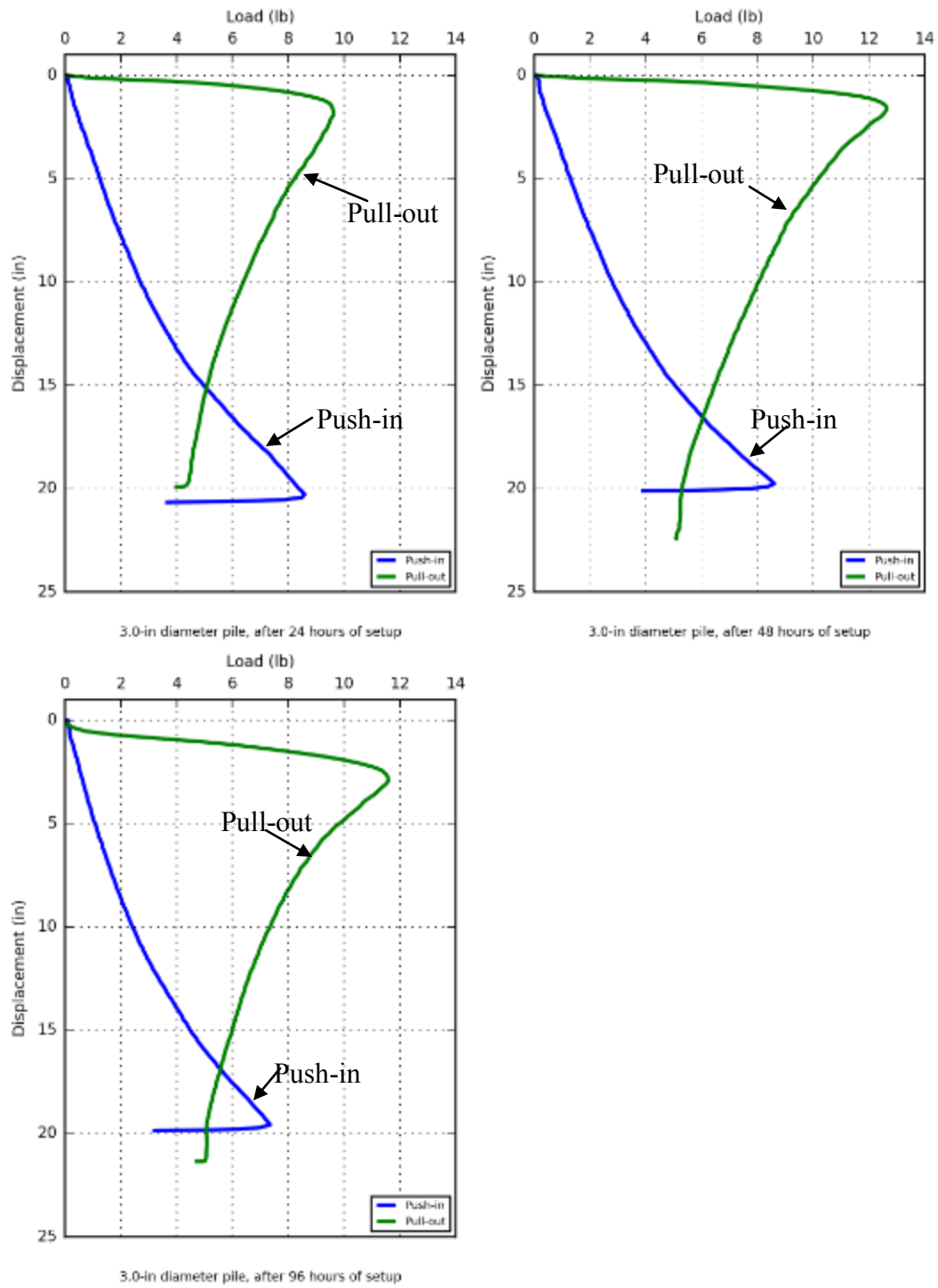


Figure 43 Continued next page.

Figure 43 Results from setup tests of 3-inch Piles

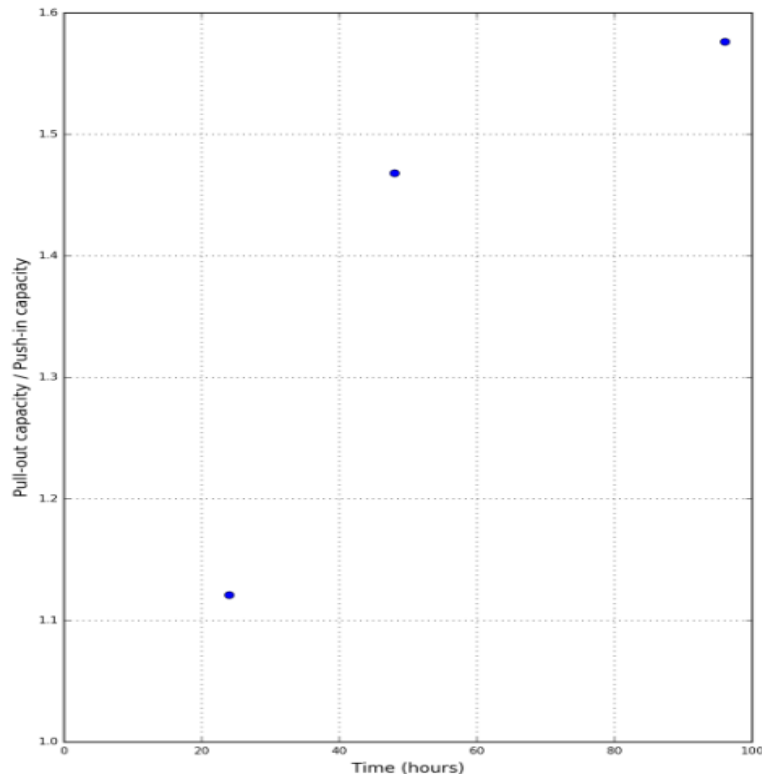


Figure 44 Pullout capacity/push-in capacity vs. time for 3-inch diameter piles

Since about 90-percent of the set-up occurs within 48 hours in both sets of tests (Figure 41 and Figure 44), a setup time of 48 hours was used in subsequent testing.

5.3 PILE OVER PILE TESTS

After a setup time of 48 hours, the outer piles were installed over the inner piles, and the series of pile over pile testing was carried out. As with the setup tests, normally consolidated kaolinite test beds were constructed in barrels. The tests were all run with three pile over pile tests and one control free field test to compare the results to in each test bed (Figure 45).



Figure 45 Typical Pile configuration used for PoP and setup testing

The results of the three pile over pile test series configurations as well as the retest of Test Series 1 are presented and summarized below.

5.3.1 Test Series 1: 2-inch over 1.5-inch

A third test bed, Test Bed 3, was created for this series of tests. A T-bar test was run after the bed was allowed to consolidate for 6 days (Figure 47).

After the T-bar was run, three 1.5-inch piles were installed and allowed to setup over 48 hours. After 48 hours of set-up, the 2-inch piles were installed over the three 1.5-inch piles, and a free field "control" 2-inch pile was installed without an inner pile (Figure 48). In every test with a 1.5-inch inner pile, the outer pile contacted the inner pile as indicated by contact observed above the mudline after the pile was installed (Figure 46).



Figure 46 Example of inner pile making contact with outer pile visible from the surface

An increase in the push-in resistance compared to the free-field case was observed to occur when there was pile-to-pile contact (Figure 46). Plug depths were measured from

the mudline to the soil level inside the pile within the inside diameter of the inner pile and within the annulus between the inner and outer pile for the outer pile (Table 6). Finally, pull-out tests were conducted for all four 2-inch diameter piles after varying periods of set-up (Figure 49). A T-bar test performed after the last pull-out test showed how the undrained shear strength increased over the four days of testing (Figure 50).

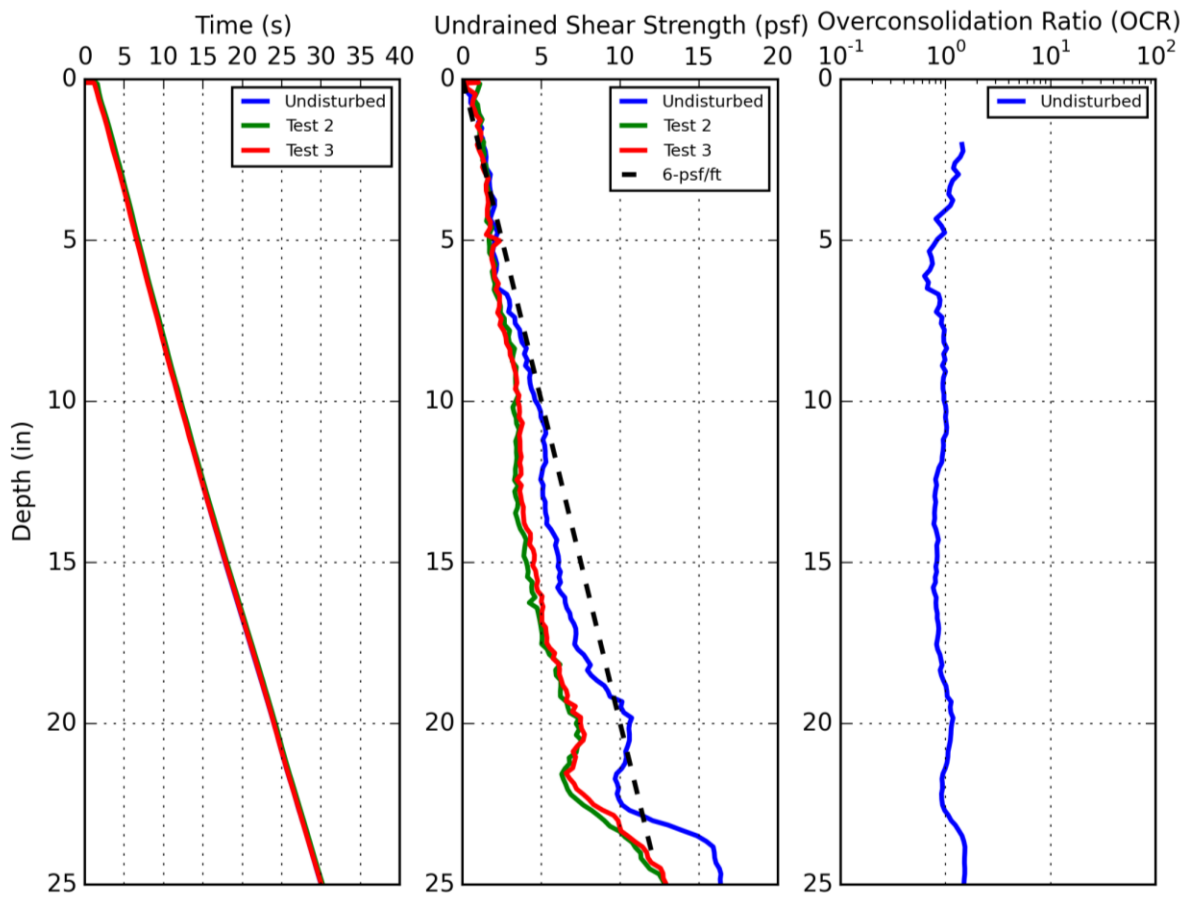


Figure 47 T-bar test results for Test Series 1, Test Bed 3 before PoP tests were run

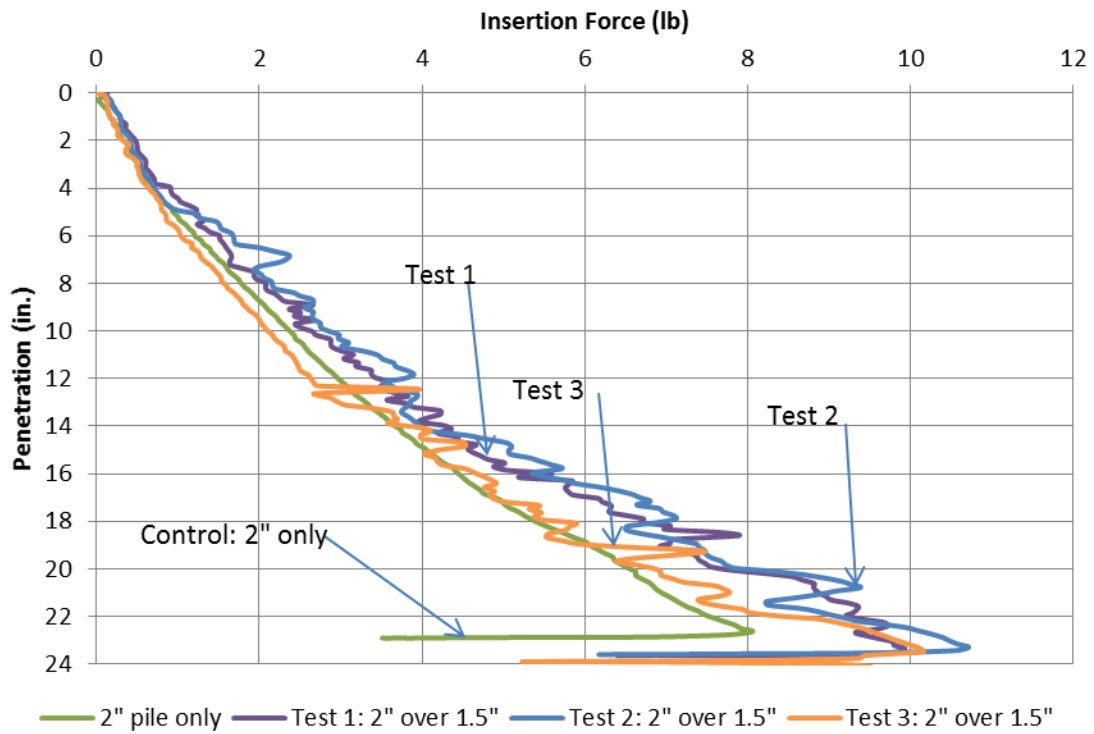


Figure 48 Push in capacities of 2-inch piles over 1.5-inch piles

		Test Series 1 (26 inch depth of soil)			
		24 hour	48 hour	96 hour	Control
Inner Pile (1.5-inch)	Pile Length (in.)	36	36	36	-
	Embedment Depth (in.)	24	24	24	-
	Plug Depth (in.)	7	7	7	-
Outer Pile (2-inch)	Pile Length (in.)	42	42	42	30
	Embedment Depth (in.)	23.5	23.8	24	22.5
	Plug Depth (in.)	-	7	7	2

Table 6 Measurements from Test Series 1

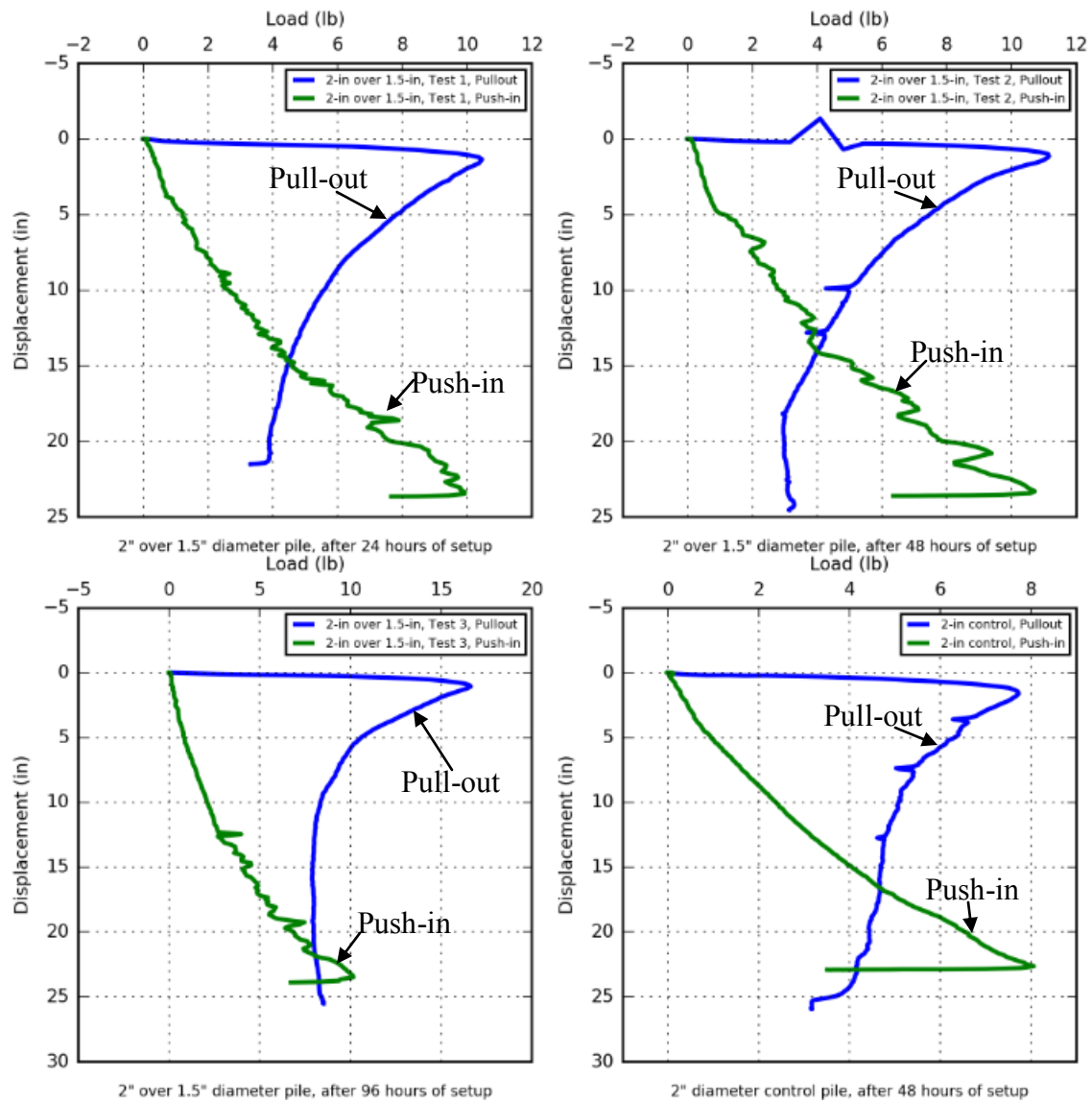


Figure 49 Push in vs. Pullout results from Test Series 1

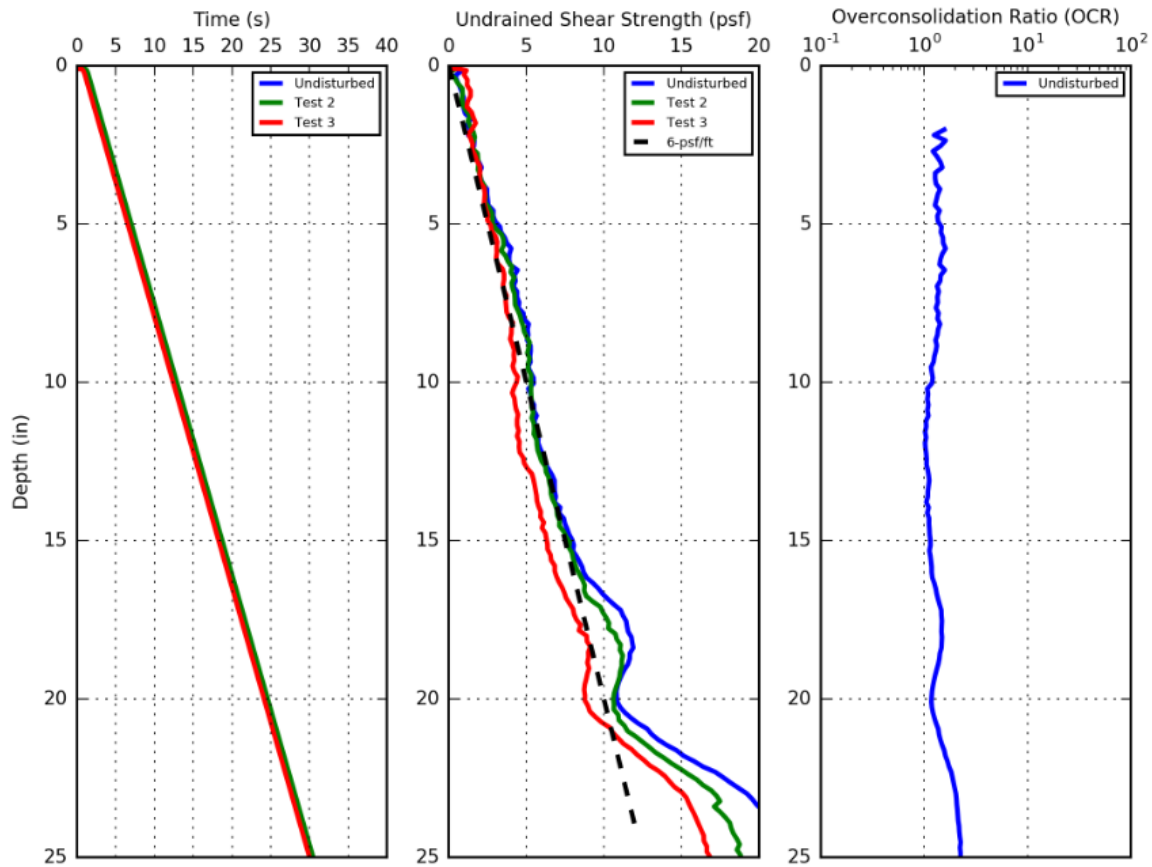


Figure 50 T-bar test results for Test Series 1, Test Bed 3 after PoP tests were run

5.3.2 Test Series 1 Retest: 2-inch over 1.5-inch

The outer piles made contact with the inner piles for every one of the PoP tests that were performed in Test Series 1 (2-inch over 1.5-inch diameter piles). The outer pile has a clearance of only 0.2 inches between its inside wall and the outside wall of the inner pile, meaning small deviations from plumb can cause the two piles to contact during installation. In order to mitigate contact from happening, each inner 1.5-inch diameter pile was fitted with two spacers. These 0.175-inch thick spacers were set 4 inches apart above the mudline to provide moment resistance to the outer pile rotating relative to the

inner pile; they were made by wrapping duct tape and covering it in a Teflon sheet to minimize friction (Figure 51).



Figure 51 Spacers used on 1.5-inch piles for retest of Test Series 2

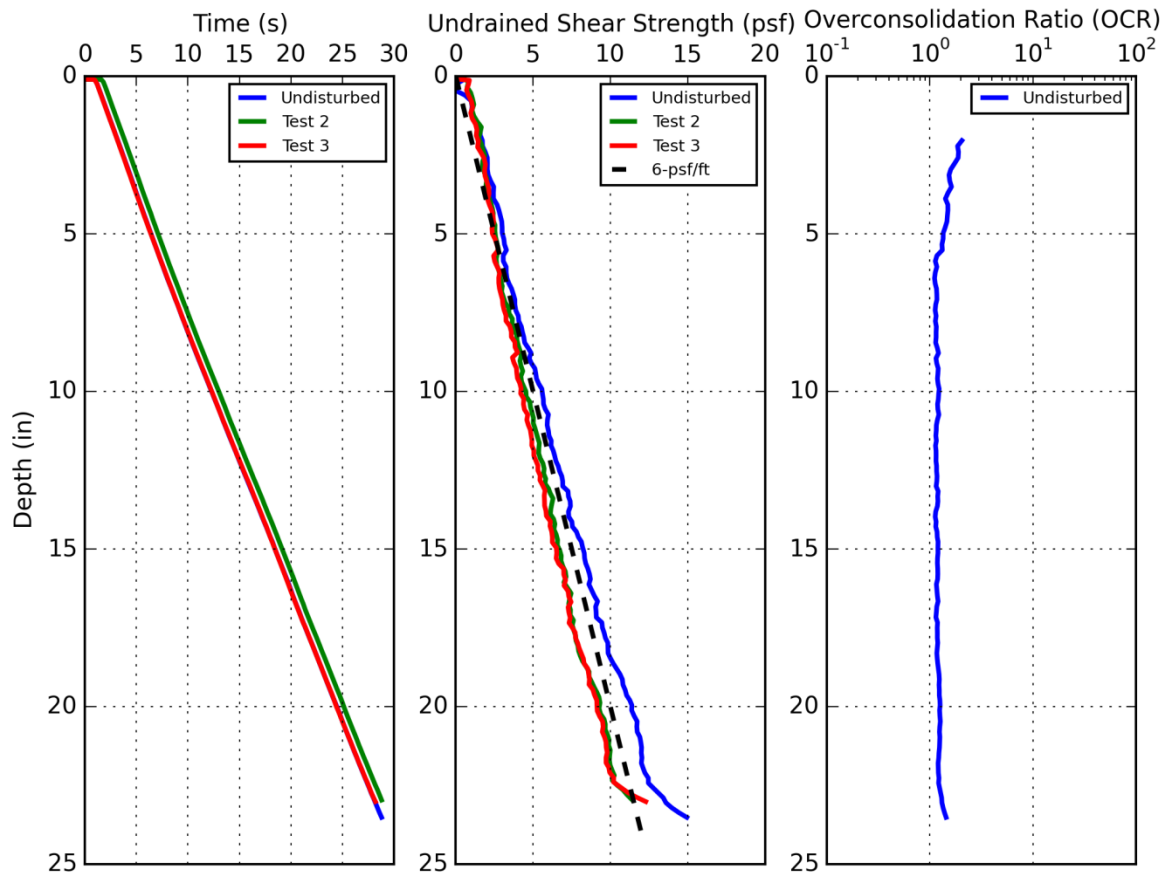


Figure 52 T-bar test results for Test Series 1 retest, Test Bed 8 before PoP tests were run

The retest of Series 1 was performed in Test Bed 8 (Figure 52). Three 1.5-inch piles were installed and allowed to setup over 48 hours. After 48 hours, the 2-inch piles were installed over the three 1.5-inch piles (Table 7 and Figure 53). Due to the spacers, it was not possible to measure the depth to the annulus between the piles used for PoP. Additionally, a test in air was conducted with the 2-inch pile installed over the 1.5-inch pile to establish the minimum possible resistance from the spacers (Figure 53). Finally,

pull-out tests and a T-bar test after pull out was completed were conducted (Figure 54 and Figure 55).

		Test Series 1 (24 inch depth of soil)			
		24 hour	48 hour	96 hour	Control
Inner Pile (1.5-inch)	Pile Length (in.)	30	30	30	-
	Embedment Depth (in.)	21.5	21.5	21.5	-
	Plug Depth (in.)	9	9	9	-
Outer Pile (2-inch)	Pile Length (in.)	36	36	36	30
	Embedment Depth (in.)	22.2	22.5	22	23.2
	Plug Depth (in.)	-	-	-	5

Table 7 Measurements from Test Series 1 retest

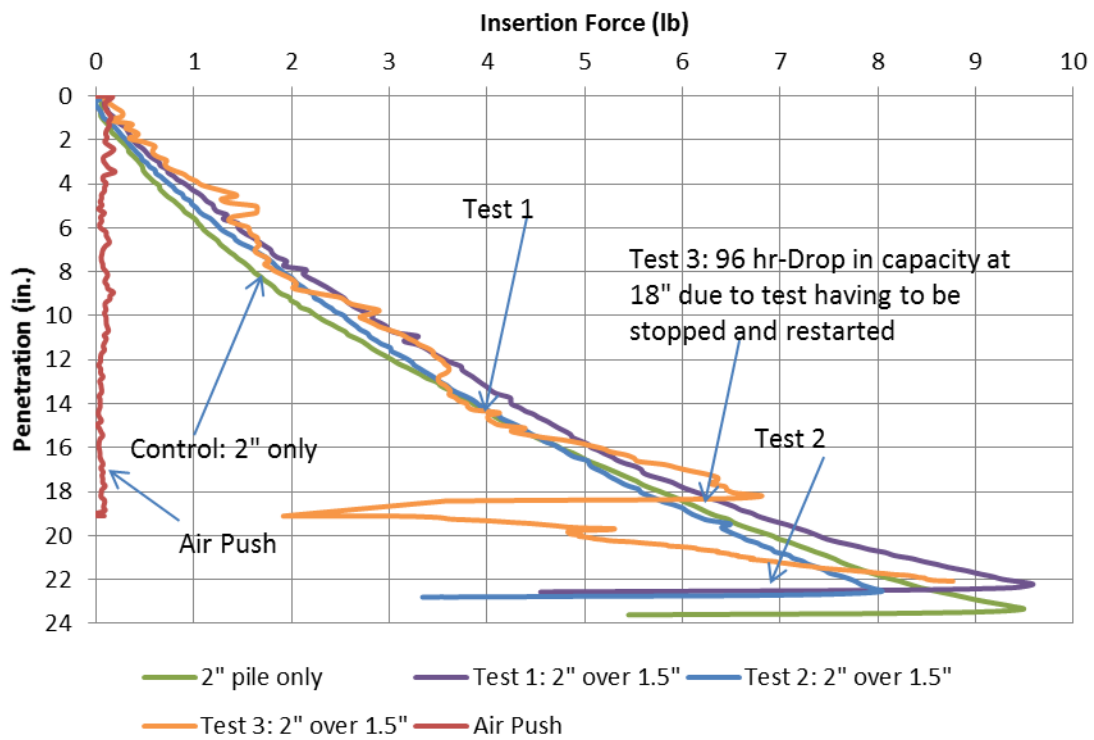


Figure 53 Push in capacities of 2-inch piles over 1.5-inch piles with spacers

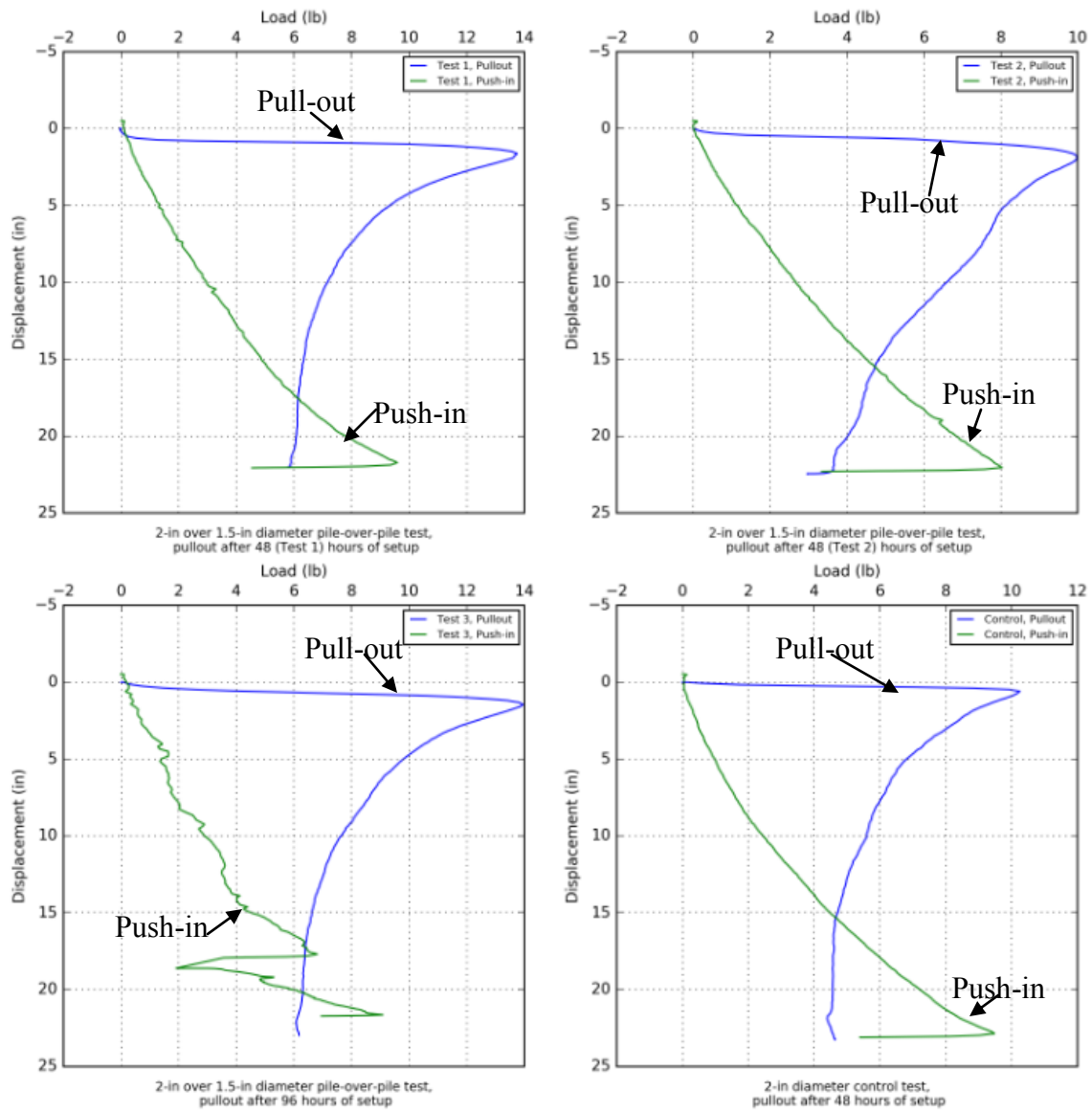


Figure 54 Push in vs. Pullout results from retest of Test Series 1 with spacers

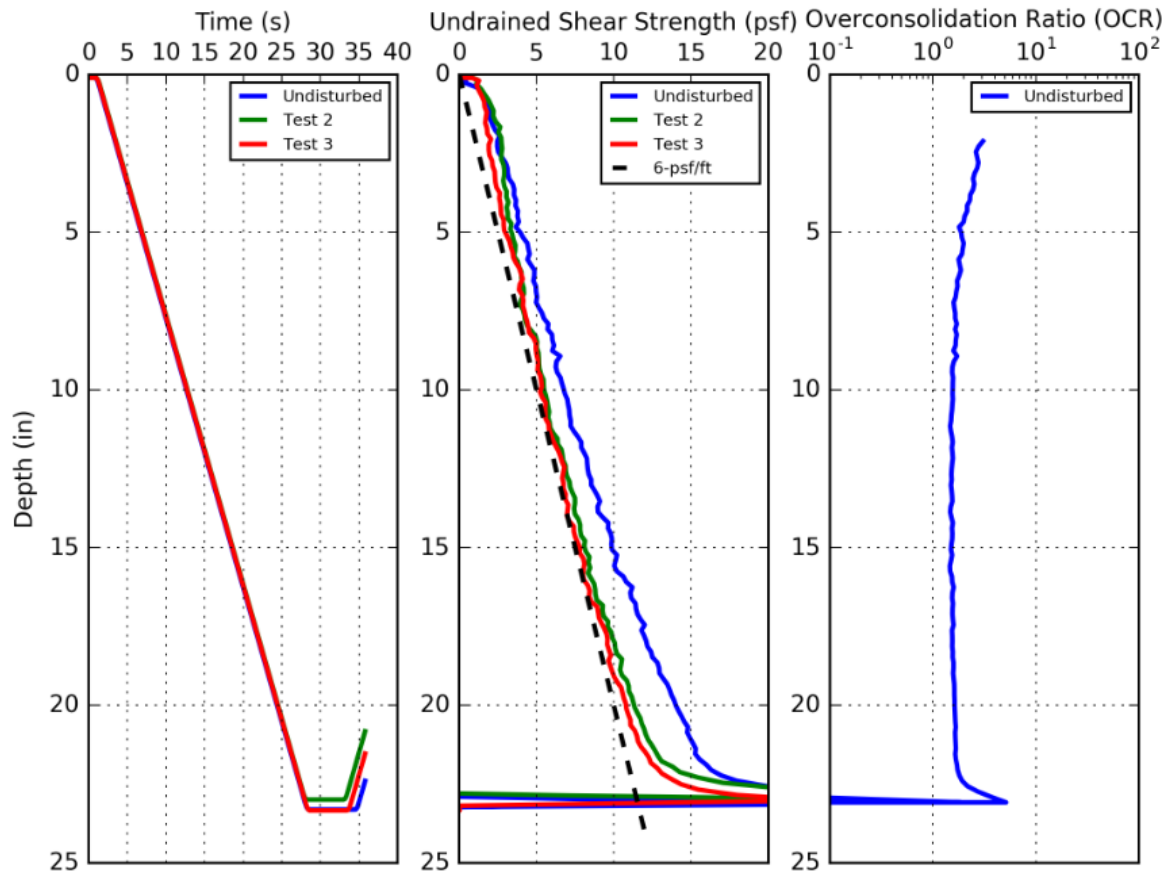


Figure 55 T-bar test results for retest of Test Series 1, Test Bed 8 after PoP tests were run

5.3.3 Test Series 2: 3-inch over 2-inch

The fourth test bed constructed was used for the second series of pile over pile tests. After the T-bar test (Figure 56), three 2-inch piles were installed and allowed to setup over 48 hours. After 48 hours, the 3-inch piles were installed over the three 2-inch piles. Additionally, a free field "control" 3-inch pile was installed (Table 8). In this series of tests, none of the outer piles were observed to have come into contact with the inner piles, and the push-in resistance for the PoP cases align with the control case with the

exception of the final 3-inches of penetration in Test 1 (Figure 57). After set-up, pull-out tests were performed (Figure 58) and a final T-bar test was conducted (Figure 59).

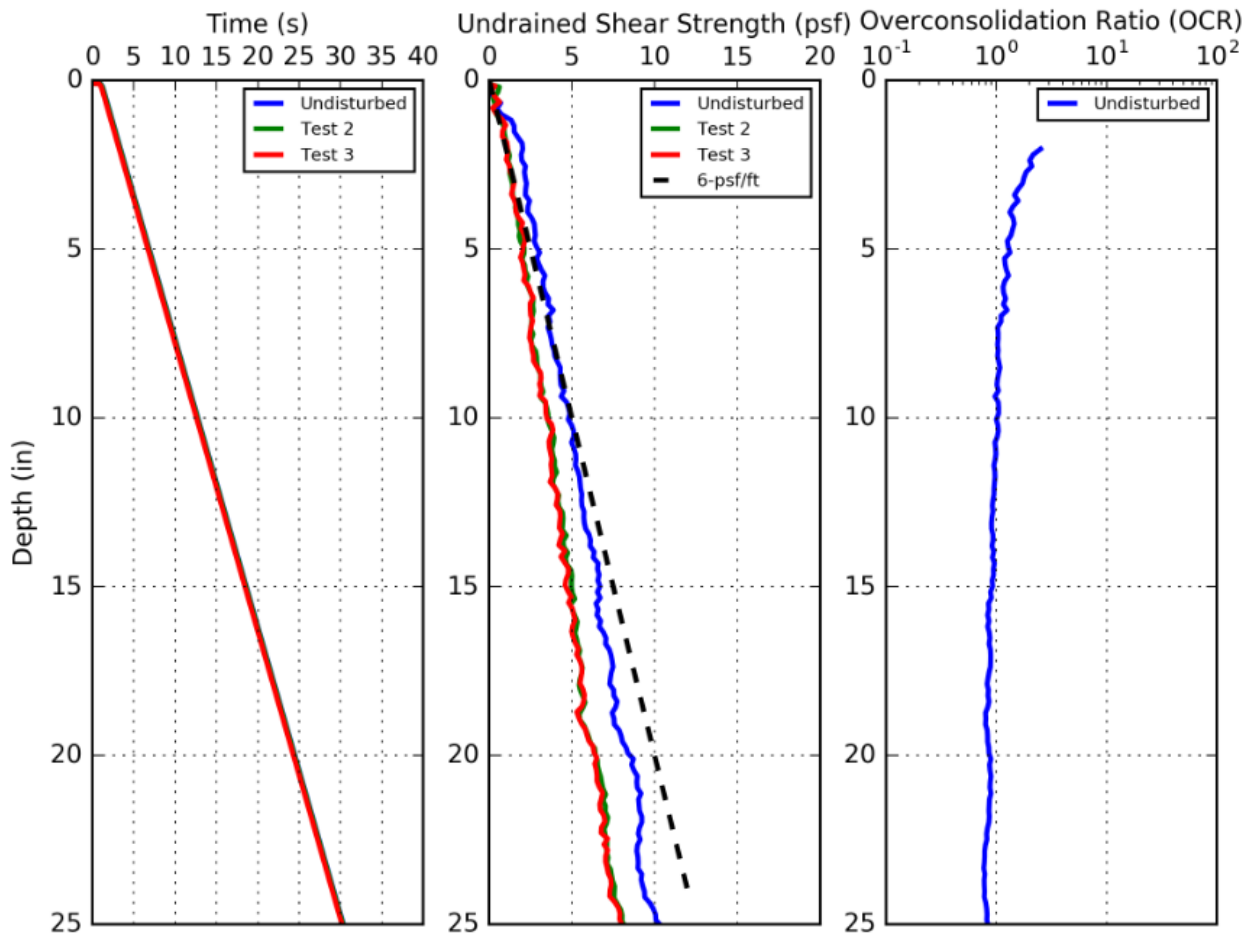


Figure 56 T-bar test results for Test Series 2, Test Bed 4 before PoP tests were run

		Test Series 2 (26 inch depth of soil)			
		24 hour	48 hour	96 hour	Control
Inner Pile (2-inch)	Pile Length (in.)	30	30	30	-
	Embedment Depth (in.)	24.2	24	23.8	-
	Plug Depth (in.)	5.2	5	5	-
Outer Pile (3-inch)	Pile Length (in.)	36	36	36	36
	Embedment Depth (in.)	24	23	23	24
	Plug Depth (in.)	8	7	7	2

Table 8 Measurements from Test Series 2

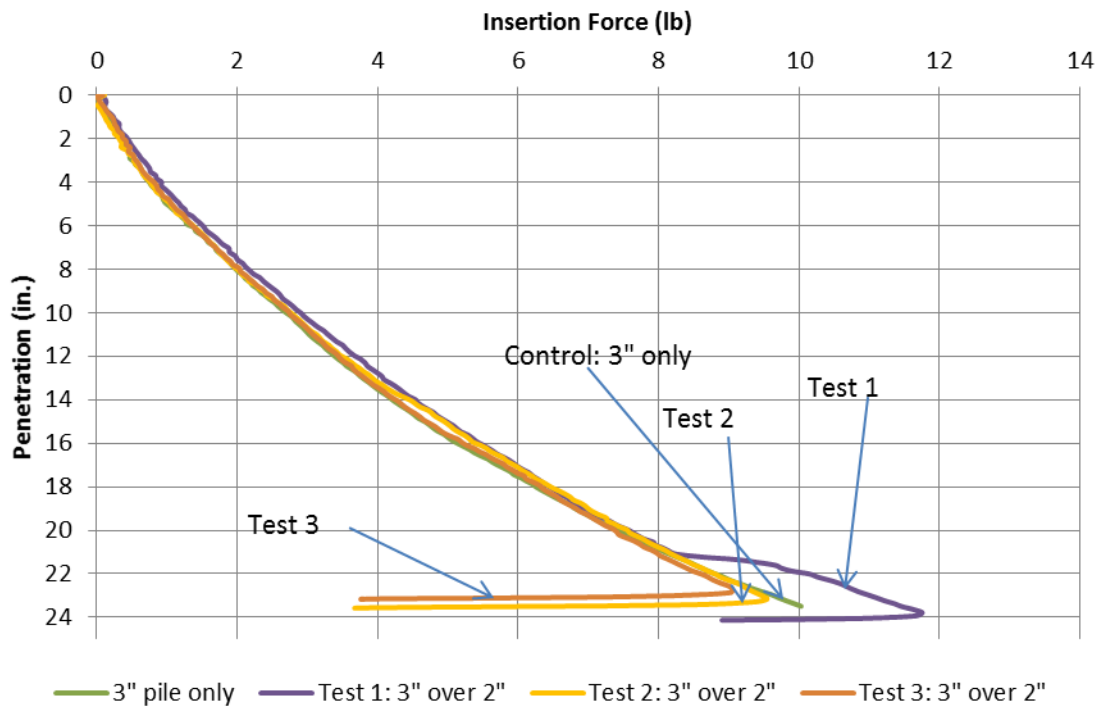


Figure 57 Push in capacities of 3-inch piles

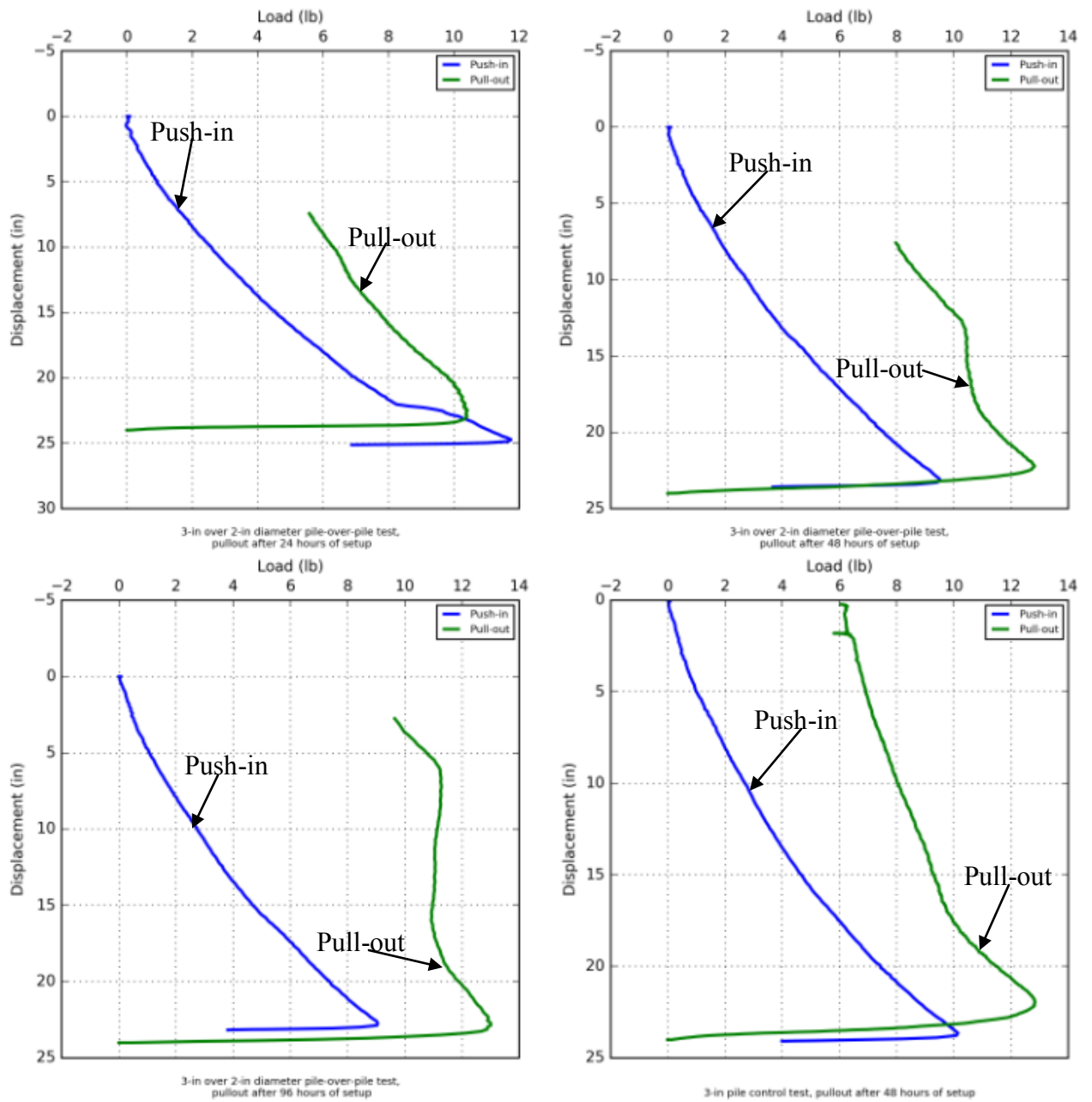


Figure 58 Push in vs. Pullout results from Test Series 2

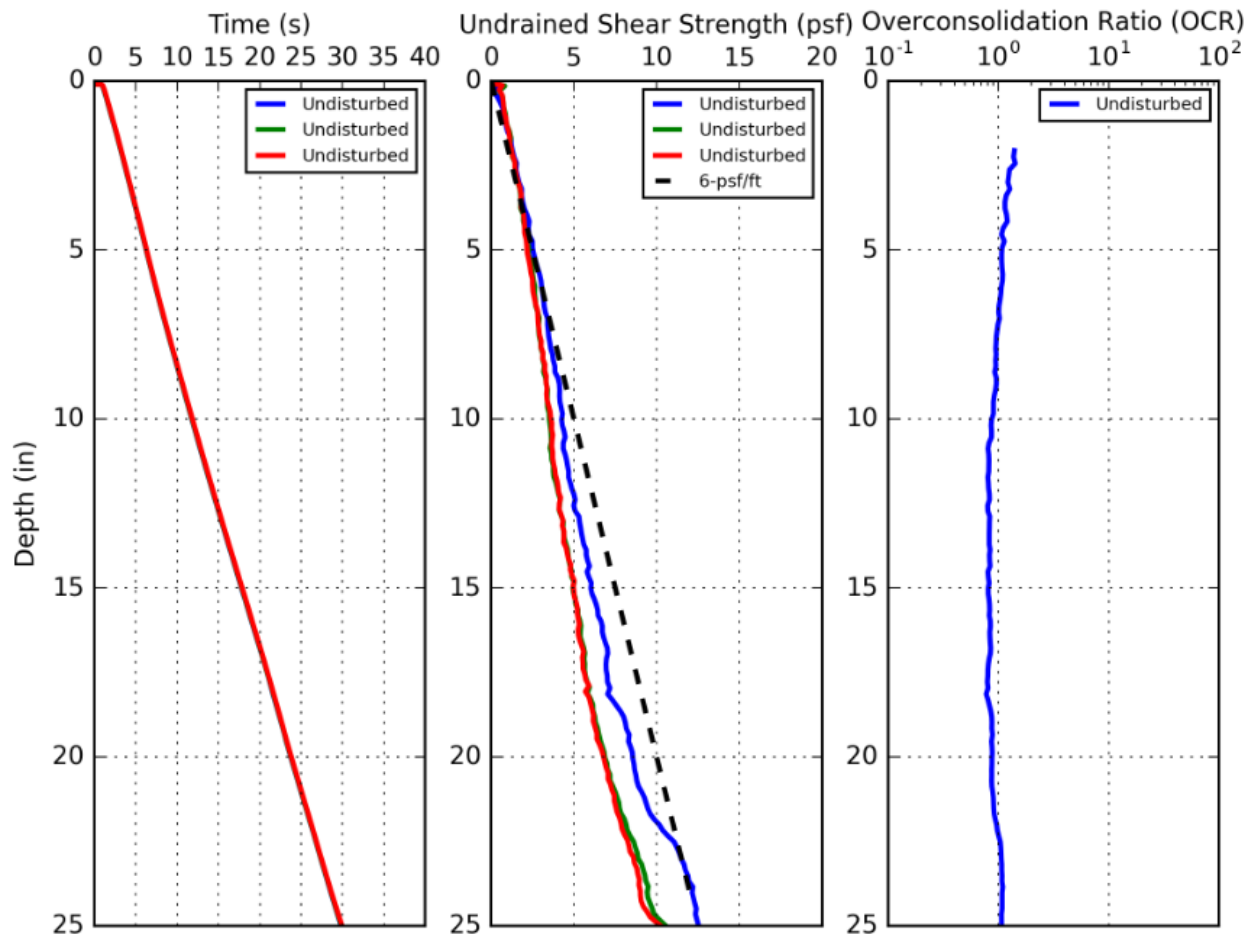


Figure 59 T-bar test results for Test Series 2, Test Bed 4 after PoP tests were run

5.3.4 Test Series 3: 4-inch over 3-inch

The sixth test bed constructed was used for the third series of pile over pile tests. After the T-bar test (Figure 60), three 3-inch piles were installed and allowed to setup over 48 hours. After 48 hours, the 4-inch piles were installed over the three 3-inch piles (Figure 61). Additionally, a free field "control" 4-inch pile was installed (Table 9). In this series of tests, two of the three outer piles came into noticeable contact with the inner piles as observed after the test from looking inside the outer pile, and sudden increases in

the push-in resistances compared to the control case were observed (Tests 1 and 2 in Figure 61). After varying periods of set-up, pull-out tests were performed (Figure 62).

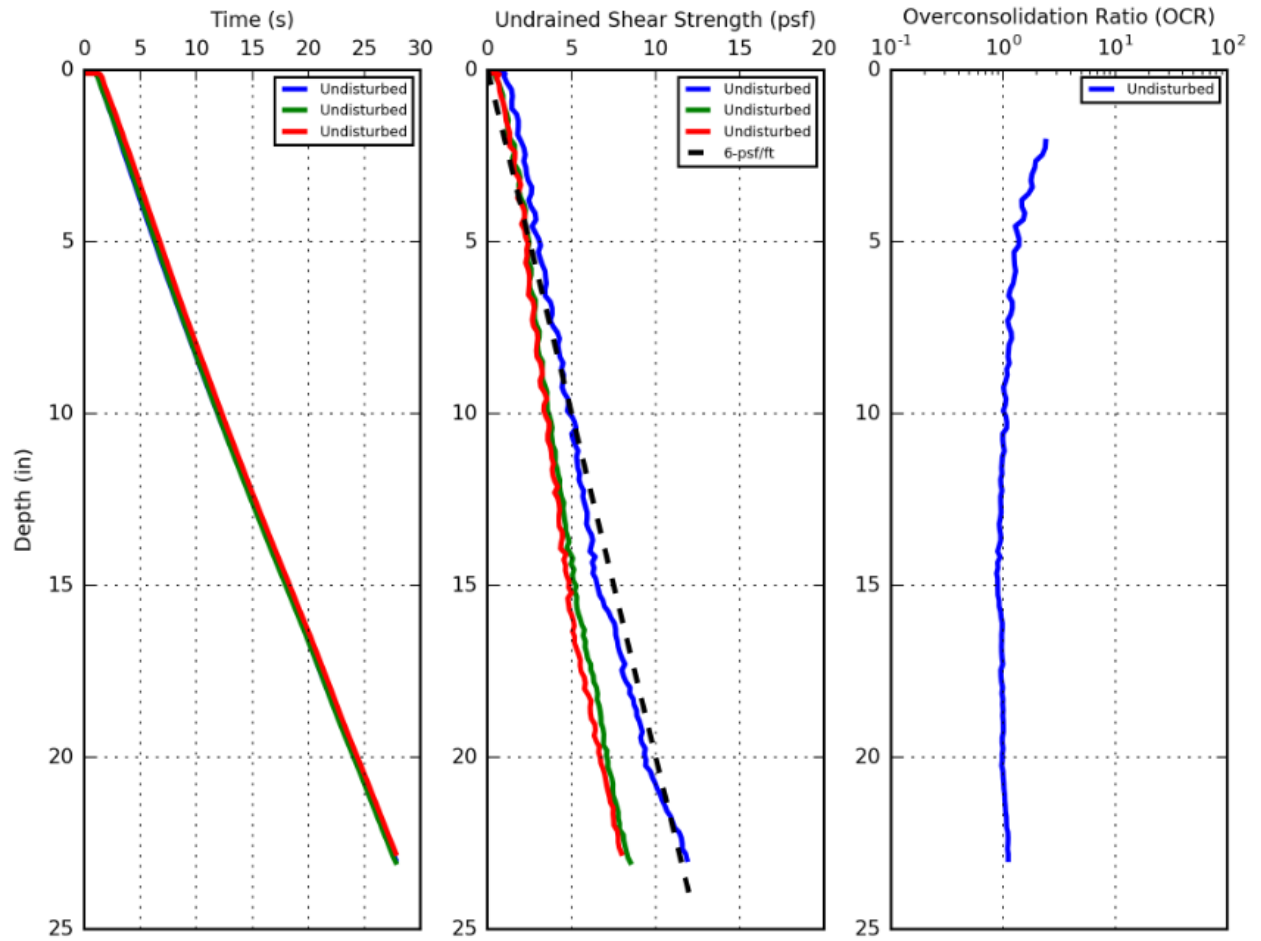


Figure 60 T-bar test results for Test Series 3, Test Bed 6 before PoP tests were run

		Test Series 3 (26 inch depth of soil)			
		24 hour	48 hour	96 hour	Control
Inner Pile (3-inch)	Pile Length (in.)	30	30	30	-
	Embedment Depth (in.)	24	24	24	-
	Plug Depth (in.)	3.5	3.5	3.4	-
Outer Pile (4-inch)	Pile Length (in.)	36	36	36	36
	Embedment Depth (in.)	22	22	22.5	22.5
	Plug Depth (in.)	6	6	6	1.5

Table 9 Measurements from Test Series 3

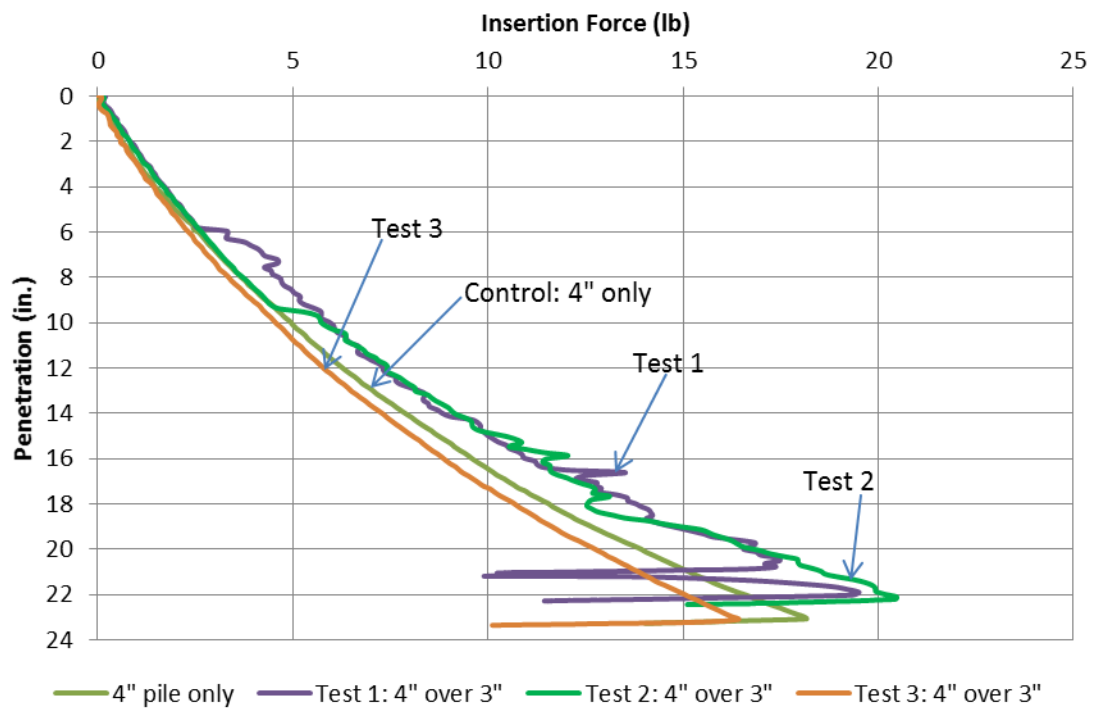


Figure 61 Push in capacities of 4-inch piles

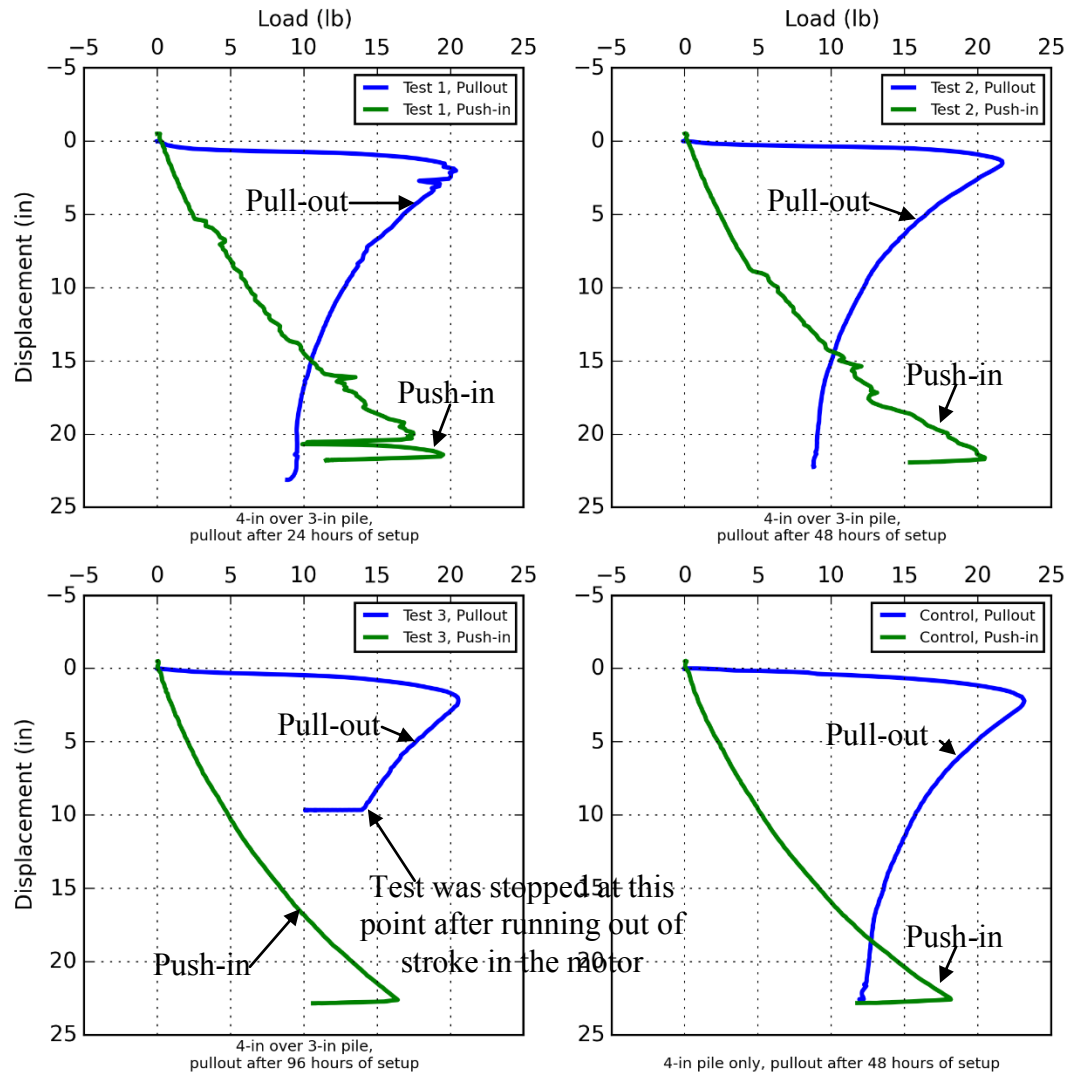


Figure 62 Push in vs. Pullout results from Test Series 3

5.4 CONCLUSION

All push in tests were conducted according to the methodology, and the raw results were presented without modification. Due to pile contact in all pile over pile tests in Test Series 1, it was necessary to conduct a retest, using spacers at the top of the piles to ensure that pile to pile contact was avoided.

All pile pull-out tests were conducted according to the methodology and the results from testing were presented without modification.

Chapter 6 ANALYSIS OF RESULTS FROM PILE OVER PILE TESTING

The results from the single pile setup tests and the pile over pile tests were analyzed and compared with theoretical models for the push-in resistance and pull-out capacity.

6.1 CORRECTING MEASURED LOAD FOR BUOYANCY

The raw data from the pile installation and the pile removal was given as a text file from the DAQ system described in Chapter 3. The raw values obtained from the system included both the effects of the pile soil interaction as well as the uplift due to buoyancy. While the data plotted in the results represents the pure output from the DAQ, to look at only the effects of the soil interaction with the pile, rather than the soil effects with buoyancy, the loads recorded by the DAQ had to be further corrected. This was done by using the following method:

$$P_{corrected} = P - (A_{pile} \times z \times \gamma_{kaol})$$

Where:

$P_{corrected}$ =Load corrected for buoyancy

P =Actual load recorded by DAQ

A_{pile} =Unplugged area of the pile

z =Embedment depth at point being corrected

γ_{kaol} =Unit weight of kaolinite (85 pcf)

While this correction was relatively small for all of the data sets obtained from pile testing, this correction was applied to all push in and pull out data set's load readings. All data present in the form of tables and figures reflects this correction.

6.2 PUSH-IN RESISTANCE

The push-in resistance was analyzed for the piles pushed into soil alone and for the piles pushed into soil over inner piles.

6.2.1 Push-In Resistance in Free-Field Soil

A simplified prediction of the net pile push-in resistance from API (API 2011)(i.e., the resistance provided by the shear strength of the soil) and modified for this testing, Q , is obtained as follows:

$$Q = Q_{side,remolded} + Q_{p,net}$$

where

$$Q_{side,remolded} = \sum_{Pile\ Length} \alpha S_{ur} C_{side} dL$$

S_{ur} = Remolded undrained shear strength from T-bar data

α = Empirical skin friction factor (assumed 1.0 for normally consolidated clay)

C_{side} = Outside circumference of pile

dL = Interval of length along pile

and where

$$Q_{p,net} = 9S_u A_{tip}$$

S_u = Undisturbed undrained shear strength from T-bar data

A_{tip} = Area of pile tip (fully enclosed area for fully plugged and 0 for unplugged)

At depth, the measurements match well with the simplified prediction assuming that the pile is fully plugged (Figure 63 and Figure 64). The measurements for all of the tests where a pile was pushed in to free field soil match well with the values predicted. For push in, the initial T-bar data was used in all the capacity prediction calculations.

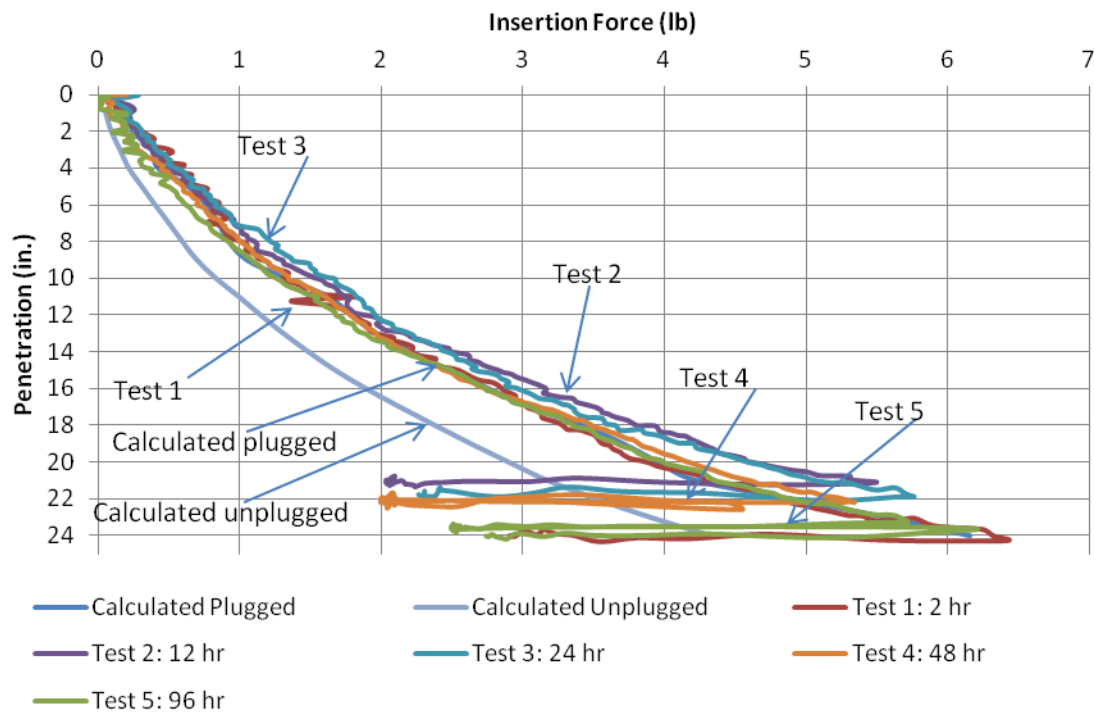


Figure 63 Predicted Push in Resistance vs. Measured Push in Resistance for 1.5-inch Piles

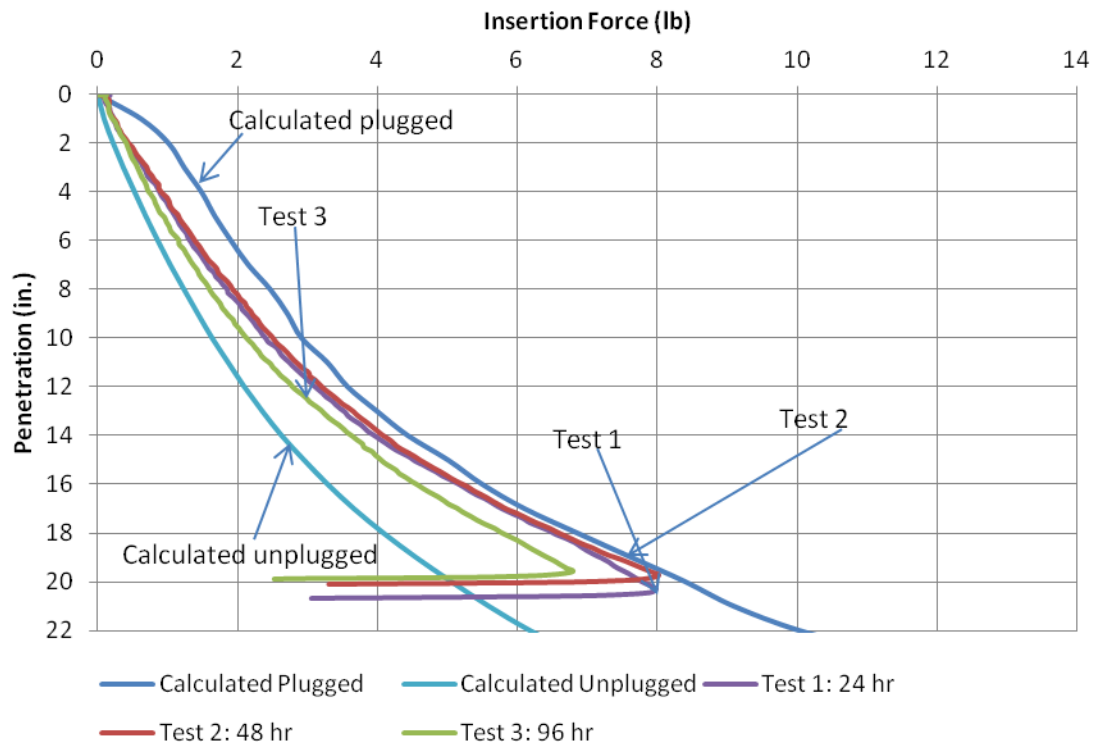


Figure 64 Predicted Push in Resistance vs. Measured Push in Resistance for 3-inch Pile Tests

6.2.2 Push-In Resistance Outer Pile

The push-in resistance for the outer pile over an inner pile was not noticeably affected when the piles did not come into contact (all tests except Test 1 in Figure 67 and Figure 68 and Test 3 in Figure 69 and Figure 70). Conversely, the push-in resistance increases when the outer pile contacts the inner pile (Tests 1 and 2 in Figure 69 and Figure 70 and all tests in Figure 65 and Figure 66); the percentage increases in push-in resistance versus the case with soil alone range between 20% and 40% when the piles come in contact (Figure 70 and Figure 66). With spacers, the push-in resistance is

increased (Figure 71), but the percentage increases at depth are less than in the case of no spacers (Figure 72 versus Figure 66). Simplistically, it seems that the spacers provide a relatively constant increase in the push-in resistance versus depth (meaning that the percentage increase decreases with penetration depth -Figure 72).

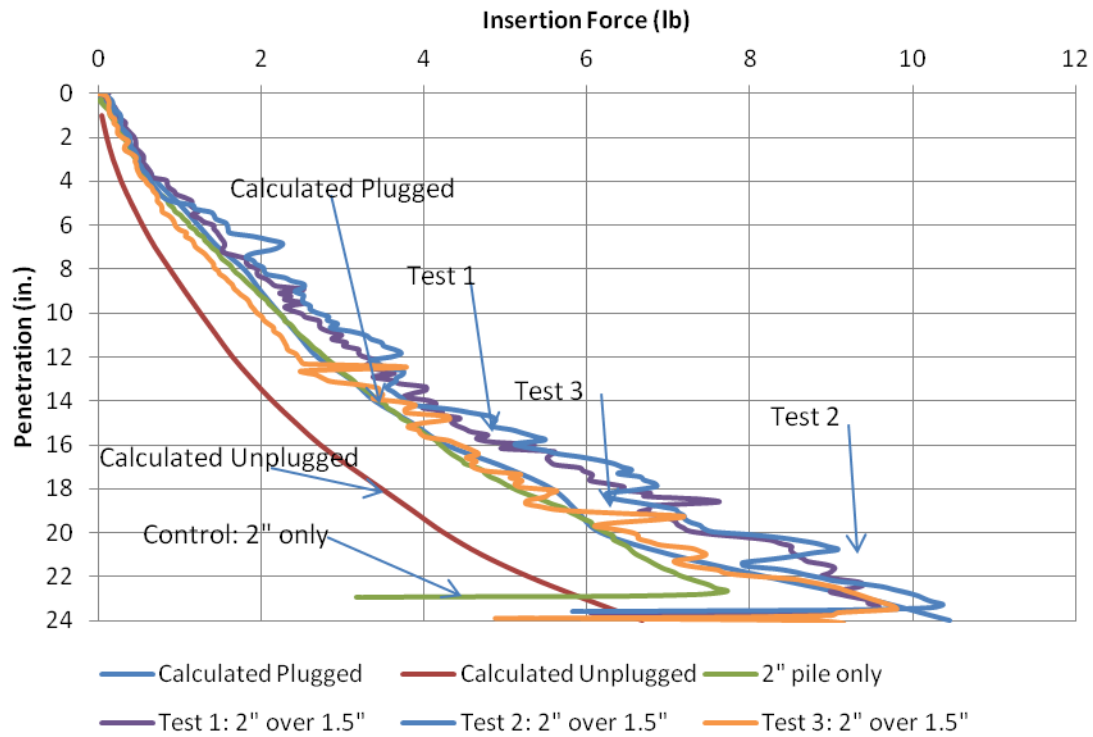


Figure 65 Predicted push in capacity vs. measured push in capacities for 2-inch piles pushed over 1.5-inch piles

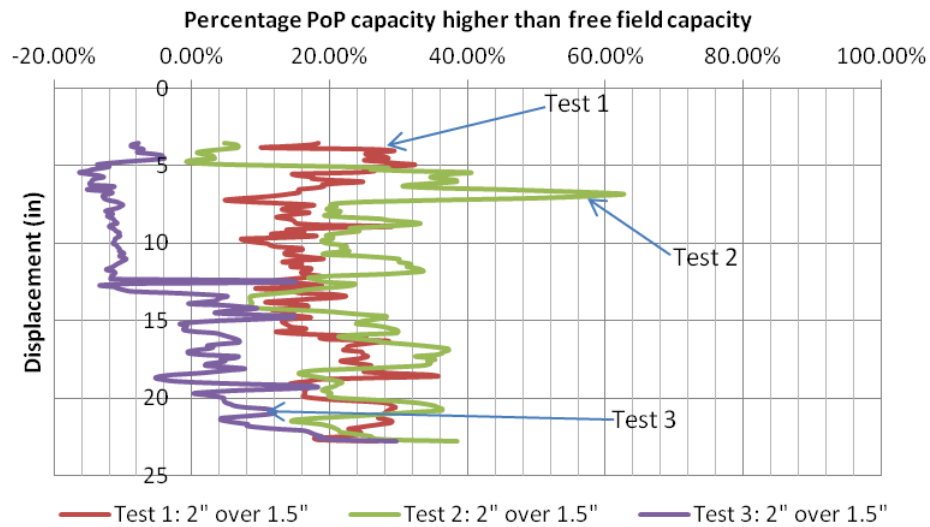


Figure 66 Percentage 2-inch PoP capacity higher than free field 2-inch capacity

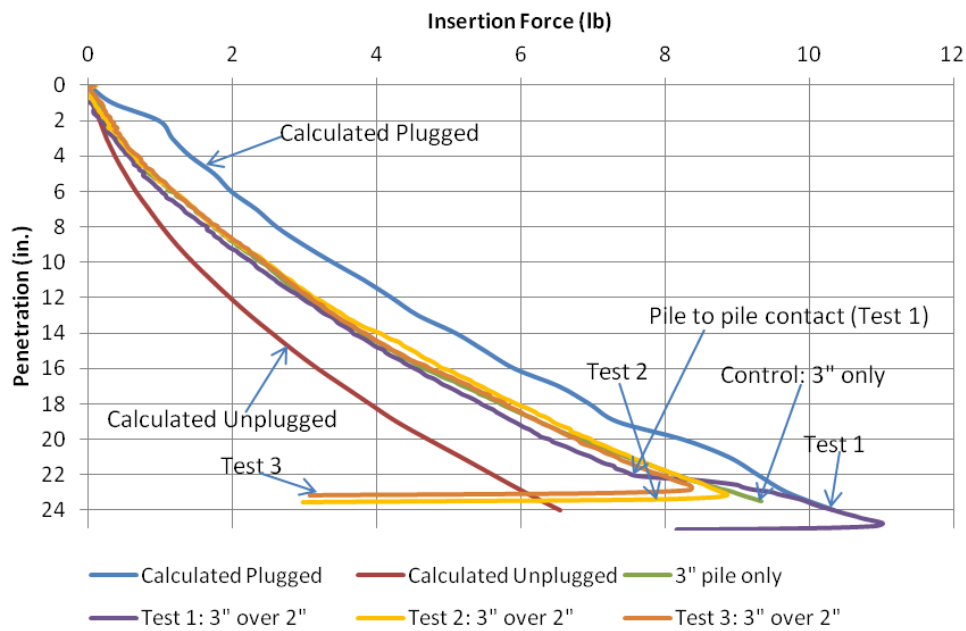


Figure 67 Predicted push in capacity vs. measured push in capacities for 3-inch piles pushed over 2-inch piles

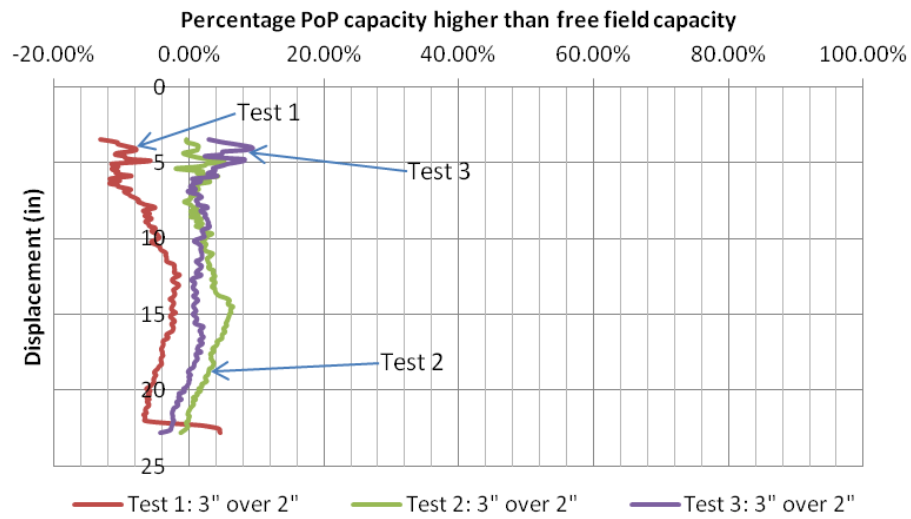


Figure 68 Percentage 3-inch PoP capacity higher than free field 3-inch capacity

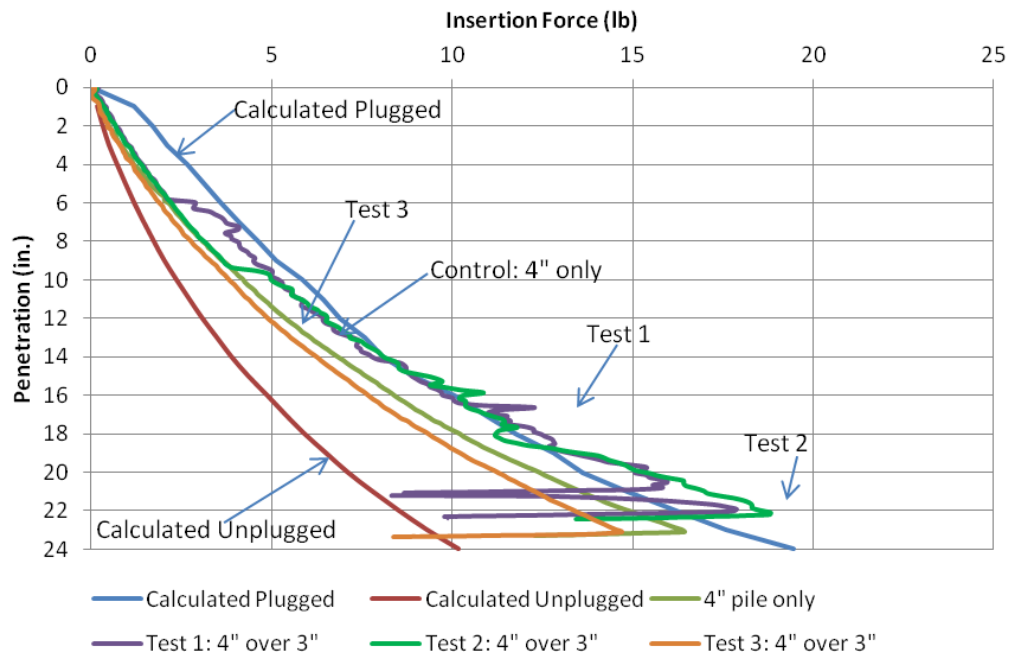


Figure 69 Predicted push in capacity vs. actual push in capacity for 4-inch piles pushed over 3-inch piles

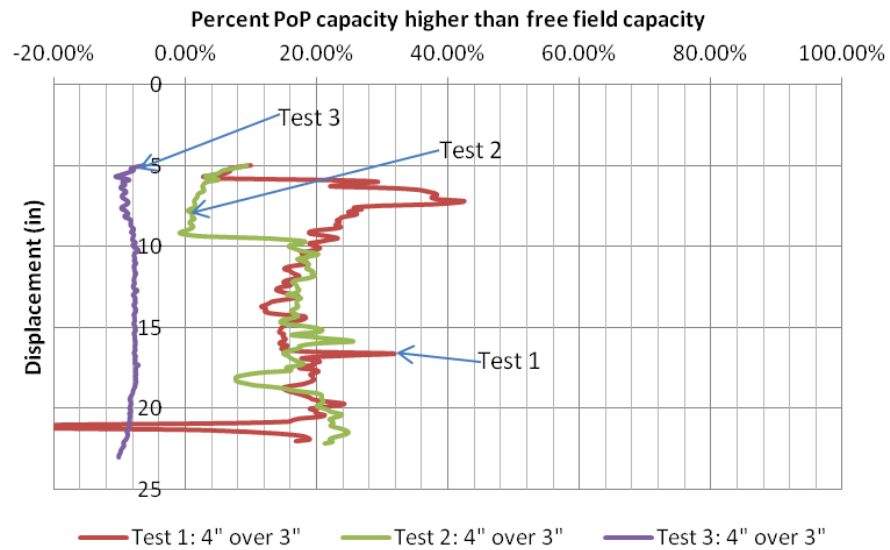


Figure 70 Percentage 4-inch PoP capacity higher than free field 4-inch capacity

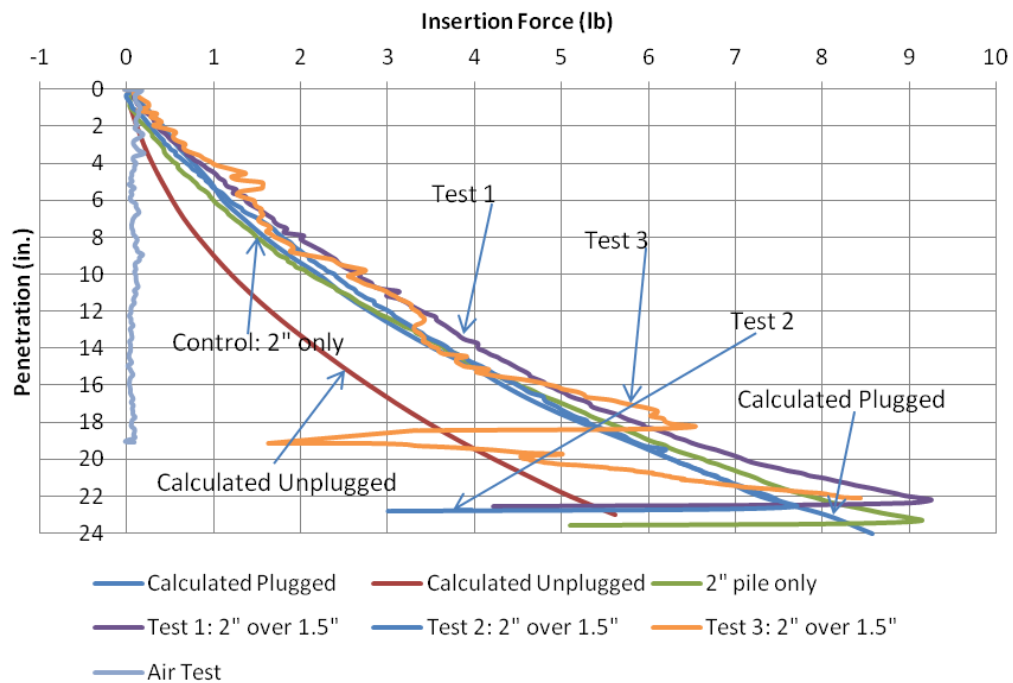


Figure 71 Continued next page.

Figure 71 Predicted push in capacity vs. actual push in capacity of 2-inch piles pushed over 1.5-inch piles with spacers

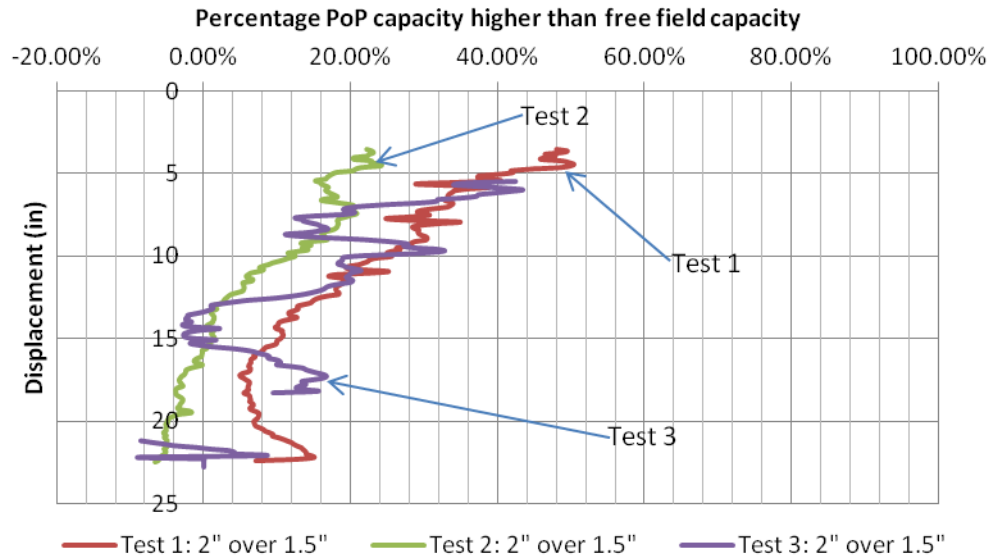


Figure 72 Percentage 2-inch PoP capacity higher than free field 2-inch capacity for test with spacers

Using moment equilibrium, an approximate limit can be placed on the increase in measured push in resistance resulting from an outer pile coming into contact with an inner pile. Using the assumption of full mobilization of the ultimate soil resistance and the point of rotation for the pile, the maximum increase in force from a pile acting on another pile can be determined. (Figure 72). Using the API method to determine P_{ult} , the maximum contact force can be determined.

$$P_{ult} = 3S_u + \gamma' z D + 0.5 S_u z$$

where

P_{ult} =ultimate soil resistance

S_u =undrained shear strength

γ' =effective unit weight of the soil

D =pile diameter

Applying this equation to the free body diagram for the 2 inch pile over a 1.5 inch pile, with its rotational moment at 12 inches of embedment, gives a resultant maximum resistance of 7.9 lbs, which assuming a coefficient of friction of one makes the maximum resultant force 7.9 lbs. While this can be used as an upper limit for the maximum contribution of the piles coming into contact, none of the instances where this occurred showed increases close to this, staying in the range of 2 to 2.5 pounds (Figure 71)

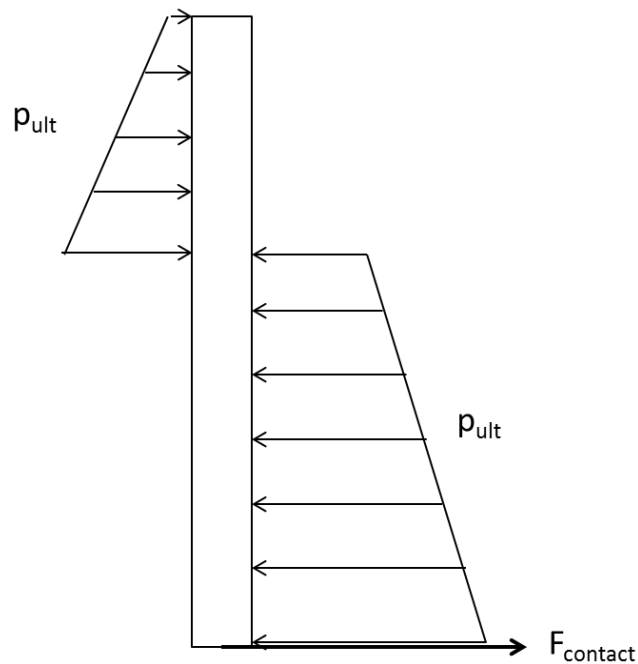


Figure 73 Free-body Diagram of Lateral Contact Force and Soil Resistance on Outer Pile

6.3 PULL-OUT CAPACITY

The pull-out capacity was analyzed for the piles during set-up and after set-up.

6.3.1 Pull-Out Capacity during Set-Up

The empirical Matlock and Bogard (1990) set-up model was fit to the measured data by adjusting the ultimate pull-out capacity and the time to 50% of the ultimate pull-out capacity for the 1.5-inch diameter pile (Figure 74). This model was then adjusted to the 3-inch diameter pile; the measured results for the 3-inch diameter pile are close to the prediction. In both cases, close to 90% of the ultimate capacity (typically defined as “full” set-up) was reached in about 48 hours. This setup time was subsequently used for all inner piles in the pile over pile testing.

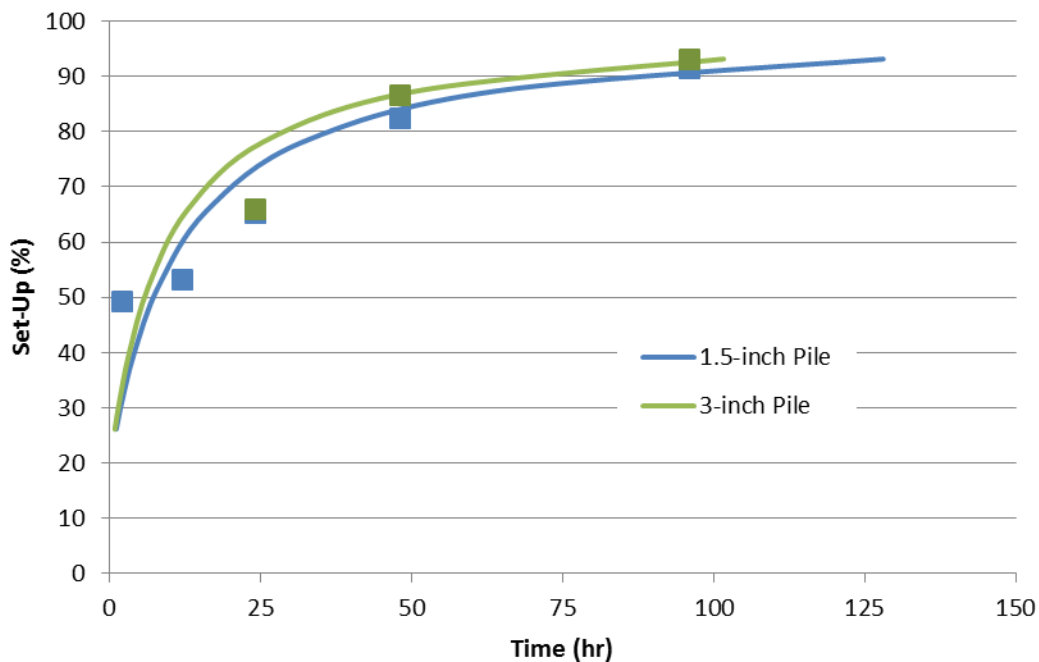


Figure 74 Predicted and actual percent setup for 1.5-inch and 3-inch diameter piles

6.3.2 Pull-Out Capacity after Set-Up

For the pullout resistance of the piles, three separate scenarios have been considered. The first is that specified in API for extension, where side shear and reverse end bearing are considered (Figure 75).

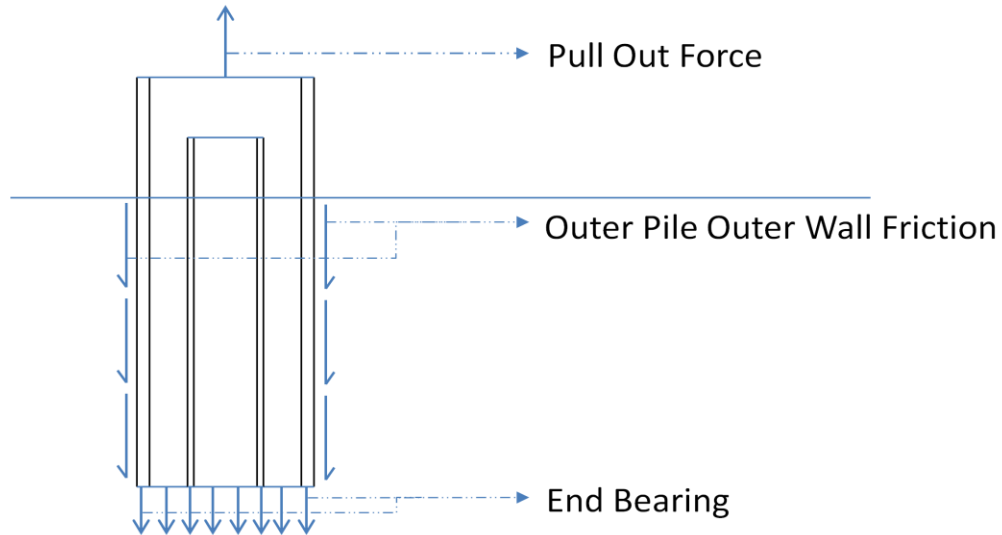


Figure 75 Free body diagram for pile pull-out with end bearing

A simplified prediction of net pile pull-out capacity (i.e., the pull-out capacity due to the shear strength of the soil), Q , is obtained as follows:

$$Q = Q_{side} + Q_{p,net}$$

where

$$Q_{side} = \sum_{Pile\ Length} \alpha S_u c_{side} dL$$

S_u = Undisturbed undrained shear strength from T-bar data

α = Empirical skin friction factor (assumed 1.0 for normally consolidated clay)

C_{side} = Outside circumference of pile

dL = Interval of length along pile

and where

$$Q_{p,net} = 9S_u A_{tip}$$

S_u = Undisturbed undrained shear strength from T-bar data

A_{tip} = Area of pile tip (fully enclosed area for fully plugged)

Second, where gapping exists at the base of the pile, and soil is retained along the outside of the pile (Figure 76).

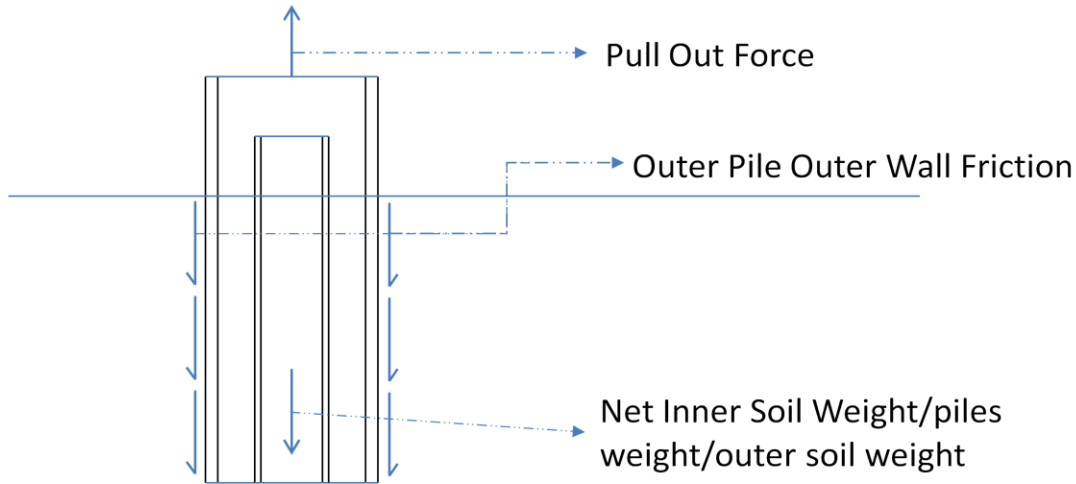


Figure 76 Free body diagram for "gapping" behavior at base of pile with no end bearing

A simplified prediction of net pile pull-out capacity for gapping behavior (i.e., the pull-out capacity due to the shear strength of the soil), Q , is obtained as follows:

$$Q = Q_{side} + Q_{p,net} + W_{pile\ system}$$

where

$$Q_{side} = \sum_{Pile\ Length} \alpha S_u C_{side} dL$$

S_u = Undisturbed undrained shear strength from T-bar data

α = Empirical skin friction factor (assumed 1.0 for normally consolidated clay)

C_{side} = Outside circumference of pile

dL = Interval of length along pile

where

$$Q_{p,net} = 9S_u A_{tip}$$

S_u = Undisturbed undrained shear strength from T-bar data

A_{tip} = Area of pile tip (fully enclosed area for fully plugged)

and where

$$W_{pile\ system} = W_{p,outer} + W_{p,inner} + W_{s,inner} + W_{s,outer}$$

$W_{pile\ system}$ = Total free hanging weight of the outer pile, inner pile, soil plug retained inside the piles, and soil retained on outside of the pile

$W_{p,outer}$ = Weight of outer pile

$W_{p,inner}$ = Weight of inner pile

$W_{s,inner}$ = Weight of soil plug

$W_{s,outer}$ = Weight of soil retained on outside of pile

In order to account for possible changes in undrained shear strength with time in the test bed between pile installation and pull-out, the measured undrained shear strengths

obtained just prior to pile installation and obtained just after the last pull-out test in a test bed were both used to bracket the predicted pull-out capacity (Table 10). In order to determine the appropriate undrained shear strength for each of the tests, linear interpolation with respect to time was used to find the appropriate value between the two T-bar tests, where possible. Although the increase in undrained shear strength would more appropriately be interpolated with the log of time, at the small intervals, a linear method was used for simplicity.

	Prediction from T-bar test before pile installation (lb)	Prediction from T-bar test after final pile removal (lb)
Setup Tests 1.5 inch piles	7.69	-
Setup Tests 3 inch piles	10.3	-
Test Series 1: 2 inch over 1.5 inch pile	9.02	12.05
Test Series 2: 3 inch over 2 inch pile	12.28	12.64
Test Series 3: 4 inch over 3 inch pile	23.2	-
Test Series 1 Retest	9.38	10.37

Table 10 Predicted pullout force based on T-bar tests run prior to pile installation and T-bar tests run after final pile removal

For single piles, the measured peak pull-out resistances generally match well with the predicted pull-out capacities for set-up times of 48 hours and greater (Figure 75 and Figure 76). Similarly for piles installed over piles, the measured peak pullout resistances generally match well with the predicted pull-out capacities for set-up times of 48 hours and greater (Figure 77, Figure 78, Figure 79 and Figure 80). In most cases, the measured resistance is within about 20 percent of the prediction with set-up times of at least 48 hours.

The undrained shear strength of the test beds in the free field continued to increase between the time of pile installation and the final pull-out test (Figure 77, Figure

78 and Figure 79); for the 96-hour set-up times, the predicted pull-out capacities using the undrained shear strengths measured after the pull-out tests are closer to the measured pull-out capacities than the predictions using the undrained shear strength measured before pile installation more than 96 hours earlier (Figure 77, Figure 78 and Figure 79).

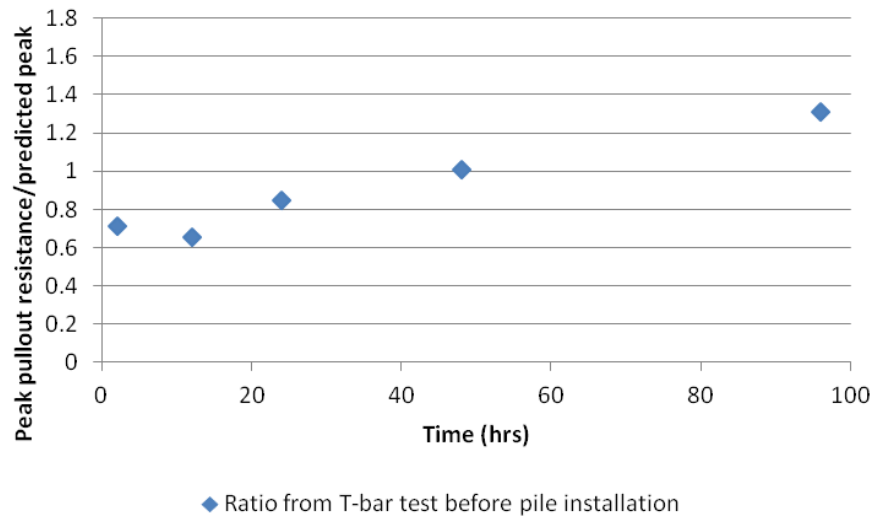


Figure 77 Ratio of predicted pull out resistance to measured pull out resistance for 1.5-inch Piles

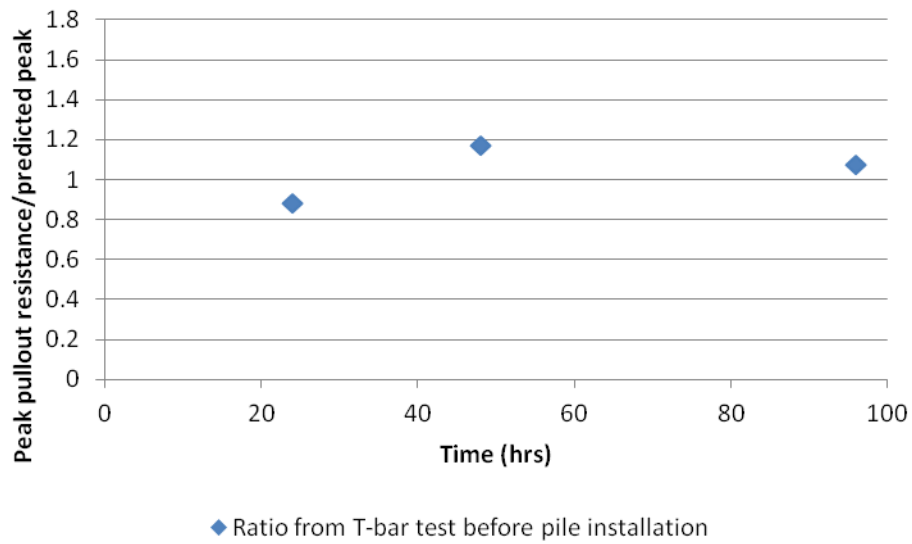


Figure 78 Ratio of predicted pull out resistance to measured pull out resistance for 3-inch Pile Tests

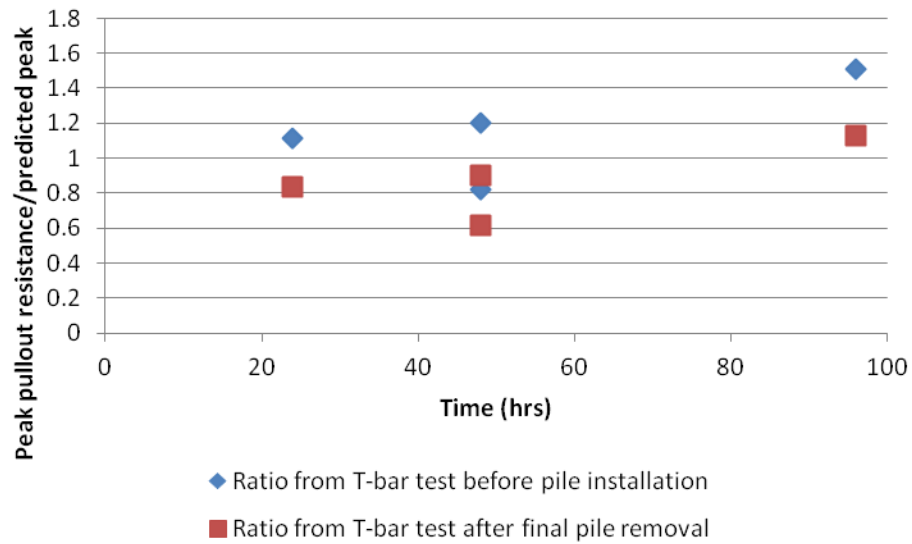


Figure 79 Ratio of predicted pull out resistance to measured pull out resistance of 2-inch piles over 1.5-inch piles

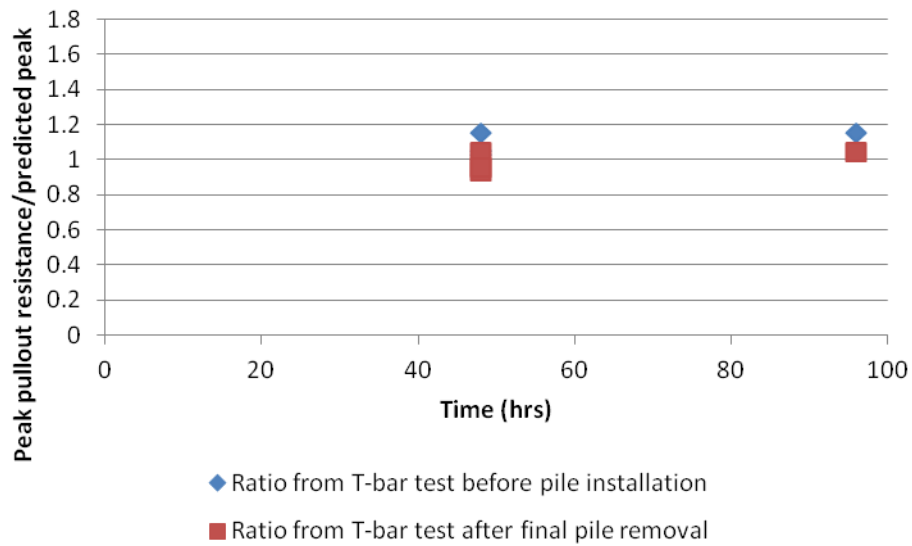


Figure 80 Ratio of predicted pull out resistance to measured pull out resistance of 2-inch piles over 1.5-inch piles – Retest with spacers

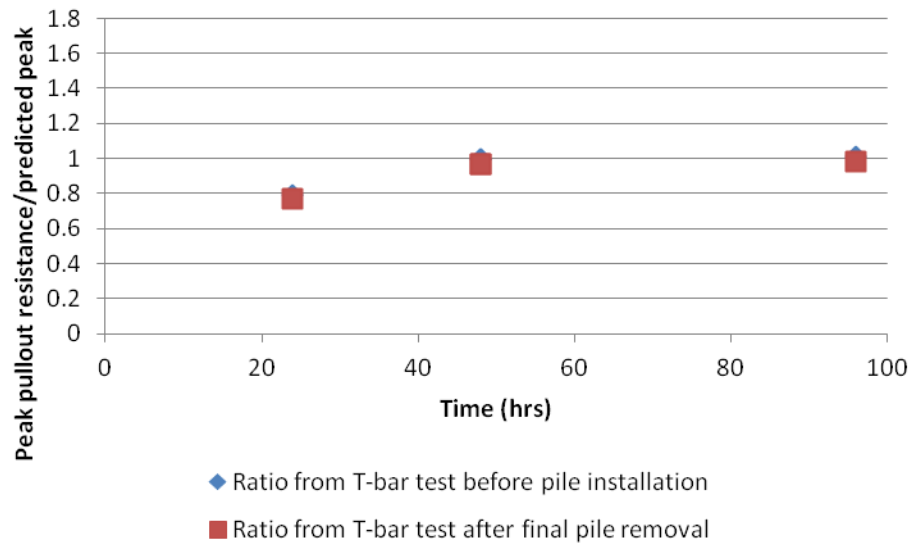


Figure 81 Ratio of predicted pull out resistance to measured pull out resistance of 3-inch piles over 2-inch piles

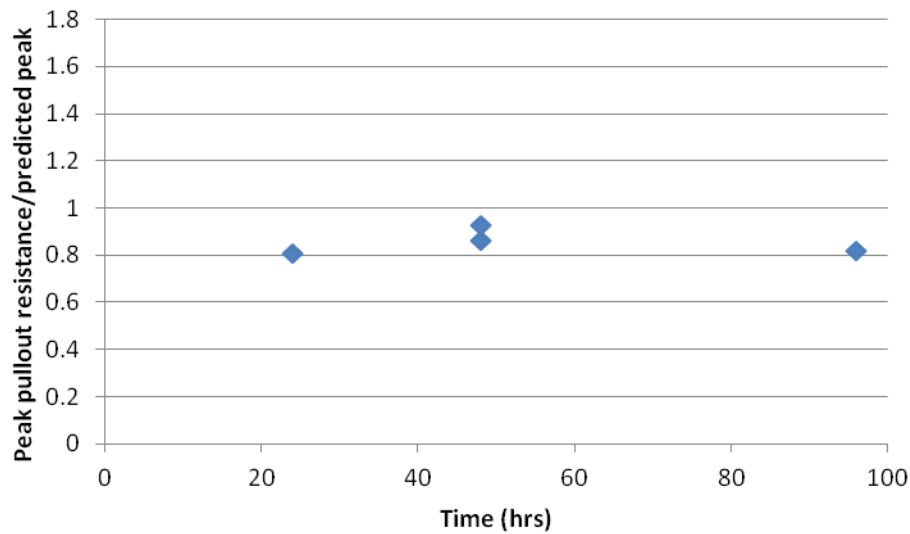


Figure 82 Ratio of predicted pull out resistance to measured pull out resistance of 4-inch piles over 3-inch piles

There are several notable outliers for pile-over-pile tests where the measured pull-out capacity was more than 20 percent greater than the predicted capacity (regardless of whether the undrained shear strengths measured before installation or after the last pull-out test were used in the predictions): the 2-inch over 1.5-inch diameter pile at 48-hours of set-up in one case (Figure 80) and at 96-hours of set-up in all cases (Figure 79 and Figure 80). In each of these tests, the soil plug, including the inner pile) was lifted up with the outer pile, indicating that the soil plug had separated from the soil at the tip. Additionally, a substantial outer ring of soil was retained on the outside of the pile itself (Figure 83).



Figure 83 Soil retained on 2 inch pile after pull-out

The added weight of the soil plug can be seen clearly in the normalized measured pull-out resistance for these three tests after the pile has pulled up 12 to 24 inches (Figure 84).

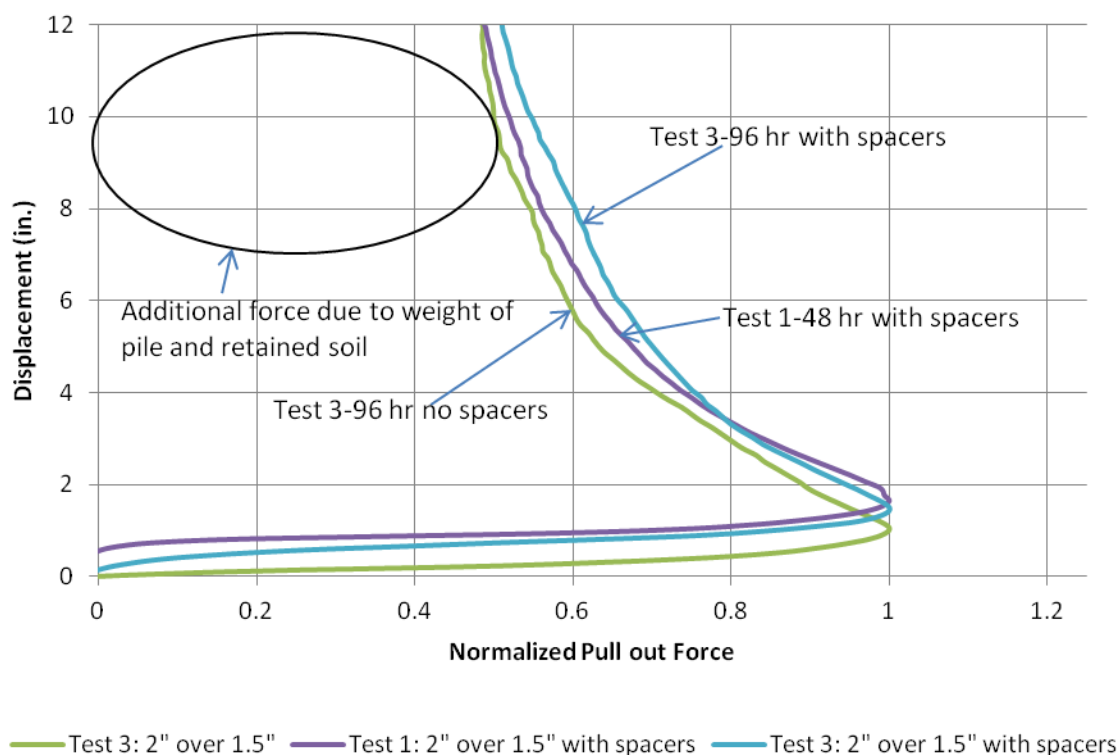


Figure 84 Normalized pull out force in tests that displayed possible gapping behavior

For these three outlier cases, using the information about the plug heights in the inner pile, and using a typical outer retained soil ring of 0.25 inch thickness, the expected weight of the pile system in the air can be calculated for each (Table 11).

	$W_{\text{outer pile (lb)}}$	$W_{\text{inner pile (lb)}}$	$W_{\text{inner soil (lb)}}$	$W_{\text{outer soil (lb)}}$	Total Weight (lb)
Test Series 1 Test 96 hour	1.23	0.78	2.38	2.09	6.48
Test 2 Series 1 Retest 48 hour	1.05	0.65	2.10	2.09	5.89
Test 3 Series 1 Retest 96 hour	1.05	0.65	2.10	2.09	5.89

Table 11 Composite weights of outlier pile systems exhibiting gapping behavior

If gapping behavior is suspected, this should become visible in the plots as the pile is fully removed from the soil. The ratio of predicted resistance as determined through the standard API method to the measured resistances shows this difference (Figure 85). However, when the API method is modified to include gapping behavior, the predicted resistance shows a much closer value to the measured results (Figure 86).

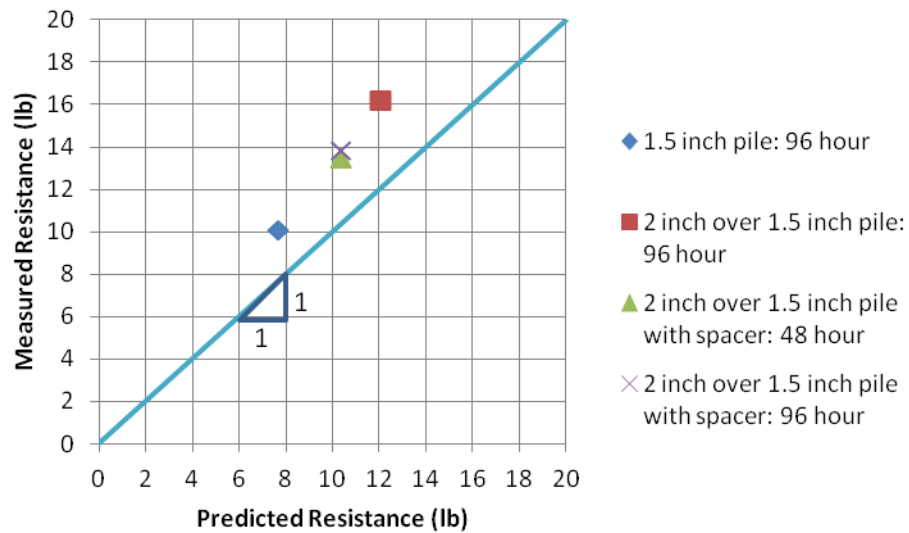


Figure 85 Comparison of predicted resistance based on fully plugged behavior to measured resistance in piles that displayed possible gapping behavior

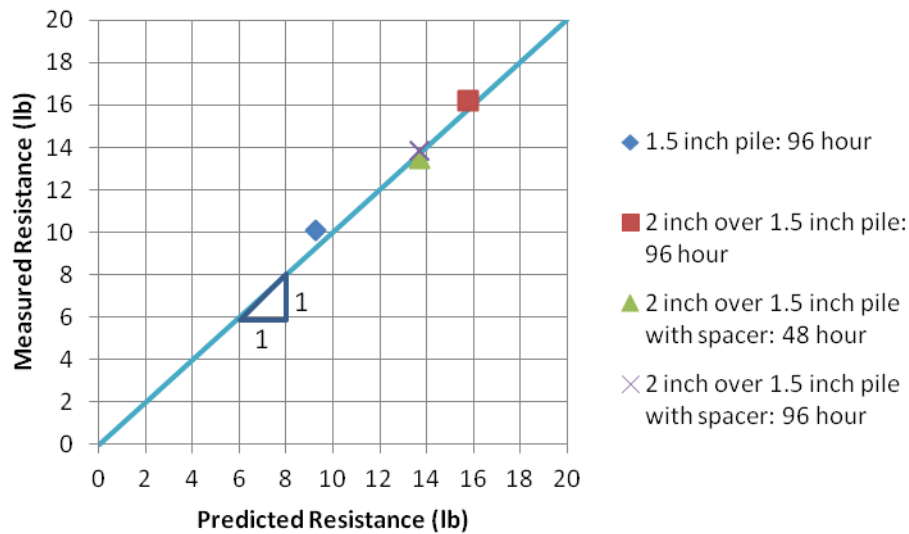


Figure 86 Comparison of predicted resistance based on fully plugged behavior with gapping at base of pile to measured resistance in piles that displayed possible gapping behavior

For these smaller diameter test series, the "gapping" behavior observed was dependent on time the inner soil was allowed to setup, as the inner plug and pile were most likely to be pulled out with the outer pile in the tests that had been allowed to sit the longest after installation.

6.4 CONCLUSION

There is no discernible increase (less than 5% to 10%) in push-in resistance due to an inner pile being present as long as the two piles do not come into contact. Using a remolded undrained shear strength for side shear, and a plugged pile tip produces results that match closely to the measured values within the scatter.

When piles did come into contact, there was an increase in push in resistance in the range of 20% to 40%. Using the theoretical upper bound based on lateral soil

resistance gave an upper limit for these cases, which were 2 inch over 1.5 inches, of approximately 9 pounds.

Using spacers at the top of the piles to prevent pile to pile contact did prevent the pile to pile contact. It did introduce its own increase in resistance in certain cases, but this stayed in the average range of around 10%.

Using the API method gave an accurate prediction for the pull-out capacities of the outer piles in the pile over pile system. In the case of the four outlier tests, gapping behavior was observed, leading to a contribution of pile weight, and retained soil weight being registered by the load cell. Once the added weight was accounted for in the API method, the outlier results matched up with the predicted results. From the testing, there was no apparent increase or decrease in the pile pull-out resistances that wasn't within the typical noise associated with the testing.

Chapter 7 SEISMIC TESTING OF MONOPILE

7.1 INTRODUCTION

Seismic testing was performed on the 4-inch diameter pile in Test Bed 7 in an attempt to understand how the soil properties are changing before and after pile installation. The test bed was constructed with geophone sensors embedded at varying depths of the bed in a spiral orientation around the pile.

7.2 RESULTS

After test-bed construction, readings were taken on the geophone sensors daily, and the shear wave arrival times were used to determine the average shear wave velocity in the soil versus time. The shear wave velocity increased with time following construction of the test bed (Figure 86), presumably due to re-arrangement of the clay particles at a nearly constant water content (i.e., thixotropy). A T-bar test was conducted about 5 days after test-bed construction (Figure 87). The measured undrained shear strengths are roughly proportional to the measured shear wave velocities (Figure 88). The insertion of the T-bar, while several bar lengths away from the geophone array, reduced the shear wave velocity in the vicinity of the geophones (Figure 86).

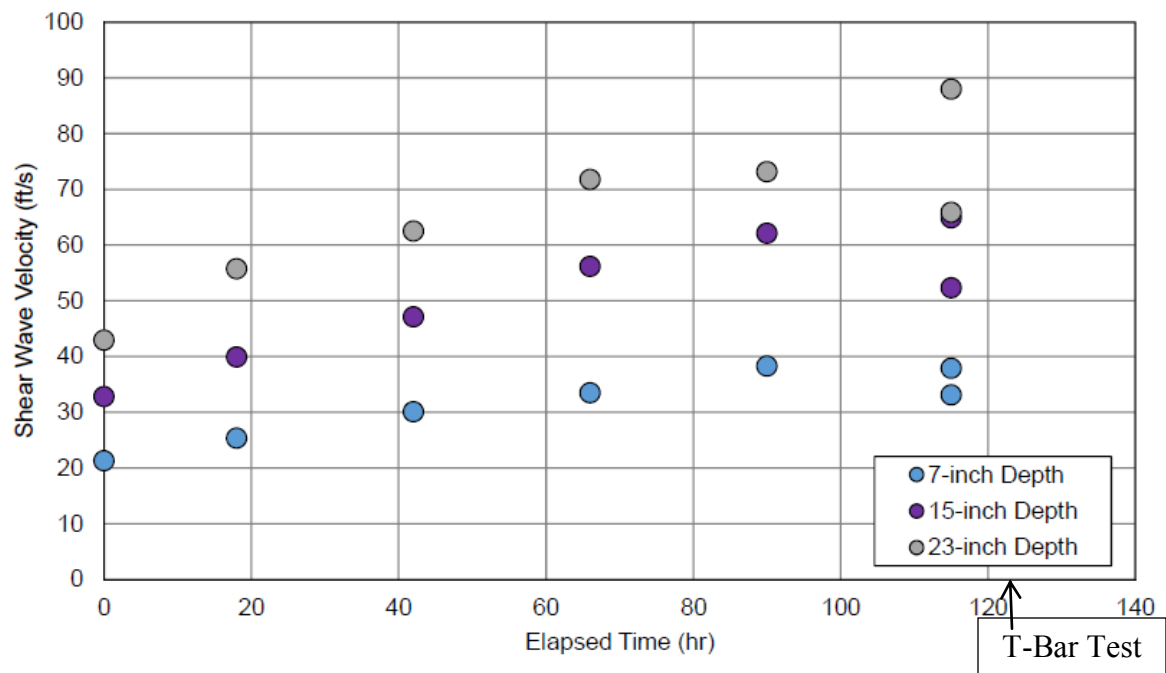


Figure 87 Average shear wave velocities vs. time from seismic test bed

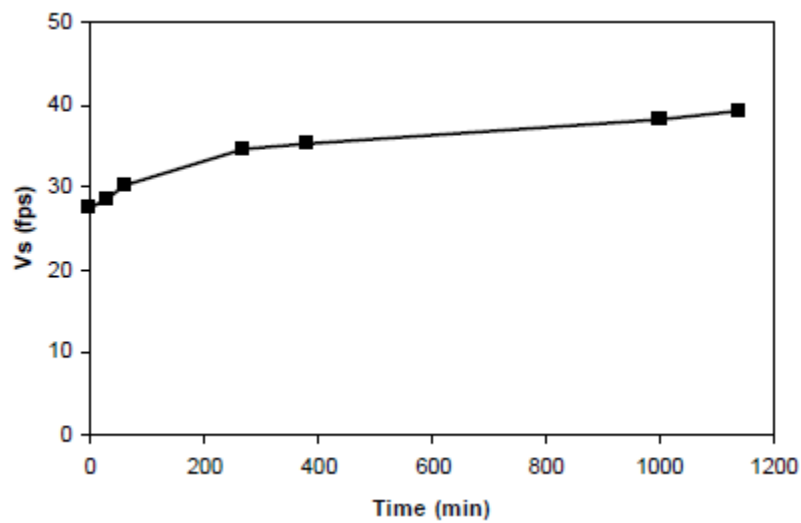


Figure 88 Change in Vs with time in the small kaolinite test bed (Jung 2005)

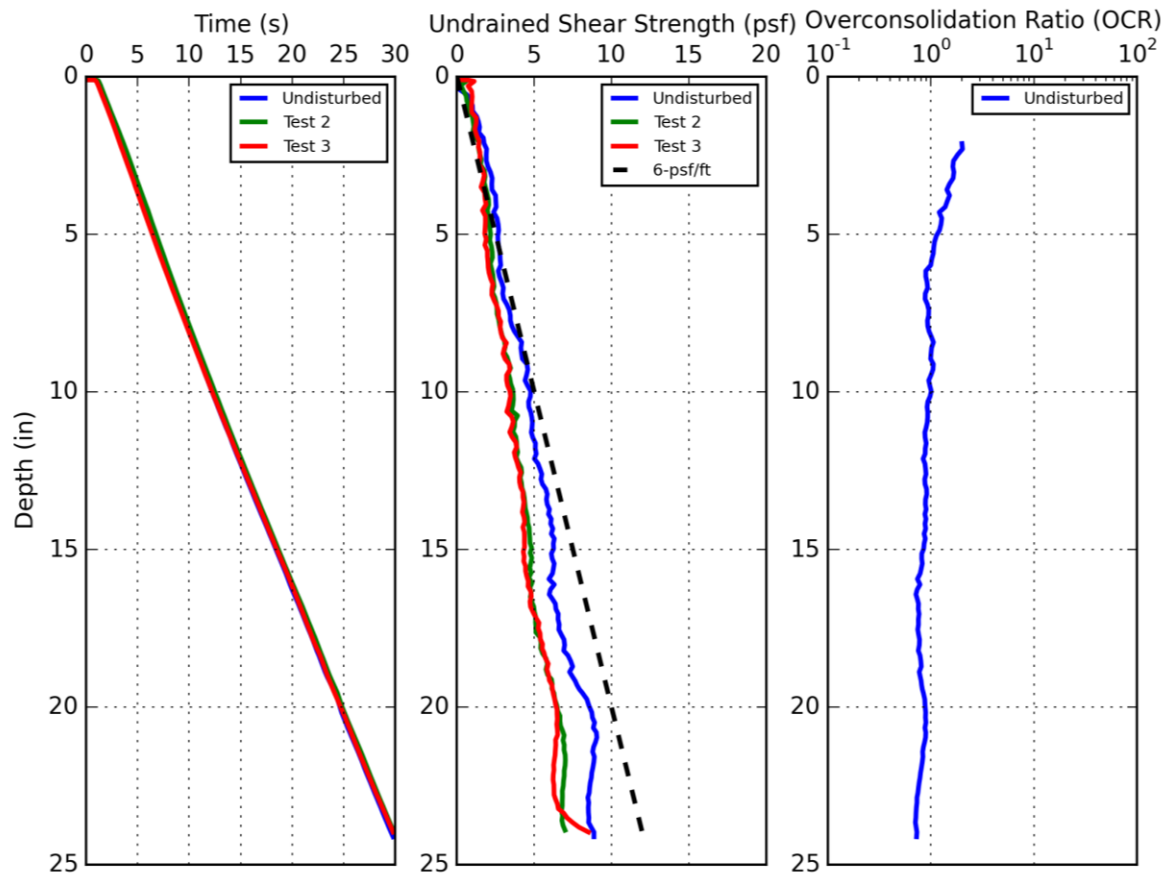


Figure 89 T-bar results for seismic test bed, Test Bed 7

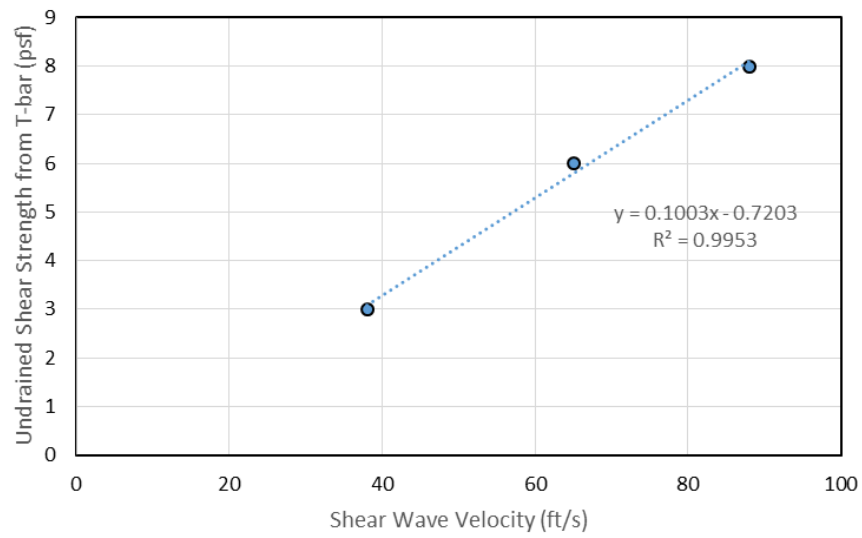


Figure 90 Undrained shear strength versus shear wave velocity

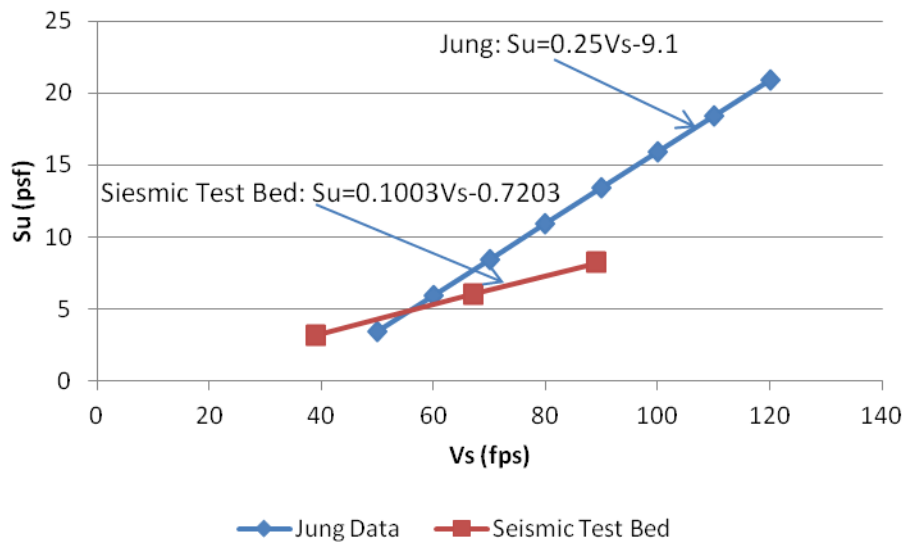


Figure 91 Undrained shear strength versus shear wave velocity in a kaolinite slurry (Jung, 2005) compared to results from seismic test bed

The comparison of the correlation from Jung to the correlation developed from the seismic test bed results shows a high level of disagreement between the data sets (Figure 90). However, both sets show a very linear correlation for a normally consolidated test bed. The linearity in both trends show that the shear wave velocity increased with time at a constant water content.

The trend established by Jung was developed from a test bed that was constructed using a slurry mix rather than the layering method. It was then allowed to consolidate for 7 months, rather than the 6 days used for the pile over pile testing.

After pile installation, the measured shear wave velocities were very irregular. The reason for the irregular readings was not apparent after further investigation, and the results were not presented in this thesis.

7.3 CONCLUSION

When taken with the T-bar test results, the shear wave velocity readings showed that the undrained shear strength and the shear stiffness of the kaolinite increased with time without any change in the water content, showing secondary compression.

The undrained shear strength showed a very linear relationship to the shear wave velocity. Comparison to the values obtained by Jung show that this relationship changes with time, but still remains linear.

The drop in shear wave velocities recorded after the second T-bar test show that the T-bar does have a not insignificant disturbance effect that was impossible to quantify in earlier testing. The T-bar itself had a disturbance known in excess of 10 T-bar diameters from the T-bar testing location. The installation of the 4 inch pile had a similar

effect, but was impossible to quantify, due to the inadmissibility of the shear wave velocities recorded following its installation.

The shear wave velocity testing shows further potential as a means of monitoring changes in soil conditions in model pile testing, but further work needs to be undertaken to limit the effects of disturbance.

Chapter 8 CONCLUSION AND RECOMMENDATIONS

8.1 CONCLUSIONS

Installing a larger diameter pile over an existing pile could be used to increase the capacity of an existing foundation, or mitigate problems with an existing foundation. Laboratory model testing was performed in order to investigate changes in pile driving resistance and pull-out capacity of a pile installed over an existing pile. This study included three test series with different pile diameters (2-in over 1.5-in, 3-in over 2-in, and 4-in over 3-in), one test series with spacers (2-in over 1.5-in), and one series of seismic testing to measure shear wave velocities versus location and time in a test bed,.

The following conclusions are drawn from this work:

- There is no discernible increase (less than 5% to 10%) in push-in resistance due to an inner pile being present as long as the two piles do not come into contact. Using a remolded undrained shear strength for side shear, and a plugged pile tip produces results that match the measurements within the typical scatter for piles alone and outer piles that do not contact inner piles.
- There is an increase in push-in capacity when the outer pile comes into contact with the inner pile. This increase is typically in the range of about 20% to 40% higher than the push-in resistance of a single pile of the same diameter. The measured increases were all less than a theoretical upper bound based on the ultimate lateral resistance of the soil to pile rotation.
- Using spacers between the piles (at the top as was done in this experiment) can mitigate the friction between the piles and limit the increase in the push-in resistance due to contact. The spacers need to provide enough moment resistance to keep the outer pile from rotating relative to the inner

pile. The spacers, as implemented in this experiment, nominally increase the push-in resistance in the model tests (less than one half the resistance without the spacers when the piles come into contact). However, the length of model piles and their effects on the resistance with spacers was not investigated.

- Measured pullout capacity for the larger diameter piles (3 inch and 4 inch) is consistent with API predictions for undrained loading, including setup and reverse end bearing.
- For the smallest diameter piles (1.5 inch alone and the 2 inch over 1.5 inch), the measured pullout capacity is greater than API predicts, probably because the inner plug separates from the surrounding soil at the tip and contributes its total weight to pullout resistance. This phenomenon could advantageously be used to increase pullout capacity for a pile over a pile.
- Both T-bar testing and shear wave velocity testing show that the undrained shear strength and the shear stiffness of the normally consolidated clay increase with time at a near constant water content (i.e., thixotropy or secondary compression).
- The undrained shear strength has a linear relationship with the shear wave velocity. However, the relationship changes with time at a constant water content because the undrained shear strength apparently increases at a different rate than the shear wave velocity with time at the same location.
- Based on the shear wave velocity measurements, the T-bar testing reduces the shear stiffness of the soil (at least temporarily) between 5 and as far away as 10 T-bar diameters away from the T-bar probe location.

8.2 RECOMMENDATIONS

From these conclusions, the following recommendations are made:

- Further consideration should be given to the pile over pile installation method. Increase in push in resistance during testing that was outside the typical noise associated with testing was attributable to pile over pile contact. Looking in to further methods to prevent this contact from occurring would be the best way to improve drivability in the pile over pile configuration.
- Further investigation should be conducted with regards to the hypothesized "gapping" behavior during pullout of the outer pile, and whether this mechanism can be utilized.
- The seismic crosshole testing method in the small scale, normally consolidated test beds needs further study. The uncertainty in the data introduced by disturbance from strength and foundation testing made much of the data inadmissible, and further work needs to be explored in remediating those effects.
- For the application of observing the increase in undrained shear strength about a model pile, using the pile as a seismic source gave poor results. The configuration used for this type of testing needs improvement.

References

- ASTM D2487-00, Standard Classification of Soils for Engineering Purposes (Unified Soil Classification System) ASTM International, 03/05/2000.
- Boylan, N., and Long, M. (2007). *Characterization of Peat Using Full Flow Penetrometers*, Department of Civil Engineering, University College of Dublin, Ireland, Taylor and France Group, London.
- Chung, and Randolph M.F. "Penetration resistance in soft clay for different shaped penetrometers." *Proceedings of ISC-2 Geotechnical and Geophysical Site Characterization*. 2004. 671-677.
- Coffman, R.A. *Horizontal Capacity of Suction Caissons in Normally Consolidated Clay*. M.S. Thesis, Austin: The University of Texas at Austin, 2003.
- El-Gharbawy, S.L. *The pullout capacity of suction caisson foundations for tension leg platforms*. Ph.D. Dissertation, Austin: The University of Texas, 1998.
- El-Gharbawy, S.L., and Roy Olson. "Suction caisson foundations in the Gulf of Mexico." *OTRC '99 Conference*. Austin, TX, 1999. pp. 281-295.
- El-khatib, S., B. Lonnie, and M.F. Randolph. "Installation and pull-out capacities of drag-in plate anchors." *Twelfth International Offshore and Polar Engineering Conference*. Kitakyushu, Japan, 2002. 648-654.
- El-Sherbiny, R. *Performance of suction caisson anchors in normally consolidated clay*. Ph.D. Dissertation, Austin: The University of Texas, 2005.
- Fugelsang, L.D., and Steensen-Bach, J.O. (1991). *Breakout Resistance of Suction Piles in Clay*. Proceedings of the International Conference on Centrifuge 1991, Boulder, Colorado, pp.153-159.

- House, A.R., and Randolph, M.F. (2001). *Installation and Pull-out of Stiffened Suction Caissons in Cohesive Sediments*, Proceedings of the 11th International Offshore and Polar Engineering Conference, Stavanger, Norway, June 17-22, Vol. 2, pp.574-580.
- Huang, Y. (2015). *Designing a Laboratory Model Test Program for Developing a New Offshore Anchor*, M.S. Thesis, The University of Texas at Austin.
- Jung, M. J. (2005). *Shear Wave Velocities of Normally Consolidated Kaolinite Using Bender Elements*. M.S. Thesis, Austin: The University of Texas.
- Kolk, H.J., and van der Velde, E. (1996). *A REliable Method to Determine Friction Capacity of Piles Driven into Clays*, Proc. Annual Offshore Technology Conf., Houston, Paper OTC 7993.
- Lee, Chun Ho. *Constructing Test Beds of Clay with a Specified Profile of Undrained Shear Strength versus Depth*. M.S. Thesis, Austin: The University of Texas, 2008.
- Luke, A.M. (2002). *Axial Capacity of Suction Caissons in Normally Consolidated Kaolinite*, M.S. Thesis, The University of Texas at Austin.
- McCarthy, K.B. (2011). *Experimental In-Plane Behavior of a Generic Scale Model Drag Embedment Anchor in Kaolinite Test Beds*. M.S. Thesis, The University of Texas at Austin.
- Mecham, E.C. (2001). *A Laboratory for Measuring the Axial and Lateral Capacity of Model Suction Caissons*, M.S. Thesis, The University of Texas at Austin.
- Morvant, M. (2008). *Model Torpedo Pile Tests in Kaolinite Test Beds*, Final Project Report Prepared for the Mineral Management Service.

- Olson, R.E. et. al. (2003). *Soil Reconsolidation Following the Installation of Suction Caissons*, Proc. Annual Offshore Technology Conf., Houston, Paper OTC 15263.
- Randolph, M.F., and Houlsby, G.T. (1984). *The Limiting Pressure on a Circular Pile Loaded Laterally in Cohesive Soil*. Geotechnique, London, England, 34(4), 613-623.
- Stewart, D.P, and M.F. Randolph. "T-Bar Penetration Testing in Soft Clay." *Journal of Geotechnical Engineering*, 1994: 2230-2235.
- Vanka, S.K.R. (2004). *Laboratory Tests to Estimate Strength Profile of Normally Consolidated Kaolinite*, M.S. Thesis, The University of Texas at Austin.
- Vijeyvergiya, V.N and Focht, J.A. (1972). *A New Way to Predict Capacity of Piles in Clay*, Proc. Annual Offshore Technology Conf., Houston, Paper OTC 4178.

Vita

John Alexander McMillan V was born in Arlington, Virginia, in 1992, the first son of Mr. and Mrs. McMillan. He spent his early years in Dallas, Texas, and Melbourne Beach, Florida until the age of 6. He grew up in Charleston, South Carolina, with his three siblings. He considers this beautiful coastal city his home. In 2010, he graduated from Bishop England High School, and went on to earn his B.S. in Civil Engineering from The Citadel, the Military College of South Carolina. After finishing his undergraduate studies in 2014, he moved to Austin to pursue his M.S. in Geotechnical Engineering. To be continued.....(Also, the author prefers to not be contacted, but if you must, the following email should do)

Permanent address: mcmillanfith@gmail.com

This thesis was written by the author